Study of the properties of channel-forming proteins of the cell walls of different *Corynebacteriae*

Dissertation

zur Erlangung des naturwissenschaftlichen Doktorgrades der Fakultät für Biologie

an der Bayerischen Julius-Maximilians-Universität Würzburg

vorgelegt von

Enrico Barth

Würzburg

Würzburg 2008

Eingereicht am: ....

Prüfungskommission:

Vorsitzender: Prof. Dr. Martin Müller, Dekan der Fakultät für Biologie

1. Gutachter: Prof. Dr. Dr. h.c. Roland Benz

2. Gutachter: Prof. Dr. Roy Gross

Tag der mündlichen Prüfung: ....

Promotionsurkunde ausgehändigt am: ....

Ich versichere, dass ich diese Dissertation selbständig angefertigt und keine anderen, als die von mir angegeben Quellen und Hilfsmittel benutzt habe.

Die von mir vorgelegte Dissertation hat noch in keinem früheren Prüfungsverfahren in ähnlicher oder gleicher Form vorgelegen.

Ich habe zu keinem früheren Zeitpunkt versucht, einen akademischen Grad zu erwerben.

....

Contents

Chapter 1

1.1 Introduction

The cell wall is the outermost boundary of bacterial cells. Due to its exposed location it has various functions, some of which are obviously contradictory. For instance, the cell wall separates the inside from the outside of the bacteria and thereby protects the cells from harmful environmental influences. On the other hand, it enables the transport of substances from the exterior to the interior of the cells and vice versa, thus allowing a communication between the bacterium and its environment. Moreover, the cell wall provides the bacteria with shape and rigidity while being still flexible enough to allow growth and multiplication of the cells. The bacterial cell wall is adapted to fulfil all these manifold functions, but solving the problem is quite different in individual bacteria. Nevertheless, in comparing the cell walls of different bacteria, structural principles common to most of them become apparent (Fig. 1.1).
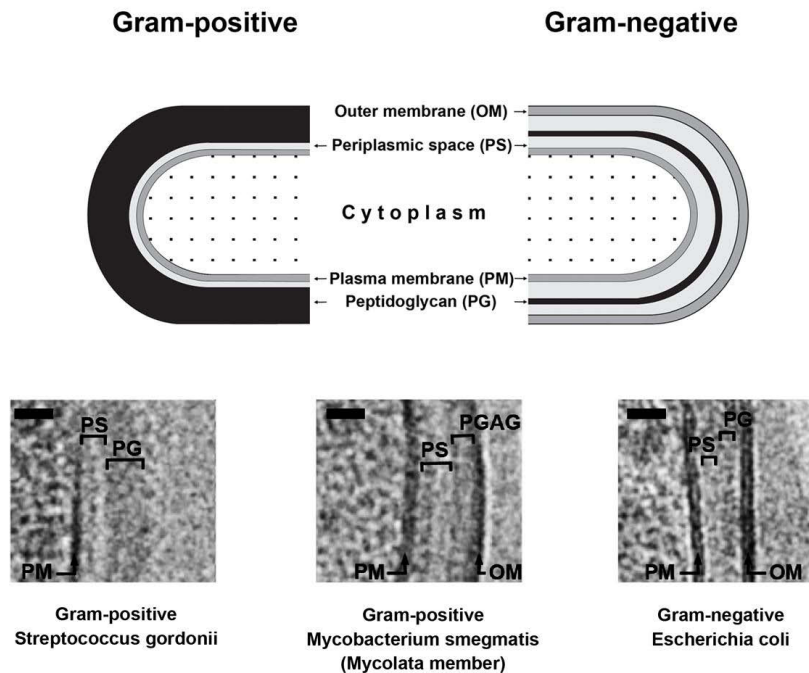
Figure 1.1: Scheme of the structure of the bacterial cell envelope (upper panel) on bases of electron micrographs (lower panel) (Zuber *et al.*, 2008). Among Gram-positive bacteria, the mycolata take an exceptional position in having an outer membrane enclosing the cell, as is the case with Gram-negative bacteria. Bars have a length of 20 nm.

Peptidoglycan (also called murein) is a structure wide-spread in nature. It has a far-reaching meaning because it allowed the Danish scientist Christian Gram, more than 100 years ago (1884), a classification of *Eubacteria* into Gram-positive and Gram-negative bacteria by a simple staining technique. By the application of a series of dyes, the Gram-positive bacteria appear under the microscope dark blue to violet, while the Gram-negative ones turn red. The difference in stain between species of both groups originates from the structure of their cell walls. More precisely, it is based on the structure of the peptidoglycan of Gram-positive microorganisms, which is considerably thicker than that of Gram-negative microorganisms. Both groups differ in further cell wall components, with the most obvious being the outer membrane of Gram-negative bacteria that does not exist in Gram-positive bacteria. Except for *Mycoplasma* containing neither a cell wall nor peptidoglycan and *Archaea* having a differently composed pseudomurein layer instead of peptidoglycan and/or a protein surface layer (S-layer), the cell walls of most *Eubacteria* resemble one of the two cell wall architectures illustrated schematically in Fig. 1.1. However, the exception proves the rule. The Gram-negative members of *Cyanobacteria* contain a thick murein layer and the Gram-positive mycolata have cell walls that look like those of Gram-negative bacteria. As a consequence, the response to Gram stain for these bacteria is ambiguous. They are called Gram-variable bacteria. It has to be noted that, despite having similar functions, the outer membranes of mycolata and Gram-negative bacteria fundamentally differ from each other.

1.2   Bacterial cell wall structures

In general, microorganisms of the above-mentioned groups differ from each other in many details of their cell envelopes. However, the cytoplasmic membrane and the peptidoglycan are two components of the bacterial cell envelope which can be found in almost all bacteria (Fig. 1.1).

1.2.1   The cytoplasmic membrane

The innermost layer of the cell envelope is the cytoplasmic membrane. It separates the cytosol from the periplasmic space and is the site of synthesis of many cell wall components (Holtje, 1998; Reeves, 1994; Ward, 1981). According to electron micrographs of cell-cross sections, the thickness of the membrane, consisting of about equal amounts of lipids and proteins,

amounts to 6 to 7 nm (Zuber *et al.*, 2008). Among the lipids that constitute the membrane, the amphiphilic (or complex) lipids are more important for the integrity of the membrane than the neutral lipids. Among the former group of lipids are glycolipids, anionic glycerophopholipids (such as phosphatidylinositol, phosphatidylglycerol, phosphatidylserine and diphosphatidylglycerol (cardiolipin)) and zwitterionic glycerophospholipids (such as phosphatidylethanolamine and phosphatidylcholine). Glycerol substituted with two fatty acids and a phosphate group builds the backbone of the phospholipids. These lipids (together with minor amounts of neutral lipids) are arranged as a fluid bilayer that forms a matrix for membrane proteins. The hydrophobic core of the bilayer is generally built by saturated, monounsaturated, hydroxylated and cyclopropane fatty acids that have in the majority chain lengths of 12 to 28 C-atoms (Seltmann & Holst, 2002). For instance, in case of *Corynebacterium glutamicum,* palmitic (16:0) and oleic (18:1) acids are the dominant fatty acids (Minnikin *et al.*, 1987). Because of the hydrophobic interior of the membrane, most polar and charged molecules cannot enter the cell through an intact membrane. Except for water, dissolved gases (such as carbon dioxide and oxygen) and lipid-soluble molecules that may cross the cytoplasmic membrane by simply diffusion, hydrophilic substances need transport pathways to cross this barrier. The uptake of nutrients and the release of waste are mediated by specialized integral or transmembrane proteins, such as carriers and porins, making the cytoplasmic membrane permeable for those substances.

1.2.2 The periplasmic space

The periplasmic space is defined as the space between the cytoplasmic membrane and the peptidoglycan layer. In contrast to the thick peptidoglycan of Gram-positive bacteria, the thin peptidoglycan of Gram-negative bacteria is hardly visible in electron micrographs (Fig. 1.1). This is because it forms part of a gel-like matrix which is limited by the inner and outer membranes. The enclosed space, called periplasm, is iso-osmolar to the cytoplasm (around 300 mOsm); an important feature that contributes to the resistance of Gram-negative bacteria towards osmotic shock (Benz, 1988). Although the exact composition of the periplasm is unknown, it is known to contain mono- and oligosaccharides, amino acids and precursors of the peptidoglycan. It further contains different kinds of polypeptides which may be classified as chaperons, transport proteins and enzymes (Seltmann & Holst, 2002). Depending on their

function, the enzymes are either involved in catabolic, detoxifying or synthesis processes, all of whom have an important role for the survival of the bacteria.

A periplasmic space presumably also exists for Gram-positive bacteria even though they (i.e. the classical representatives) do not possess an outer membrane as is the case with Gram-negative ones (Dijkstra & Keck, 1996; Merchante *et al.*, 1995). This assumption is supported by electron micrograph analysis (Fig. 1.1) showing between the inner membrane and the thick peptidoglycan layer of Gram-positive bacteria a corresponding interspace (Matias & Beveridge, 2006; Zuber *et al.*, 2008). Given the fact that the peptidoglycan mesh itself acts like a molecular sieve retaining hydrophilic molecules larger than 50 kDa (Demchick & Koch, 1996), the space between the murein and the cytoplasmic membrane of Gram-positive bacteria presumably contains elevated levels of proteins and other high molecular compounds, similar to the situation in the periplasm of Gram-negative microorganisms. Microscopy analyses indicate that the periplasmic space of Gram-positive bacteria has on average a thickness of 11 to 18 nm (Zuber *et al.*, 2008).

1.2.3   The peptidoglycan layer

The peptidoglycan acts as an exoskeleton. It is an astonishingly widespread element of bacterial cell walls that is only missing in a few bacterial genus such as *Mycoplasma* and *Archaea* (Brock *et al.*, 2001). It consists of polysaccharide chains cross-linked via peptide bridges, thereby building a net-shaped bag. The chain of the polysaccharide moiety is build from alternating, ($\beta1\rightarrow4$) linked N-acetylglucosamine (GlcNAc) and N-acetylmuramic acid (MurNAc) sugars (Holtje, 1998). The latter is simply GlcNAc esterified at O-3 with lactic acid (Fig. 1.2). The 1,6-anhydro form of MurNAc forms the reducing end of the glycan chain (Holtje, 1998). In principle, the structure of this polysaccharide strand shows little variation. Alterations such as *O*-acetylation of the MurNAc residue at C-6 or modification of the *N*-acetyl groups are frequently found in pathogenic species where they may contribute to the resistance of bacteria to host defence factors (Vollmer, 2008). One such factor is lysozyme that specifically cleaves the β-1,4-glycosidic bond between MurNAc and GlcNAc. Other than in corynebacteria, the *N*-acetyl function on the muramic acids of mycobacteria and nocardia are further oxidized to yield *N*-glycolyl-muramic acids (Uchida & Aida, 1979).

For the cross-linkage of the glycan chains each MurNAc residue carries a tetrapeptide unit attached to the lactyl residue of the muramic acid. Commonly, the sequence of this peptide unit is L-alanyl-D-isoglutaminyl-L-meso-diaminopimelyl-D-alanine (Fig. 1.2). Besides minor variations in the amino acid composition of this tetrapeptide, L-lysine fairly substitutes the second last amino acid (i.e. meso-diaminopimelic acid (DAP)) (Schleifer & Kandler, 1972).
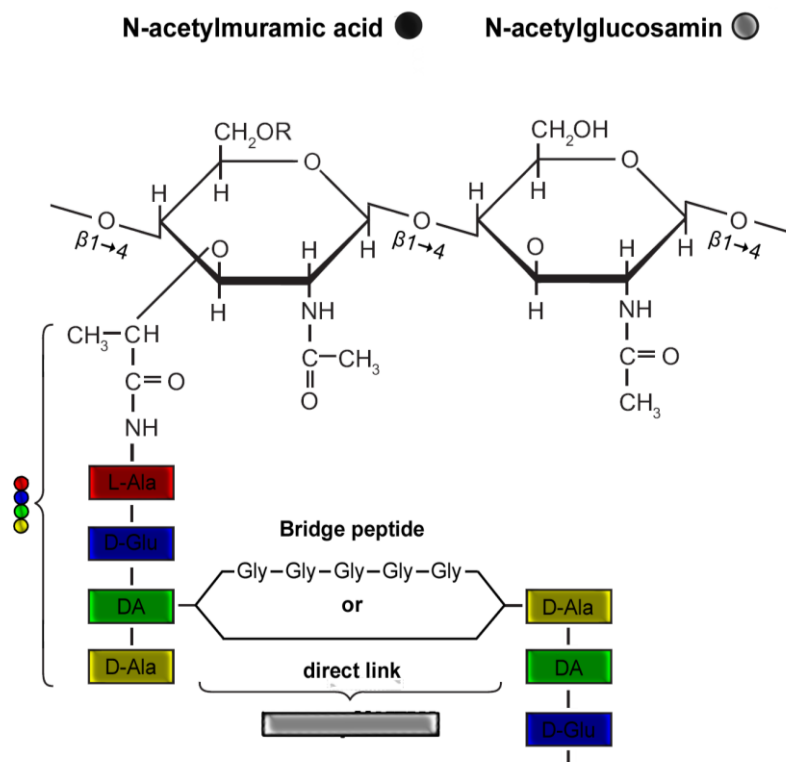
Figure 1.2: Chemical components and structure of peptidoglycan (Brock *et al.*, 2001). The pentaglycine residues corresponds the characteristic interpeptide bridge of *Staphyloccocus aureus*.

Cross-linking of peptide subunits may happen from the D-alanine of one subunit to the diamino acid (DA; i.e. L-Lys or DAP) of another subunit either via a bridge peptide, as is generally the case with Gram-positive bacteria, or directly. The direct connection between tetrapeptides often occurs in Gram-negative bacteria, such as *Escherichia coli*. However, it was also found in mycobacteria, corynebacteria and nocardia, i.e. for Gram-positive members of the mycolata (Schleifer & Kandler, 1972). These bacteria have, according to the peptidoglycan classes introduced by Schleifer and Kandler in 1972, a peptidoglycan structure of the A1γ type. In all cases, transpeptidases localized in the periplasmic space catalyse the cross-reaction between the peptide moieties (Holtje, 1998).

According to the species of bacteria, the murein sacchulus can amount to 10 to 90% of the cell wall mass (Brock *et al.*, 2001). The value is higher in Gram-positive than in Gram-negative bacteria because the latter have a thin murein skeleton consisting of 1 to 3 peptidoglycan layers (each about 2.5 nm thick), whereas the former have a multilayered, 10 times thicker exoskeleton (Dijkstra & Keck, 1996; Holtje, 1998). In this context, it is noteworthy that Gram-positive bacteria, as indicated in Fig. 1.3, exhibit a significant higher cross-linkage of their murein (70 to 90%) than Gram-negative bacteria (25 to 50%) (Dijkstra & Keck, 1996).
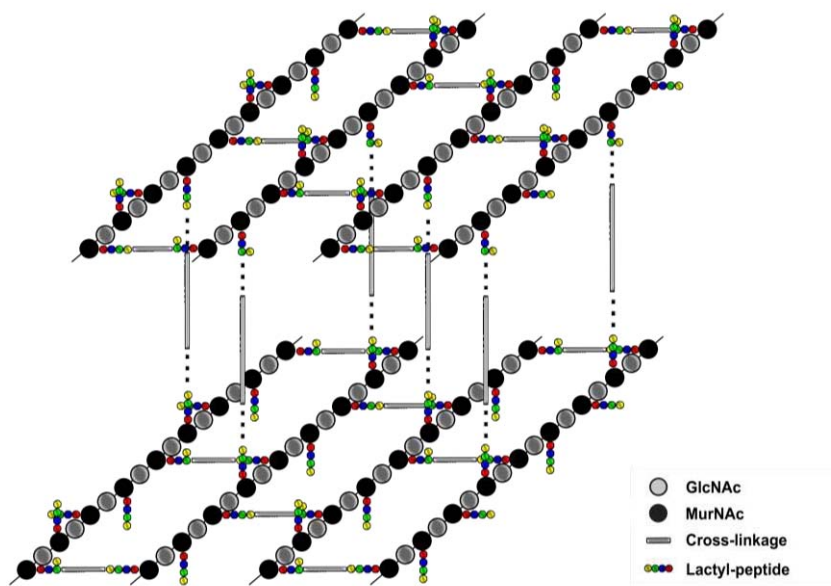
Figure 1.3: Structure of the peptidoglycan sacculus. The sketch was taken from Höltje (1998) and modified according to Fig. 1.2. It shows two peptidoglycan layers of a multilayered murein.

In accordance with models proposed by Ghuysen and McNeil (Ghuysen, 1968; McNeil & Brennan, 1991), the subsequent sketches that expand on the cell envelopes of Gram-positive, Gram-negative and mycolic acid-containing bacteria show peptidoglycan drawn in parallel to the cytoplasmic membrane. However, on basis of molecular modelling Dmititrev (Dmitriev *et al.*, 1999; Dmitriev *et al.*, 2000) suggested a different model in which the peptidoglycan strands are arranged as coils perpendicular to the cell surface. In his model the thicker murein sacculus of Gram-positive bacteria may be explained through the assumption of longer glycan strands. More research is needed to clarify the real structure and arrangement of this cell wall component of high importance.

1.2.4   The cell wall of Gram-positive bacteria

The cell walls of Gram-positive bacteria contain besides a distinct, 30 to 40 nm thick peptidoglycan layer mainly proteins and polysaccharides. With a few exceptions, they are poor in lipids and lack an outer membrane. The Gram-positive mycolata have an unusual cell envelope composition and architecture as described in section 1.2.6. A schematic overview of the structure and composition of the typical Gram-positive cell wall is provided in Fig. 1.4. These cell walls contain considerable amounts (10 to 60%) of mostly anionic polysaccharides that are either anchored to the peptidoglycan or the cytoplasmic membrane. Among the former are teichoic acids, teichuronic acids and anionic polysaccharides. Among the latter are lipoteichoic acids and lipoglycans. Because of their marked hydrophilic character, these polysaccharides allow a good suspension of the bacteria. However, the polymers possess a broad range of further features that indicate their importance for bacterial vitality. Besides their contribution in the supply of the bacteria with metal cations, the polysaccharides may also function as adhesion molecules that facilitate bacterial binding to various surfaces. Moreover, they represent potential antigenic structures that may be involved in phage binding and that may provide activities in immune modulation (Brock *et al.*, 2001; Seltmann & Holst, 2002; Ward, 1981).
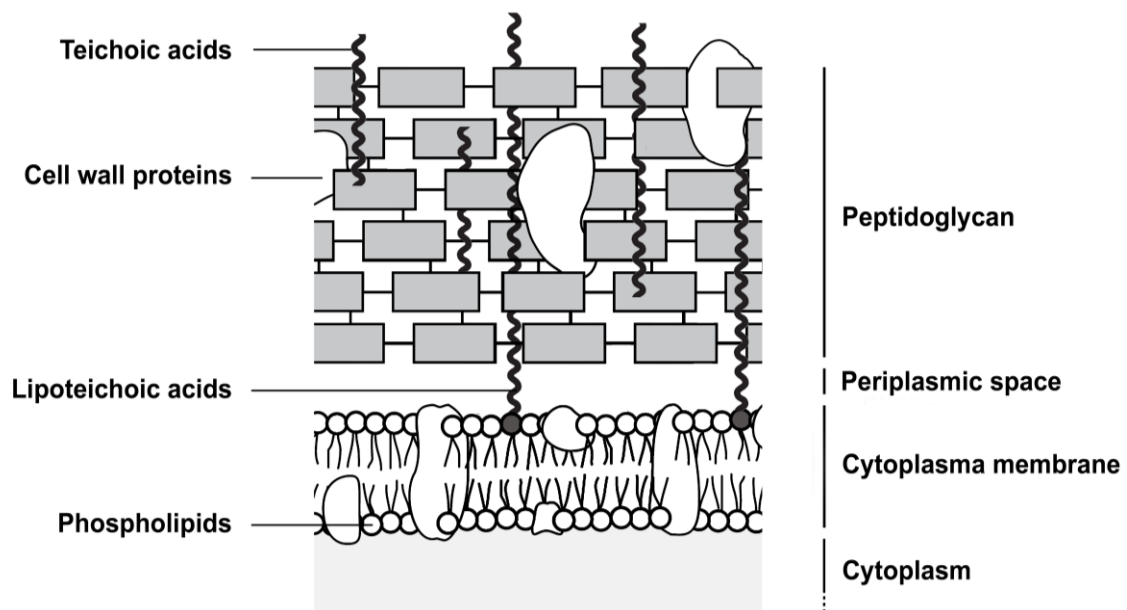
Figure 1.4: Sketch of the structure and the components of the Gram-positive cell envelope.

Both teichoic acids and the thick murein represent major and important parts of the Gram-positive cell wall. The structure of the latter constituent was described in section 1.2.3. The former cell wall polymers (i.e. teichoic acids) are built up from 16 to 40 repeating units of glycerol phosphate or ribitol phosphate that are linked via phosphodiester bonds. Rarely, mannitol or erythritol appears as polyol component. The polymers may further have additional sugar phosphates in the main chain as well as D-alanine, L-lysine, sugars or amino sugars which establish side chains (Brock *et al.*, 2001; Ward, 1981). The thereof resulting heterogeneity of teichoic acids may explain the various intrinsic properties of these cell wall elements. Their attachment to the murein sacculus occurs at O-6 of the *N*-acetylmuramic acid through a special linkage unit (Ward, 1981).

Under normal growth conditions, teichuronic acids unlike teichoic acids are marginally present in the Gram-positive cell wall. That is because former acids are primarily synthesized under phosphate starvation, while at the same time the synthesis of teichoic acids is reduced (Ward, 1981). The negative charged backbone of teichuronic acids is formed of complex repeating units containing uronic acid residues which take over the functions of the phosphate residues in teichoic acids.

The composition of lipoteichoic acids basically correspond to that of teichoic acids. But instead of being anchored to the cell wall skeleton, lipoteichoic acids possess a lipid part by means of which they are incorporated into the cytoplasmic membrane. Carrier molecules that fix lipoteichoic acids to this membrane are generally glycolipids bound by phosphodiester linkage (Brock *et al.*, 2001; Ward, 1981).

As apparent from Fig. 1.4, Gram-positive bacteria lack an outer membrane. To prevent the loss of cell wall proteins into the surrounding environment, the bacteria retain the proteins by covalently linking them to components of the cell envelope. Although teichoic acids and lipoteichoic acids are also a possibility, the peptidoglycan and the cytoplasmic membrane are the only cell wall elements that are seemingly used by Gram-positive bacteria for the anchoring of extracellular proteins. However, the site of attachment is not randomly chosen. A translocated polypeptide is covalently linked to peptidoglycan via its C-terminus, when it possesses a special C-terminal anchor signal (Navarre & Schneewind, 1999; Schneewind *et al.*, 1993). A hexapeptide (with the consensus sequence X-Leu-Pro-X-Thr-Gly) is of

importance in this process of protein fixation, because it contains the site for protease cleavage. In contrast, proteins containing at their N-termini the consensus sequence Leu-X-Y-Cys (X, Y are neutral amino acids) may be linked to lipids of the cytoplasmic membrane via their N-termini (Gilson *et al.*, 1988; Sutcliffe & Russell, 1995). For this purpose, a signal peptidase cleaves off the first three amino acids of the tetrapeptide and a diglyceride unit is added to the terminal cysteine. Thus the secreted polypeptide is fixed in the inner membrane.

1.2.5   The cell wall of Gram-negative bacteria

The electron micrographs of cell cross-sections of *E. coli* and *M. smegmatis* in Fig. 1.1 clearly show an electron-dense layer beyond the peptidoglycan, representing the outer membrane (OM) of these bacteria. The figure also contains a cross-section of *S. gordonii* which does not have an OM, as is commonly the case for Gram-positive bacteria. This indicates that the cell walls of Gram-negative bacteria and mycolata differ from those of Gram-positive bacteria in having an additional cell wall component. Though the cell envelopes of *E. coli* and *M. smegmatis* look similar to each other in the electron micrographs, they are not identical, because cell walls of Gram-negative bacteria and mycolata exhibit significant structural and compositional differences. Nevertheless, the OMs of both bacterial groups represent an effective penetration barrier (Benz, 1994; Jarlier & Nikaido, 1990; Nikaido, 2003).

Figure 1.5 provides a schematic overview of the architecture of the cell envelope of Gram-negative bacteria. Within the periplasm the rigid peptidoglycan layer constitutes a rather thin skeleton (1 to 3 layers), as compared to Gram-positive species (Holtje, 1998). Electron micrographs of Gram-negative bacteria evidence that the OM possesses the typical trilaminar structure of the cytoplasmic membrane (Matias *et al.*, 2003). Despite this similarity, it is clear that the former has a different composition and a higher mechanical stability than the latter. The OM of Gram-negative bacteria is composed of about 35% proteins, 40% lipopolysaccharides (LPS) and 25% phospholipids, where the latter mainly consists of phosphatidylethanolamine (75%), in addition to phosphatidylglycerol (20%) and cardiolipin (5%) (Seltmann & Holst, 2002). LPS and Braun`s lipoprotein are cell wall components specific for Gram-negative bacteria and both make significant contributions to the assembly and maintenance of the OM. LPS are restricted to the outer leaflet of the OM. There, the glycolipids are important for the function of most OM proteins and contribute decisively to

the permeability properties of the OM. However, LPS is also a potential pathogenic factor of Gram-negative bacteria (endotoxin), which might cause an intense systemic inflammatory reaction (Brock *et al.*, 2001).
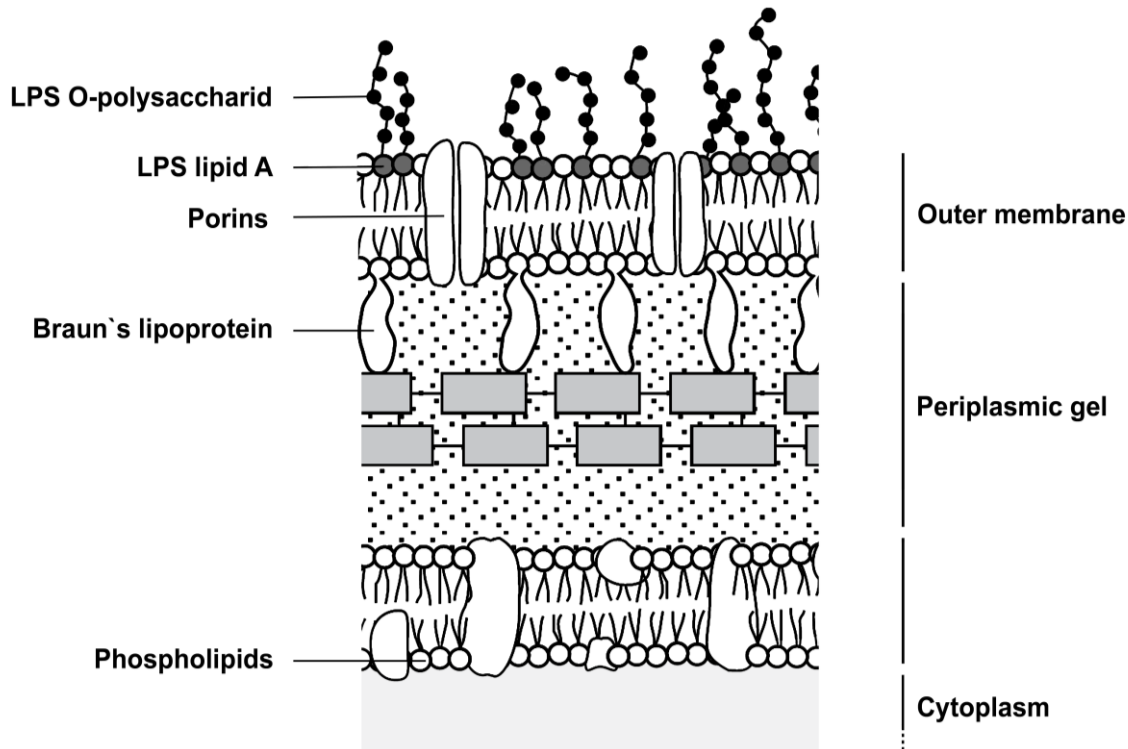
Figure 1.5: Sketch of the structure of the Gram-negative cell envelope.

The Braun lipoprotein, the molecular mass of which is about 7.2 kDa, is localized in the periplasm and connects the middle and outermost layers of the Gram-negative cell envelope with each other. Braun and Rehn (1969) were the first to report on this linking function which is of importance for the maintenance of the cell envelope integrity. The covalent linkage of the protein to murein takes place between the ε-amino group of the C-terminal lysine and the carboxyl group of approximately every 10th meso-diaminopimilic acid. In addition, the N-terminal cysteine of the polypeptide is coupled via a thioether linkage to glycerol carrying three fatty acids (two ester- and one amide-linked) that are usually the same as for the phospholipids. In this way, the N-terminus of Braun`s lipoprotein is anchored to the inner leaflet of the OM and thereby the protein fixes the outermost lipid layer to the cell wall skeleton.

LPS have like the Braun lipoprotein an amphiphilic structure, but these molecules are entirely localized on the exterior of the OM, anchored there through the lipid A moiety. In most (but not all) Gram-negative bacteria the lipid component is responsible for the endotoxic properties of LPS, whereas the immunogenic ones are determined by a hydrophilic polysaccharide part (Brock *et al.*, 2001; Caroff & Karibian, 2003). The latter, amounting to up to 90% of the LPS molecule, consists of a long-chained polysaccharide that can be subdivided into a large, highly variable domain (the O-specific region) and a small, less variable domain (the core region). The O-specific region is composed of 20 to 40 repeating units, with each unit being comprised of 2 to 8 monosaccharides. In contrast, the core region only contains about 15 monosaccharides (Caroff & Karibian, 2003; Seltmann & Holst, 2002). Considering the large variety of different kinds of monosaccharides (around 60) that have been found in the polysaccharide domain of LPS, it becomes apparent that this domain represents a highly variable region of LPS. Further structural diversity of LPS may occur in the O-specific region, e.g., through phosphorylation, acetylation and acylation. In contrast to this, the structure of the lipid A moiety is relatively invariable. In enterobacteria, the lipid A molecules consist of a D-glycosaminyl-(β1$\rightarrow$6)-D-glucosamine disaccharide that is substituted in positions 2, 3, 2' and 3' with long-chained, 3-hydroxylated fatty acids and carries in positions 1 and 4' phosphates (Caroff & Karibian, 2003). The chain length of the fatty acids corresponds to the thickness of a membrane monolayer. Two of the bound fatty acids are usually further acylated at their 3-hydroxyl group. The pattern of lipid A acylation varies depending on the type of bacteria. As the fatty acids tightly pack against each other, this results in a decrease of the mobility of the chains and the fluidity of the lipid interior (Cullis & Hope, 1985). For this reason, and because of the special surface structure of the OM, the permeability for hydrophobic substances through the OM is poor. It is only about 1 to 2% of that of typical glycerophospholipid bilayers (Plesiat & Nikaido, 1992; Vaara *et al.*, 1990). This fact contributes to the high resistance of Gram-negative bacteria towards hydrophobic antibiotics, bile salts and detergents and, moreover, protects the cells from the activity of proteases, lipases and lysozyme (Nikaido, 2003; Plesiat & Nikaido, 1992; Vaara *et al.*, 1990).

In order to ensure nutrient supply, Gram-negative bacteria contain channel-forming proteins (porins) in their OMs, which permit hydrophilic solutes to enter (Fig. 1.5). The uptake of solutes through the membrane may either occur via general diffusion pores or specific pores, but it is usually limited to molecules smaller than 600 daltons (Benz, 1988). Among the

former are, e.g., the preferentially cation-selective pores OmpC, OmpF and the anion-selective PhoE channel of *E. coli* (Benz, 1988; Nikaido & Rosenberg, 1983). Among the latter are, e.g., the nucleoside-specific channel Tsx, the maltooligosaccharide-specific LamB-channel (maltoporin) and the sucrose-specific ScrY-channel (sucroseporin) of enteric bacteria (Benz *et al.*, 1988; Schmid *et al.*, 1991; Szmelcman & Hofnung, 1975). Besides the mentioned porins, there exists a considerable number of porins that have been identified in various Gram-negative bacteria. The cell wall channels usually appear in the OM as a trimer consisting of three identical subunits ranging in molecular mass from 30 to 50 kDa. This means that cell wall channels of Gram-negative bacteria actually consist of three individual channels. There are only a few exceptions from this rule, such as the *E. coli* OmpA protein which forms only a monomer (Schulz, 2004). The common structure of the monomer is a β-barrel cylinder, which is mostly formed by 16 or 18 antiparallel β-strands that are connected through short periplasmic and long extracellular loops (Schulz, 2004). The function of the extracellular L3 loop is noteworthy in that it narrows the passage through the channel by folding into the lumen of the channel. As a consequence, the free cross-section of channels of Gram-negative bacteria is usually constricted to an opening of around 1 nm (Schulz, 2004).

1.2.6   The cell wall of mycolic acid containing bacteria

Members of the suborder *Corynebacterineae* of the order *Actinomycetales* within the class *Actinobacteria*, as defined by Stackebrandt *et al.* (1997), form a noticeable exception to the rule that Gram-positive bacteria have cell walls of high permeability (Lambert, 2002). Despite their allocation to the separate families of *Corynebacteriaceae*, *Dietziaceae*, *Gordonaceae*, *Mycobacteriaceae*, *Nocardiaceae* and *Tsukamurellaceae*, members of this suborder possess similar cell envelopes which differ in their chemical and structural composition from those of the remainder of the bacteria. Apart from peptidoglycan, the ubiquitous bacterial cell wall component, the cell walls of *Corynebacterineae* contain large amounts of unusual lipids and lipopolysaccharides (not to be confused with LPS) (Barksdale, 1981; Goodfellow *et al.*, 1976; Ochi, 1995). Major constituents of the lipids are mycolic acids, α-alkyl β-hydroxy fatty acids, which are unique to members of the above mentioned families and which is why these bacteria are called mycolata.

Most research on the cell envelope of *Corynebacterineae* has been focused on different *Mycobacterium* species (Brennan & Nikaido, 1995; Chatterjee, 1997; Lee *et al.*, 1996), because of the medical importance of some of these bacteria such as *M. tuberculosis*, the causative agent of tuberculosis. However, other members of the *Corynebacterineae* have also been investigated (Puech *et al.*, 2001; Sutcliffe, 1998). Although there are some apparent differences in the molecular structure of some cell wall components, especially in the mycolic acids, it can be assumed that bacteria belonging to the *Corynebacterineae* group have similar cell wall compositions. A schematic overview of the structure and composition of the cell envelope of members of the *Corynebacterineae* is given in Fig. 1.6. As apparent in this figure, the mycolyl-arabinogalactan-peptidoglycan (MAP) complex makes up the largest part of the cell wall of species of the mycolata. The arabinogalactan moiety is covalently attached to the peptidoglycan and the mycolic acids, so it represents the connecting part between both latter cell wall elements. Free lipids, in the main trehalose mono-and dimycolates, complete the inner leaflet of cell wall fixed mycolic acids to an asymmetric bilayer. Thereby, the mycolic acid chains which are unequal in length allow free lipids to intercalate.
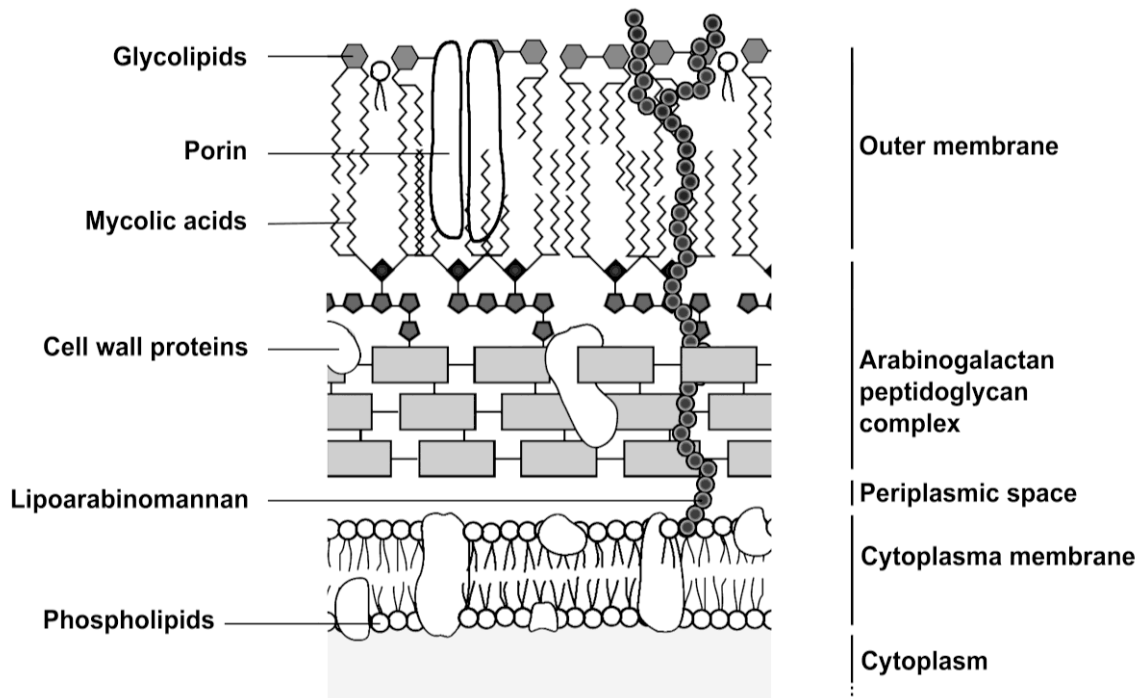
Figure 1.6: Sketch of the structure of the cell envelope of mycolic acid containing bacteria

The model is based on a model proposed by Minnikin (1982) for the structure of the mycobacterial cell wall. He suggested that the chains of the mycolic acids are packed side by side in a direction perpendicular to the cell surface. He also suggested that the thereby formed inner monolayer of mycolic acids is covered by an outer monolayer composed of extractable lipids. As a result, the whole structure would form an asymmetric lipid bilayer. From X-ray diffraction of the cell wall of *Mycobacterium chelonae*, Nikaido and coworkers (1993) presented substantial evidence for the existence of such a structure. In all other current cell wall models (Liu *et al.*, 1995; Rastogi, 1991; Sutcliffe, 1998), the outer permeability barrier of mycolata consists of a monolayer of mycolyl residues linked to the arabinogalactan-peptidoglycan complex and lipids arranged in a fashion allowing them to establish a bilayer with the mycolyl residues. This molecular arrangement is responsible for the permeability properties of cell walls of mycolata species whose cell walls are less permeable than those of Gram-positive and even Gram-negative bacteria. This was shown by Jarlier and Nikaido (1990) for *M. chelonae*. The cell wall of this bacterium is 100 to 1000 fold less permeable to hydrophilic substances than that of *E. coli*. It is easily conceivable that the intrinsic antimicrobial resistance of pathogenic representatives of the *Corynebacterineae*, such as *M. tuberculosis* and *Mycobacterium leprae*, is primarily related to their special cell wall structure (Fig. 1.6). In this context, it is noteworthy that the cell wall of mycolata contains unusual lipopolysaccharides (lipoarabinomannans) which may possess immunomodulatory properties. The lipoarabinomannans may also contribute to pathogenesis by abolishing T-cell activation or inhibiting macrophage activity (Hunter *et al.*, 1986; Kaplan *et al.*, 1987).

As with Gram-negative bacteria, the outermost membrane in mycolata is a permeability barrier defined by channel-forming proteins which enable the exchange of nutrients and waste products with the environment (Mailaender *et al.*, 2004; Stahl *et al.*, 2001; Wolschendorf *et al.*, 2007). To date, the best characterized and analysed outer membrane protein of mycolic acid bacteria is MspA of *Mycobacterium smegmatis* (Niederweis *et al.*, 1999). MspA as well as OmpATb of *M. tuberculosis* (Senaratne *et al.*, 1998) are porins suggested to be involved in drug efficiency. Although the pathway of tuberculosis drugs is not clearly known, there are indications that three of the four first-line tuberculosis drugs (namely isoniazide, ethambutol and pyrazinamide) presumably cross the mycolate membrane because of their small and hydrophilic attributes through channels (Lambert, 2002; Niederweis, 2003).

1.2.6.1   The arabinogalactan moiety

Studies over a period of 50 years have demonstrated that the arabinogalactan polymer is rather unusual as it is exclusively composed of the furanosidic forms of D-galactose and D-arabinose, two compounds that are rarely found in nature. The basic chain of the polymer consists of a linear poly-D-galactofuranose chain in which about 32 Gal*f* residues are coupled by alternating (β1→5) and (β1→6) linkages (Fig. 1.7) (Brennan & Nikaido, 1995; Crick *et al.*, 2001; Pathak *et al.*, 2007). Three poly-(α1→5)-D-arabinofuranose chains, each with about 27 Ara*f* units, are bound to O-5 of Gal*f* residues, but the exact branching pattern of the arabinan proximal to the galactan is unknown (Chatterjee, 1997). Partially, the polyarabinose chains carry Ara*f* residues which further branch from the O-3 position. The non-reducing polysaccharide ends are capped by a branched penta-arabinose motif that contains O-2 linked Ara*f* units. They, in turn carry the mycolic acids which form the inner leaflet of the asymmetric outer membrane of mycolata and represent the non-extractable lipids. The mycolyl-arabinogalactan molecule is linked to O-6 of some of the muramic acids of the peptidoglycan via the phosphate residue of the disaccharide structure α-L-Rha*p*-(1→3)-α-D-Glc*p*NAc-1-*P* (pyranosides rhamnose and *N*-acetyl-glucosamine) (Crick *et al.*, 2001; Pathak *et al.*, 2007).
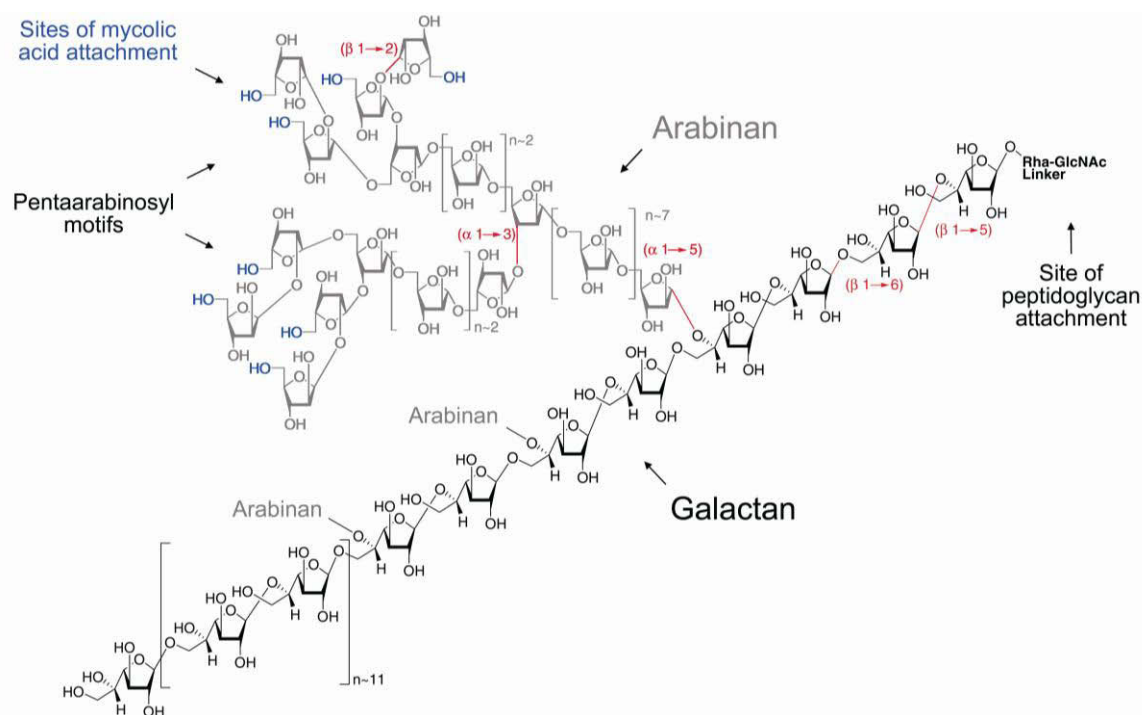
Figure 1.7: Structure of the mycolated arabinogalactan of *Mycobacterium tuberculosis* linked to peptidoglycan (taken from Pathak *et. al* (2007) and modified according to Crick and Brennan (2001).

1.2.6.2 The mycolic acid moiety

Mycolic acids are high-molecular fatty acids that are alkylated in the α-position (α-chain) and hydroxylated in the β-position (meromycolate chain) (Fig. 1.8A) (Brennan & Nikaido, 1995). They occur in the cell walls either free, loosely associated or bound to polysaccharides (in particular to pentaarabinofuranosyl clusters) and represent the main component of the cell walls of mycolata species (Chatterjee, 1997). The free mycolic acids are linked to trehalose (in form of trehalose dimycolate and trehalose monomycolate) and can be extracted from cells by organic solvents, such as chloroform/methanol. In contrast, the cell wall bound lipids need alkaline treatment for their isolation.

A)   B)
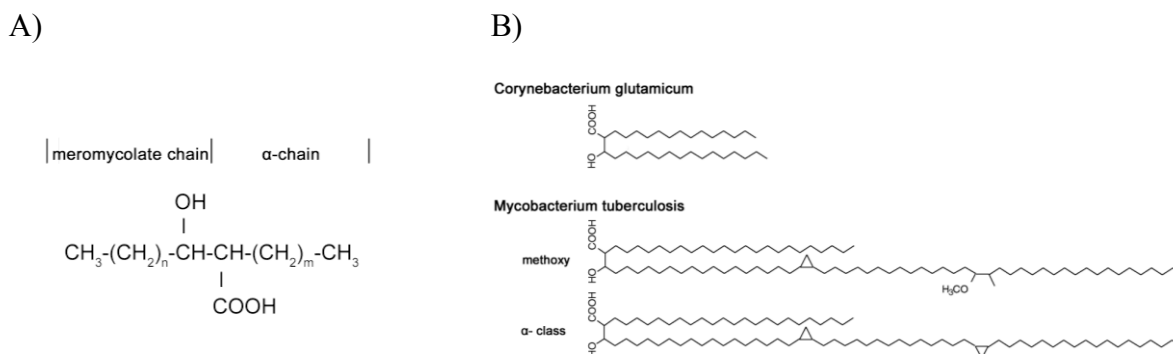
Figure 1.8: (A) The general structure of mycolic acids. (B) Structural variations between mycolic acids of the genera *Corynebacterium* and *Mycobacterium*. Two of three mycolic acid classes found in *Mycobacterium tuberculosis* are shown.

By using thin-layer chromatography to separate the mycolic acids from each other, they can serve as valuable taxonomic markers to distinguish between individual genera of mycolata and even between species within the genera (Barry *et al.*, 1998). As shown in Table 1.1, mycolic acids of mycobacteria count up to 90 carbon atoms, i.e. that species of this genus have the largest molecules among mycolata, whereas corynebacteria, with about 30 carbon atoms, have the smallest.

A further differentiation of mycolic acids is possible by comparing the chemical structures of split α- and β-chains. The cleavage of the mycolic acids into the meromycolate- and the α-branch is achieved by pyrolysis (Barry *et al.*, 1998). For instance, by mass spectrometry combined with NMR (nuclear magnetic resonance) spectroscopy, the chain length of fatty

acids as well as the position of double bonds can be determined. In contrast to the meromycolate chain, the α-branch represents a rather conservative part of mycolic acids.

Genus	Total number of C-atoms	Number of double bonds	C-atoms in the α-branch
Corynebacteria	22-38	0-2	14-18
Rhodococcus	34-48	0-4	12-18
Nocardia	44-60	0-3	12-18
Gordonia	48-66	1-4	16-18
Tsukamurella	64-78	1-6	20-22
Mycobacteria	60-90	2[#]	20-26

Table 1.1: Variations in the mycolic acid-size in dependence of the genus (Barry *et al.*, 1998). [#] Mycolates from *Mycobacterium tuberculosis* lack double bonds (Lee *et al.*, 1996).

Besides a small variation in the number of C-atoms, this chain is straight-chained, unbranched, unsubstituted and saturated. The larger meromycolate chain generally has the same properties as the α-branch, but it can contain *cis*- or *trans*-double bonds, cyclopropane and epoxy rings as well as methyl, methoxyl and oxo groups at various positions (Brennan & Nikaido, 1995). Although the substituents and the *cis*-double bonds induce kinks in the β-chain, they are located rather far from the carboxyl group of mycolic acids, which in principle allows the α- and β-branch to pack densely. According to the modifications in the carbon chains, mycolic acids are classified into α, α', epoxy, keto, methoxy and wax ester classes. Among the mycolata, the most complex structured mycolic acids are produced by mycobacteria; the simplest structures are found in corynebacteria (Fig. 1.8B).

1.2.6.3 Lipoarabinomannan

Besides the mycolyl arabinogalactan polymer, mycolata contain in their cell walls lipoarabinomannans (LAMs) of a likewise complex structure. Phosphatidylinositol mannosides (PIMs) and lipomannans (LMs) are also components of the mycolata cell wall. They are proposed precursors in the formation of LAMs (Tatituri *et al.*, 2007). Although the structure of LAM has not yet been completely elucidated, it is known to consist mainly of the sugars arabinose and mannose. In addition, it contains glycerol, inositol, phosphate as well as

palmitate, tuberculostearate and other fatty acids (Hunter *et al.*, 1986; Nigou *et al.*, 2003; Sutcliffe & Russell, 1995).
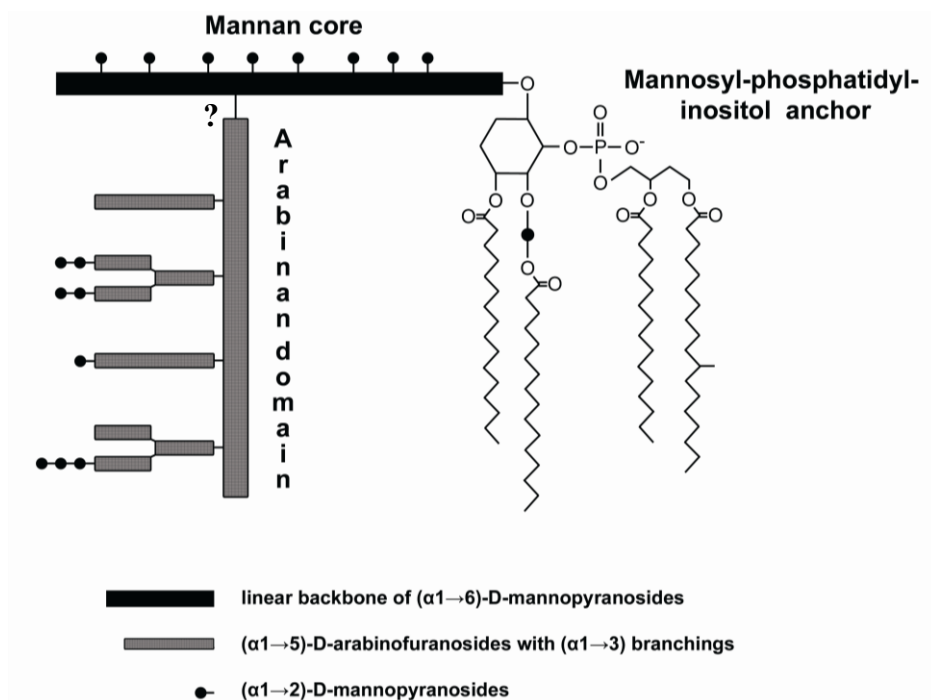
Figure 1.9: Scheme of the tripartite structure of the mycobacterial lipoarabinomannan.

The common structural element of PIMs, LMs and LAMs is an anchor molecule (MPI anchor) which presumably fixes these cell wall components into the cytoplasmic membrane (Hunter & Brennan, 1990). The MPI anchor consists of a *sn*-glycero-3-phospho-(1-D-*myo*-inositol) unit and a single D-mannopyranose (Man*p*) unit attached to the inositol via (α1→2) linkage. In mycobacteria, the most abundant fatty acids esterified with the glycerol part are palmitic acid and tuberculostearic acid. Besides these fatty acids, small amounts of stearic acid, myristic acid and other fatty acids are found (Nigou *et al.*, 2003). On average, three fatty acid residues are bound per LAM molecule, which means that acylations cannot occur only in position 1 and 2 of the glycerol unit. Indeed, more acylation sites are present in both the inositol unit and the Man*p* unit linked at O–2 of inositol (Fig. 1.9) (Brennan & Nikaido, 1995; Nigou *et al.*, 2003). The linkage of the polysaccharide moiety of LAM to the MPI anchor occurs at O-6 of the inositol residue via the mannan chain.

The polysaccharide moiety of LAM is composed of two homopolysaccharides, mannan and arabinan. Both polymers are linked to each other but the site of attachment is unknown. The

mannan domain consists of a poly-(α1→6)-D-mannopyranosyl (Man*p*) chain that branches at O-2 to varying degrees with single Man*p* residues. The size as well as the branching degree of the mannan chain can vary depending on the species. For instance, the branching degree in *M. tuberculosis* is around 70% compared with about 50% in *M. smegmatis* (Nigou *et al.*, 2003). The arabinan polymer consists of a linear backbone of (α1→5) linked D-arabinofuranosyl (Ara*f*) units, partially substituted by Ara*f* residues which branch at O-5 and O-3. However, the exact branching site(s) within the arabinan are also not known. The non-reducing ends of the arabinan may be capped, e.g., by mannosyl, (α1→2) dimannosyl and (α1→2) trimannosyl units (Nigou *et al.*, 2003) (Fig. 1.9).

1.2.6.4   Extractable lipids

Among the free or extractable lipids that cover the arabinogalactan bound mycolic acids are lipooligosaccharides (LOS), phenolic glycolipids (PGL), glycopeptidolipids (GPL), sulpholipids (SL), phthiocerol dimycoserate as well as small amounts of phospholipids (Brennan & Nikaido, 1995; Puech *et al.*, 2001). In the sections below, the focus is on the structure of LOS because the highest proportion of extractable lipids belongs to this class. Nevertheless, SL are also shortly addressed because they share a similar structure.

The common structural element in LOS and SL is a polyacylated trehalose unit (Fig. 1.10). In LOS, this unit usually contains two to four straight-chained or methyl-branched fatty chains that are not necessarily distributed equally to the α-D-glucopyranosyl-**(**1→1)-α-D-glucopyranose disaccharide (Fig. 1.10A) (Besra *et al.*, 1992; Brennan & Nikaido, 1995). The trehalose carrier of LOS may further be substituted at O-3, O-4 or O-6 by an oligosaccharide consisting of a tetraglucose unit that contains specific carbohydrates, such as xylose, fucose or *N*-acylkanosamine (Fig. 1.10B) (Brennan & Nikaido, 1995). It is noteworthy that there are also reports on more heavily acylated glycolipids. For instance in *Mycobacterium phlei*, lipids were found in which each hydroxyl-group of the trehalose unit is substituted by an unusual fatty acid (Asselineau *et al.*, 1972).

Besides the mentioned glycolipids, the cell walls of mycolata contain large amounts of trehalose monomycolates and dimycolates. These extractable lipids are also among the LOS and represent the most frequent ones in the outer mycolate membrane (Fig. 1.10C). They are

likely involved in the transfer of mycolic acids to the arabinogalactan-peptidoglycan complex (Belisle *et al.*, 1997; Gebhardt *et al.*, 2007; Tropis *et al.*, 2005). A prominent toxic component in the cell envelopes of pathogenic *Mycobacteria* and *Nocardia* species that shows a variety of biological activities is the cord factor (Spargo *et al.*, 1991). Its chemical structure, revealed in 1956 by Noll *et al.*, shows a 6,6'-diester of species specific mycolic acids with trehalose (see Table 1.1). Thus, the cord factor, the name of which is derived from the cord-forming growth of virulent tubercle bacilli, belongs to the trehalose dimycolates.
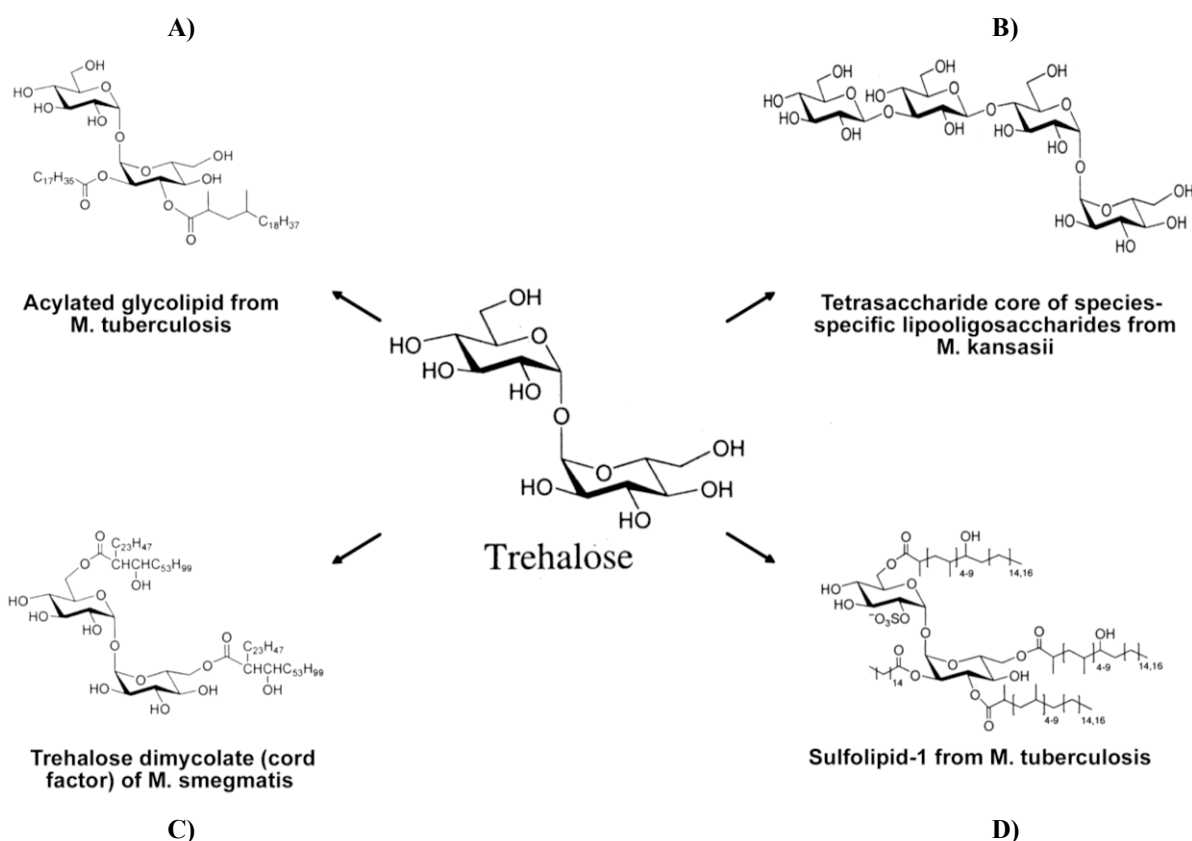
Figure 1.10: Overview of trehalose-based lipids which comprise acylated, glycosylated and mycolated trehalose lipids as well as sulfolipids.

In comparing Fig. 1.10D with Fig. 1.10A and C, it becomes apparent that there is a difference, though a minor one, between the core units of SL and LOS. SL differ from LOS in having a glucose residue in the acylated trehalose unit that is esterified at O-2 with sulphuric acid (Brennan & Nikaido, 1995; Leigh & Bertozzi, 2008). In comparison with the cord factor, the trehalose core of SL carries three to four acyl chains on various positions; often palmitate or stearate at O-2', phthioceranate at O-3' and hydroxyphthioceranat at O-6,6' (Leigh & Bertozzi, 2008). So far, these lipids have exclusively been found in virulent strains of *M. tuberculosis*. Therefore they are suggested to support the intracellular survival of this pathogen.

1.2.6.5   Porins penetrate the mycolic acid layer

Similar to the situation in Gram-negative bacteria, the outer membrane of mycolata builds a permeability barrier that contributes to the protection of included species to noxious compounds (Benz, 1994; Jarlier & Nikaido, 1990; Nikaido, 2003). However, in terms of nutrient supply and waste product deposition, both groups of bacteria make use of specialized pore-forming proteins to facilitate the passage of small hydrophilic molecules across their outer membranes.

To date, the envelopes of five species of mycobacteria are known to contain cell wall channels. This includes those of *M. chelonae*, *M. phlei* and *M. smegmatis* belonging to the fast-growing group of mycobacteria, and those of *M. tuberculosis* and *M. bovis* BCG representing slow growers with generation times of more than 5 hours (Kartmann *et al.*, 1999; Lichtinger *et al.*, 1999; Riess *et al.*, 2001; Senaratne *et al.*, 1998; Trias *et al.*, 1992; Trias & Benz, 1994). However, the MspA channel of *M. smegmatis* is by far the best-characterized cell wall pore. This resulted rather from cloning of the *mspA* gene (Niederweis *et al.*, 1999) which allowed producing the 20 kDa channel-forming protein in yields sufficient for crystallization than from established biophysical channel properties. In case of the MspA channel, these show a cation-selective and voltage-dependent pore with an ion-conductance of 4.6 nS in 1 M KCl (Niederweis, 2003; Trias & Benz, 1994). The 3D-structure of the MspA channel presented in Faller *et al.* (2004) exhibits no structural similarities to porins of Gram-negative bacteria. There, cell wall pores usually are trimers with one channel per monomer. In contrast to this, X-ray diffraction revealed the mycobacterial MspA porin as an octamer with eightfold rotational symmetry that resembles a goblet-like structure with a central channel (Fig. 1.11) (Faller *et al.*, 2004). In this goblet, each MspA monomer contributes 134 amino acid residues to the thick rim domain at the top and 50 amino acid residues to two 16-stranded, consecutive β-barrels at the bottom. The overall dimensions of the MspA channel are 9.6 nm (length) and 8.8 nm (maximum outer diameter) whereas the inner channel diameter varies between 4.8 and 1.0 nm at the pore eyelet.

Apart from *mspA*, the genome of *M. smegmatis* possesses three homologous genes named *mspB*, *mspC* and *mspD*, coding for very similar proteins as compared to MspA. In fact, these proteins differ only in 2, 4 and 18 positions, respectively, from MspA (Stahl *et al.*, 2001; Stephan *et al.*, 2005). As knockout experiments demonstrated, MspA provides the main

diffusion pathway for the bacterium. By deleting the *mspA* gene, the permeability of the *M. smegmatis* cell wall is reduced around ninefold for cephaloridine and fourfold for glucose in comparison to the wild-type (Stahl *et al.*, 2001).

Figure 1.11: Structure of the octameric MspA channel from *M. smegmatis*. The goblet-like porin consists of a thick rim-domain at the top, a stem and a base containing two consecutive β-barrels at the bottom. Each colour corresponds to one subunit (created with WebLab viewer).

Not long ago, the cell walls of *M. phlei* and *Tsukamurella inchonensis* were evidenced to contain channels with biophysical properties similar to those of the MspA channel (Dörner *et al.*, 2004; Riess *et al.*, 2001). Interestingly, the genomes of both strains harbour genes that are identical to *mspA* of *M. smegmatis*, which means that *mpp*A of *M. phlei* and *tip*A of *T. inchonensis* represent presumably the corresponding channel-coding genes for these species (Dörner *et al.*, 2004). A further interesting observation was made by Riess *et al.* (2001) who noticed under low stringency conditions hybridization of a *mspA* derived probe with genomic DNA of *Nocardia farcinica* and *Rhodococcus equi* indicating that MspA-like porins could also appear in the genera *Nocardia* and *Rhodococcus*. However, this would be an astonishing finding because the *mspA* gene itself is seemingly not even present in all species of mycobacteria. In fact, it has yet only been found with members of the fast-growing group (Niederweis *et al.*, 1999). The impaired growth of *M. tuberculosis*, *M. bovis* BCG and affiliated slow-growers could therefore be the result of a less permeable cell wall in comparison with their fast-growing relatives. This hypothesis is fostered by a twofold faster glucose uptake and an accelerated growth of *M. bovis* BCG as a result of MspA expression (Mailaender *et al.*, 2004; Niederweis *et al.*, 1999). Nevertheless, it is hardly conceivable that the different growth rates of mycobacteria are solely determined by the presence or absence of

a special kind of porin (i.e. MspA). In addition, it was demonstrated that also the slow growing species *M. tuberculosis* and *M. bovis* BCG contain channel-forming proteins in their cell walls (Kartmann *et al.*, 1999; Lichtinger *et al.*, 1999). These proteins, which were extracted from whole cells by use of detergent and organic solvent, caused channels with a conductance of about 0.7 to 4 nS in artificial lipid membranes. Unfortunately, the amount of protein was too low to allow purification and identification of the channel-forming proteins.

An alternative method to identify channel-forming proteins in mycobacteria was used by Senaratne *et al.* (1998) who searched the *M. tuberculosis* genome for sequences homologous to those of porins of Gram-negative bacteria. This approach resulted in the report of the *M. tuberculosis* porin OmpATb (38 kDa), which shows significant homology to OmpA proteins of Gram-negative bacteria. However, there is still a debate if OmpA-like proteins form channels. This is because the crystal structure of OmpA of *E. coli* does not show an open water-filled pore as is the case for the true porins, such as OmpF and PhoE. On the other hand, the recombinant expressed mycobacterial homologue was shown to cause 0.7 to 3.5 nS channels in lipid bilayer experiments with a diameter of 1.4 to 1.8 nm (Niederweis, 2003; Senaratne *et al.*, 1998). Thus, further work is required to elucidate this contradiction.

Though this section focused mainly on mycobacterial porins, it has to be noted that porins also determine the cell wall permeability for members of the genera *Corynebacteria*, *Nocardia* and *Rhodococcus* (Lichtinger *et al.*, 2000; Riess *et al.*, 1998; Riess *et al.*, 1999; Riess & Benz, 2000; Riess *et al.*, 2003). However, in most of these cases a deeper insight into the channel structure is hampered because of insufficient biochemical data. Cell wall channels of *C. glutamicum* and *C. efficiens* represent the only exceptions as the genes were identified that encode the responsible channel-forming proteins. These proteins, named PorH, PorA and PorB, have molecular masses of only 5 to 10 kDa but cause cell wall pores with 0.7 to 5.5 nS ion-conductance (Costa-Riu *et al.*, 2003b; Hünten *et al.*, 2005b; Lichtinger *et al.*, 1998). Further, neither of them shows homology to the mycobacterial MspA protein or any other channel-forming protein known to date. Thus, it is assumed that the architecture of corynebacterial porins could completely differ from those of established porins.

1.3   Aims of the work

Despite the extensive research on the components and the structure of cell envelopes of mycolata species, the knowledge about pore-forming proteins embedded in their outer mycolate membranes is still low. Meanwhile, it is widely accepted that the outer membrane of mycobacteria represents a permeability barrier to the free passage of hydrophilic solutes and that some members of this genus possess cell wall channels that facilitate the uptake and release of nutrients. However, considering the similar cell wall architecture of mycolata, it can be hypothesised that all members of this taxon presumably possess cell wall pores. This assumption gets support from reports on channels in species of the genera *Corynebacteria*, *Nocardia*, *Rhodococcus* and *Tsukamurella*, all of whom are counted among the mycolic acid-containing Gram-positive actinomycetes. However, in only a few studies have researchers achieved to identify the gene coding for the channel-forming protein. Nowadays, most of them are homologues of the MspA protein of *M. smegmatis*. On the other hand, in the closely related *Corynebacterium* species *C. glutamicum* and *C. efficiens*, *porA* and *porH* genes encode small polypeptides that clearly differ from the MspA protein. In these corynebacteria, PorA and PorH proteins assemble large, water-filled cell wall pores. Therefore, one aim of this thesis was to extend our knowledge about these known corynebacterial channels. We also aimed to obtain a more general view of the distribution of porins within the genus *Corynebacterium* by extending the search for cell wall channels to pathogenic representatives, the avirulent *C. diphtheriae* strain ATCC 11913 and the *C. jeikeium* strain K411.

Chapter 2

Corynebacterium diphtheriae: Identification and characterization of a channel-forming protein in the cell wall

2.1 Summary

The cell wall of the Gram-positive, non-toxic *Corynebacterium diphtheriae* strain C8r(-) Tox[-] (ATCC 11913) contained a channel-forming protein, as judged from reconstitution experiments with artificial lipid membranes. The channel-forming protein was present in detergent-treated cell walls and organic solvent extracts of whole cells. According to Tricine-containing SDS-PAGE, the protein had an apparent molecular mass of about 66 kDa and consisted of subunits with a molecular mass of about 5 kDa. Single-channel experiments with the purified protein revealed that it forms channels with a single-channel conductance of 2.25 nS in 1 M KCl. Further single-channel analysis indicated that the cell wall channel is wide and water-filled because it has an only slight selectivity for cations over anions and its conductance followed the mobility sequence of cations and anions in the aqueous phase. Antibodies raised against CgPorA, the subunit of the *Corynebacterium glutamicum* cell wall channel, detected both monomers and oligomers of the isolated protein. This suggests that there are highly conserved epitopes in the cell wall channel of *C. diphtheriae* and CdPorA of *C. glutamicum*. Localization of the protein on the cell surface was confirmed by an enzyme-linked immunosorbent assay. The prospective homology of CgPorA with the cell wall channel of *C. diphtheriae* was used to identify the cell wall channel gene, *cdporA,* within the known genome of *C. diphtheriae*. The gene and flanking regions were cloned and sequenced. Its protein, CdPorA, is 43 amino acids in size and does not contain a leader sequence. c*dporA* was expressed in a *C. glutamicum* strain that lacked the major outer membrane channels CgPorA and CgPorH. Organic solvent extracts of the transformed cells formed in lipid bilayer membranes the same channels as the purified CdPorA protein of *C. diphtheriae* formed. This suggests that the expressed protein is able to complement CgPorA and CgPorH deficiency of the *C. glutamicum* strain. The study is the first report of a cell wall channel in a pathogenic *Corynebacterium* species.

2.2 Introduction

The suborder *Corynebacterineae* belongs to a distinctive suprageneric actinomycete taxon, the mycolata, which also includes *Mycobacteria*, *Nocardia*, *Rhodococci* and closely related genera. These bacteria share with corynebacteria the property of having an unusual cell envelope composition and architecture (Daffe & Draper, 1998). They have a thick peptidoglycan layer, which is covered by lipids in form of mycolic acids and other lipids (Barksdale, 1981; Goodfellow *et al.*, 1976; Ochi, 1995). The mycolic acids are covalently linked through ester bonds to the arabinogalactan which is attached to the murein of the cell wall (Minnikin, 1987). The chain lengths of these 2-branched, 3-hydroxylated fatty acids vary considerably within the mycolic acid-containing taxa (Brennan & Nikaido, 1995; Holt *et al.*, 1994; Minnikin *et al.*, 1974). In mycobacteria mycolic acids are long, but in corynebacteria mycolic acids are short (Daffe *et al.*, 1990; Yano & Saito, 1972). Despite this difference, the cell walls of corynebacteria and closely related genera are very similar to that of mycobacteria, especially in terms of ultrastructure and cell wall chemical composition (Barksdale, 1970; Marienfeld *et al.*, 1997; Sutcliffe, 1997). This means that in members of the mycolata the cell wall builds a permeability barrier comparable with the outer membrane of Gram-negative bacteria (Jarlier & Nikaido, 1990; Nikaido & Jarlier, 1991; Nikaido *et al.*, 1993; Nikaido, 2003). There, channel-forming proteins, the so-called porins, are responsible for the passage of hydrophilic solutes (Benz, 1994; Benz, 2003; Nikaido, 1992). Analogous to the situation in the outer membrane of Gram-negative bacteria, channels for the passage of hydrophilic compounds are present in the mycolate layer of the mycobacterial cell wall (Trias *et al.*, 1992; Trias & Benz, 1993) and the cell wall of *Corynebacterium glutamicum* (Costa-Riu *et al.*, 2003a; Costa-Riu *et al.*, 2003b; Hünten *et al.*, 2005a; Lichtinger *et al.*, 2001). In recent years, the assumption that the mycolic acids represent a permeability barrier on the surface of members of the mycolata has been confirmed by the investigation of porins in different members of the *Corynebacterineae*, such as in *Mycobacterium bovis* (Lichtinger *et al.*, 1999), *Rhodococcus erythropolis* (Lichtinger *et al.*, 2000), *Nocardia corynebacteroides* (Riess & Benz, 2000), *Nocardia farcinica* (Riess *et al.*, 1998) and *Mycobacterium phlei* (Riess *et al.*, 2001).

The genus *Corynebacterium* is of considerable interest because some of its members, such as *C. glutamicum* and *Corynebacterium callunae* are potent producers of glutamate, lysine and other amino acids through fermentation processes on an industrial scale (Eggeling & Sahm,

1999; Keilhauer *et al.*, 1993; Leuchtenberger, 1996; Sahm *et al.*, 1996). Otherwise, this genus also contains a few pathogens. The main pathogen, *Corynebacterium diphtheriae* (MacGregor, 1995), is well known as the cause of diphtheria, which is an acute, communicable respiratory disease. Other pathogens are *Corynebacterium urealyticum* and *Corynebacterium jeikeium* (Oteo *et al.*, 2001). Diphtheria disease is caused by exotoxin-producing *C. diphtheriae* cells that infect the throat or nose and sometimes the eyes or skin, inducing the formation of an inflammatory pseudomembrane. The exceedingly potent toxin is absorbed into the circulation and damages remote organs, potentially resulting in death (Dixon *et al.*, 1990; Holmes, 2000). In 1990 a re-emergence of the pathogen was observed by the World Health Organization (WHO), which led to a worldwide launch of immunization programs. A total of 1214 declared diphtheria cases unleashed at that time an epidemic which spread through Russia, Ukraine and neighbouring countries and even reached a few subjects in Europe and North America (Bonnet & Begg, 1999; Bricaire, 1996). Especially disturbing is the fact that non-toxigenic *C. diphtheriae* strains are associated with invasive diseases (Harnisch *et al.*, 1989) and non-toxigenic strains can change to toxigenic strains by lysogenic conversion (Anderson & Penfold, 1973; Pappenheimer & Murphy, 1983). Furthermore, the epidemiological pattern of the disease has changed (Galazka & Robertson, 1995; Prospero *et al.*, 1997). The current situation clearly demonstrates that the risk of a diphtheria epidemic still exists, even in Western countries. These results emphasize the importance of further studies of this microorganism in order to understand the metabolic pathways and to find new mechanisms of prevention and treatment.

In this study, we extended the search for cell wall channels to the *C. diphtheriae* strain C8r(-) Tox$^-$ (ATCC 11913) that is another member of the genus *Corynebacterium*. It is known that the cell wall of this strain contains a channel-forming protein but it has not been investigated in detail (Puech *et al.*, 2001). Using lipid bilayer experiments, we could demonstrate that the extracts of cell walls and whole *C. diphtheriae* cells contain a protein that forms wide and water-filled channels similar to the porins found in Gram-negative bacteria (Benz, 1994; Benz, 2003). The gene encoding the channel-forming protein, named CdPorA, was identified within the accessible genome of *C. diphtheriae* NCTC 13129 (Cerdeno-Tarraga *et al.*, 2003) by using the homology of CdPorA to CgPorA of *C. glutamicum*. CdPorA was expressed in a CgPorH/CgPorA-deficient strain of *C. glutamicum* (Hünten *et al.*, 2005a; Lichtinger *et al.*, 2001). We present in this study the characterization of the first channel-forming protein of a pathogenic strain within the genus *Corynebacterium*.

2.3 Materials and methods

2.3.1 Bacterial strains and growth conditions

The *C. diphtheriae* strain C8r(-) Tox$^-$ (ATCC 11913) (Barksdale, 1959) was used in all experiments. The strain was routinely grown in 500 ml Erlenmeyer flasks containing 250 ml brain heart infusion (BHI) medium (Difco Laboratories) at 37°C using a New Brunswick shaker at 120 rpm for 24 hours. *C. glutamicum* ATCC 13032 cells were routinely grown in BHI medium as described previously in detail (Hünten *et al.*, 2005a). The CgPorH- and CgPorA-deficient *C. glutamicum* strain ATCC 13032 Δ*porH*Δ*porA* (see below) was used to complement for PorA deficiency.

2.3.2 Construction of *C. glutamicum* strain ATCC 13032 Δ*porH*Δ*porA*

The up- and downstream regions of target genes were amplified by PCR with primers FP KO1/RP KO2 (containing *Eco*RI and *Apa*I restriction sites) and primers FP KO3/RP KO4 (carrying *Apa*I and *Bam*HI restriction sites) (Table 2.1). The FailSafe PCR System (Biozym Scientific, Oldendorf, Germany) and buffer G were used according to the manufacturer`s instructions. The PCR products were separately digested using *Apa*I (Fermentas, St. Leon-Rot, Germany) and ligated overnight with T4 DNA ligase. The ligation product served as a template for another PCR with primers FP KO1/RP KO4. After double digestion with *Eco*RI and *Bam*HI the knockout fragment was inserted into the multiple cloning site of *Bam*HI-*Eco*RI cleaved pk18mobsacB, which resulted in the plasmid pK18mobsacBΔ*porH*Δ*porA*. This plasmid was transformed by electroporation into competent *C. glutamicum* ATCC 13032 cells.

Integration of the plasmid into the chromosome, which indicated that the first single crossover event occurred, was tested by plating the cells on BHIS (9.1% D-sorbitol brain heart infusion) plates supplemented with 25 μg/ml kanamycin. For deletion of the target genes one of the colonies on a plate was grown overnight in liquid LB and spread on BHIS plates containing 10% sucrose. Cells that grew on this plate were tested for kanamycin sensitivity by parallel picking on BHIS plates which contained either kanamycin or sucrose. Sucrose-resistant and

kanamycin-sensitive cells indicated that the second crossover happened. The deletion was verified by PCR and by DNA sequencing (data not shown).

Oligonucleotides	Sequence 5'→ 3'	Position
Cdiph_XbaI_for	GCTTTTGCTATT<u>TCTAGA</u>GGAGGTATTGAC	2073825-2073796†
Cdiph_KpnI_rev	CCTAGCCAGCTA<u>GGTACC</u>AAGCCAACAAAC	2073038-2073067†
FP KO 1	GACGAGGCAACCG<u>GAATTC</u>GCATCGTCCGCG	2862508-2862538‡
RP KO 2	GTTGCCAGTTTGCTG<u>GGGCCC</u>TCAGGACGTC	2861687-2861717‡
FP KO 3	AACTTCGCCCAC<u>GGGCCC</u>AGTTTTCAAAAAC	2861216-2861246‡
RP KO 4	ATTCGACTTGATGG<u>GGATCC</u>ACGGGGACTC	2860356-2860385‡

Table 2.1: Oligonucleotides used in this study. The sequences of the primers were derived from the prospective gene of the cell wall channel and its flanking regions from the genome of *C. diphtheriae* NCTC 13129 (Cerdeno-Tarraga *et al.*, 2003). The accession numbers for the genome of *C. diphtheriae* NCTC 13129 and *C. glutamicum* ATCC 13032 are NC_002935 (†) and NC_003450 (‡), respectively.

2.3.3 Preparation of the cell wall, plasma membrane and cytosol fractions

The cell fractions were produced as previously described for mycobacteria (Daffe *et al.*, 1990; Raynaud *et al.*, 1998). Wet cells (5g) were suspended in 20 ml phosphate buffer (50 mM, pH 7.5). The resulting bacterial suspension was passed through a cell disrupter and then centrifuged at 4000 rpm for 15 min to remove unbroken cells. From the supernatant cell walls were recovered by centrifugation at 10000 rpm (8300 × g) for 60 min. To obtain the membrane fraction pellet, the 10000 rpm supernatant was 60 min long centrifuged at 50000 rpm (170000 × g) in an ultracentrifuge (Beckmann Omega 90 XL, rotor 70.1 Ti) at 4°C. The supernatant was considered as the cytosol fraction. The pellets were washed and lyophilized (Daffe *et al.*, 1990) or were directly used for the experiments. All fractions were analyzed for their protein content by sodium dodecyl sulfate (SDS)-polyacrylamide gel electrophoresis (PAGE) and for their pore-forming activity by reconstitution experiments with the black lipid bilayer assay following detergent treatment of the different fractions. NADH oxidase activity was used to verify the correct separation of the different fractions. The enzymatic activity was measured by detecting the decrease in absorbance at 340 nm (Osborn *et al.*, 1972); it followed a first order kinetics. The specific activity was calculated by dividing the appropriate rate constant k_1 by the relative protein concentration of the sample.

2.3.4 Isolation and purification of the channel-forming protein from the cell wall fraction

Whole cells of *C. diphtheriae* were extracted with the organic solvents chloroform and methanol mixed in a 1:2 (v/v) ratio. For this purpose, 1 part cells was solved in 5 to 8 parts organic solution (Lichtinger *et al.*, 1998). The chloroform/methanol extracted proteins were precipitated with ice-cold diethyl ether at –20°C for 24 hours and the resultant protein pellet was dissolved in 1% Genapol X-80. Further purification was achieved by excising bands at different molecular masses from preparative SDS-PAGE gels. The gel-embedded proteins were extracted with 1% Genapol X-80. Possible oligomers of the channel-forming protein were obtained by adding to the protein solution a volume of ethanol that was 2.5-fold greater than the volume of the solution. The protein was then 24 h long precipitated by incubation at 4°C. Subsequent to centrifugation at 4°C, the resulting pellet was dried under vacuum to completely remove the remaining ethanol.

2.3.5 Digestion of the polypeptide

The purified polypeptide with a molecular mass of about 5 kDa was treated for 5 min with 50 U/ml proteinase K (Sigma, St.Louis, MO) in a buffer containing 1% Genapol X-80.

2.3.6 SDS-polyacrylamide gel electrophoresis

Analytical and preparative SDS-PAGE was performed according to Laemmli (1970) or, because of the low resolution of this gel system at low molecular mass, according to Schägger and von Jagow (1991) with Tris-Tricine-containing gels. For protein visualization, the gels were either stained with Coomassie brilliant blue or with colloidal Coomassie brilliant blue G-250 (Neuhoff *et al.*, 1988). Application of the latter dye resulted in improved staining of proteins with sensitivity similar to that of silver stain.

2.3.7 Immunological techniques

2.3.7.1 Western blot analysis

In Western blot experiments, the proteins were separated by 10% Tricine-PAGE and transferred onto nitrocellulose sheets (Protran, BA83, 0.2 μm, Schleicher&Schuell) in a semidry blotting apparatus (Schägger & von Jagow, 1991). This method is a modified procedure described by Kyhse-Andersen (1984), taking into account the higher ionic strength of Tricine-containing SDS gels. The reactive sites on the membrane were blocked for 1 h with 5% skimmed milk in TBS-T (0.1% Tween, 0.01 M NaCl, 20 mM Tris-HCl, pH 7.5). Subsequent to three TBS-T washing steps, the blots were incubated for 1 h (or overnight) with 1:100 diluted rabbit polyclonal antibodies against *C. glutamicum* PorA (Lichtinger *et al.*, 1998) at RT. The membranes were then washed again three times with TBS-T. Bound primary antibodies were detected by using 1:1000 diluted rabbit immunoglobulins coupled to horseradish peroxidase (DAKO, Denmark). These secondary antibodies were visualized by a colour or a chemiluminescent detection method. For the colour detection, a mixture of 94% Tris-buffered saline, 6% chloronaphtol (0.3%) and 0.075% hydrogen peroxide was used which resulted after 10 min of incubation in the appearance of bands. For the chemiluminescent detection of the monomer, we used the ECL Western blot detection system (GE Healthcare, UK) providing an extremely sensitive method to detect small amounts of protein. Following the manufacturer`s instructions, signal detection was achieved by incubating the membrane in the detection mixture for 1 min, draining off the mixture and wrapping the blot in Saran Wrap. Then, the blot together with a piece of autoradiography film (HyperfilmMP, GE Healthcare, UK) on top of it were placed into a film cassette for 15 seconds to 5 minutes, as required by the sample. The exposed film was developed by use of X-omat M35 (Kodak).

2.3.7.2 Enzyme-linked immunosorbent assay

Enzyme-linked immunosorbent assay (ELISA) experiments were carried out as described previously (Burkovski, 1997). The applied method allowed us to perform a fast, simple and sensitive ELISA suitable for the detection of bacterial surface proteins. Briefly, different amounts of *C. glutamicum* ATCC 13032 or *C. diphtheriae* ATCC 11913 cells were coupled

per well (MaxiSorp immunoplates, Nunc, Roskilde, Denmark). Cells of *C. glutamicum* were used as positive control. The corresponding preimmune serum and wells containing either only cells of *C. glutamicum* or *C. diphtheriae* without any primary antibody were used as negative controls. The absorption at 405 nm was measured using a microplate reader (Thermomax, Molecular Devices).

2.3.8 Polymerase chain reaction and construction of the expression plasmid

The region containing the gene that encodes the PorA homolog of *C. diphtheriae* was isolated with the FailSafe PCR system (Epicentre Biotechnologies). The PCR amplicon was produced using primers Cdiph_XbaI_for/Cdiph_KpnI_rev (Table 2.1), chromosomal DNA of *C. diphtheriae* strain C8r(-) Tox⁻ (ATCC 11913) and Failsafe polymerase and buffer E according to the manufacturer`s advice. The PCR program was as follows: initial denaturing at 95°C for 5 min, 30 cycles at 95°C for 1 min, 45°C for 1 min, 72°C for 2 min and a final extension at 72°C for 10 min. Fifty microliters of the reaction mixture were loaded on a 0.8% agarose gel and compared to a 1 kb ladder (Gibco-BRL Life Technologies Ltd., Paisley, UK). The PCR product was cut out of the gel, ligated into the TOPO 2.1 cloning vector and transformed in One Shot Top10 F' cells. Plasmids of minipreped *Escherichia coli* cells were used for sequencing the PCR product with primers M13 forward and M13 reverse. The gene coding for the prospective cell wall channel and its flanking regions were cut out of the TOPO 2.1 vector using the restriction enzymes *EcoR*I and *Xba*I. The DNA piece was then ligated in the similar cut shuttle vector pXMJ19, which yielded pX$_{Cd}$-WT. A slightly modified standard electrotransformation method (van der Rest *et al.*, 1999) was used to inject pX$_{Cd}$-WT in *C. glutamicum* ATCC 13032 Δ*porH*Δ*porA* cells. The transformed cells were grown to an OD$_{600}$ of about 3. Then, protein expression was induced with 1 mM isopropyl-β-D-thiogalactopyranoside (IPTG) and the culture was grown for another 16 hours. Subsequent to centrifugation, the cells were extracted with a 1:2 mixture of chloroform and methanol by using 1 part cells and 5 to 8 parts organic solvent. The protein was precipitated with ether in the cold.

2.3.9 Lipid bilayer experiments

The methods used for the lipid bilayer experiments have been previously described in detail (Benz *et al.*, 1978). The instrumentation consisted of a Teflon chamber with two aqueous compartments connected by a small circular hole. The hole had a surface area of about 0.3 mm^2. Black lipid bilayer membranes were obtained by painting a 1% (w/v) solution of diphytanoyl phosphatidylcholine (PC) or phosphatidylserine (PS) (Avanti Polar Lipids, Alabaster, AL) in *n*-decane onto the hole. Membranes were also formed from PC/mycolic acids (MA) (Sigma) or PC/PS/MA mixtures to study the effect of mycolic acids on channel formation. During all experiments, the temperature was maintained at 20°C. All salts were obtained from Merck (Darmstadt, Germany) at analytical grade. Zero-current membrane potential measurements were performed by establishing a fivefold salt gradient across membranes, which contained 100 to 1000 cell wall porins (Benz *et al.*, 1979).

2.4 Results

2.4.1 Isolation and purification of the channel-forming protein

An homogenate of *C. diphtheriae* C8r(-) Tox$^-$ (ATCC 11913) cells was twice-centrifuged at different speeds and separated into pellets that should have contained the cell walls and the cytoplasmic membranes. The supernatant from the second centrifugation was the cytosol of the cells. The pellets as well as the supernatant were inspected to determine their protein contents, channel-forming abilities and NADH oxidase activities. The greatest channel-forming ability was observed for Genapol X-80 extracts of the cell wall fraction. Cytosol and cytoplasmic membrane extracts showed only a very weak single-channel activity, indicating that the cell wall contained most of the channel-forming protein. As assessed by NADH oxidase activity, the cell wall fraction was essentially free of cytoplasmic membrane. The specific NADH oxidase activity of the proteins of this fraction was relative to the protein concentration 0.10. The corresponding specific NADH oxidase activities of the proteins of the cytoplasmic membrane fraction and the cytosol relative to their protein concentrations were 0.87 and 0.03, respectively. The total NADH oxidase activity was defined as 1.0.
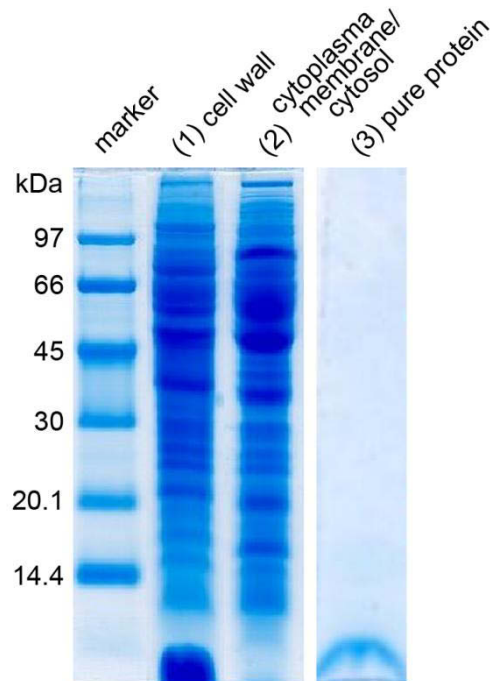
Figure 2.1: Tricine (10%)-PAGE according to Schägger and von Jagow (1987) of the cell wall fraction and the cytoplasmic membrane/cytosol fraction of *C. diphtheriae* ATCC 11913. The marker lane, lane (1) and lane (2) were stained with Coomassie blue; lane (3) was stained with colloidal Coomassie blue. Lane 1, 15 μl of the cell wall fraction (8300 × g pellet) solubilised at 40°C for 30 min in 1% Genapol X-80 and 5 μl sample buffer; lane 2, 15 μl of the 8300 × g supernatant containing the cytoplasmic membrane and cytosol solubilised at 40°C for 30 min in 5 μl sample buffer; lane 3, 3 μg of the pure cell wall channel protein of *C. diphtheriae* ATCC 11913 incubated at 100°C for 30 min in 5 μl sample buffer.

Tricine-PAGE of the detergent-solubilised material from the cell wall fraction produced so many bands in Coomassie stained gels that it was impossible to relate a single band to the channel-forming activity (although a strong band in the low-molecular-mass region was noticeable) (Fig. 2.1). Hence, whole cells of *C. diphtheriae* ATCC 11913 were treated with organic solvents. This method provided in the case of the cell wall channel of *C. glutamicum* a simple purification procedure for the channel-forming protein (Lichtinger *et al.*, 1998). Tricine-PAGE of the ether precipitate following chloroform/methanol extraction showed that a protein with a molecular mass of about 5 kDa was enriched in this fraction (data not shown). The channel-forming protein was further purified by excising the enriched band from preparative Tricine-PAGE gel and extracting it with 1% Genapol X-80 from the gel slice (Fig. 2.1). Addition of the extracted 5 kDa band to black lipid bilayer membranes resulted in very fast reconstitution of channels. When regions at different molecular masses were excised from the same Tricine-PAGE gel, the highest channel-forming activity was always observed with the 5 kDa band. However, we also noticed that minor channel-forming activity was spread across the molecular mass region between about 5 and 70 kDa of the Tricine-PAGE gel. This

result indicated that the 5 kDa band may represent a channel-forming monomer, as is the case for CgPorA of *C. glutamicum* (Lichtinger *et al.*, 2001). This was confirmed by Tricine-PAGE of the ethanol precipitate of the 5 kDa protein eluted from the preparative Tricine-PAGE gel. The corresponding gel showed that the oligomer of the channel-forming protein has an apparent molecular mass of about 66 kDa (data not shown; see also below).

2.4.2   Interaction of the cell wall protein with lipid bilayer membranes

The interaction of the cell wall protein with lipid membranes was studied by using the black lipid bilayer assay and conductance measurement experiments. Membranes were formed from 1% PC or 1% PC/PS mixtures (molar ratio 4:1) dissolved in *n*-decane. The 5 kDa cell wall protein resulted in a strong increase in conductance, when it was added at a low concentration (100 ng/ml) to one or both sides of lipid membranes. This increase was apparently not sudden, but it was rather a function of time. Within about 20 to 30 min the membrane conductance increased by several orders of magnitude above that of membranes without the protein (from about 0.05 μS/cm^2 to 150 μS/cm^2). After that time, only a small further increase occurred in comparison with the initial one. The effect of mycolic acids on channel formation was examined by forming membranes from PC/PS/MA mixtures. However, similar results were obtained suggesting that mycolic acids did not influence channel formation. Control experiments with Genapol X-80 alone (used at the same concentration as in the experiments with protein) demonstrated that the membrane activity was caused by the presence of the cell wall protein and not by the detergent. Furthermore, proteinase K digestion carried out for 5 min completely destroyed the channel-forming ability of the purified 5 kDa protein.

2.4.3   Single-channel analysis

Resolution of stepwise conductance increases was achieved by adding low amounts of the *C. diphtheriae* cell wall protein (10 ng/ml) to PC/*n*-decane membranes. Figure 2.2A shows a single-channel recording in the presence of the 5 kDa protein. A few minutes after the addition of the protein to a membrane in the black state, the current increased in step-like fashion. This was caused as the protein reconstituted long-lasting channels with a mean lifetime larger than 5 min, which led to the superposition of single-steps.

A)

B)
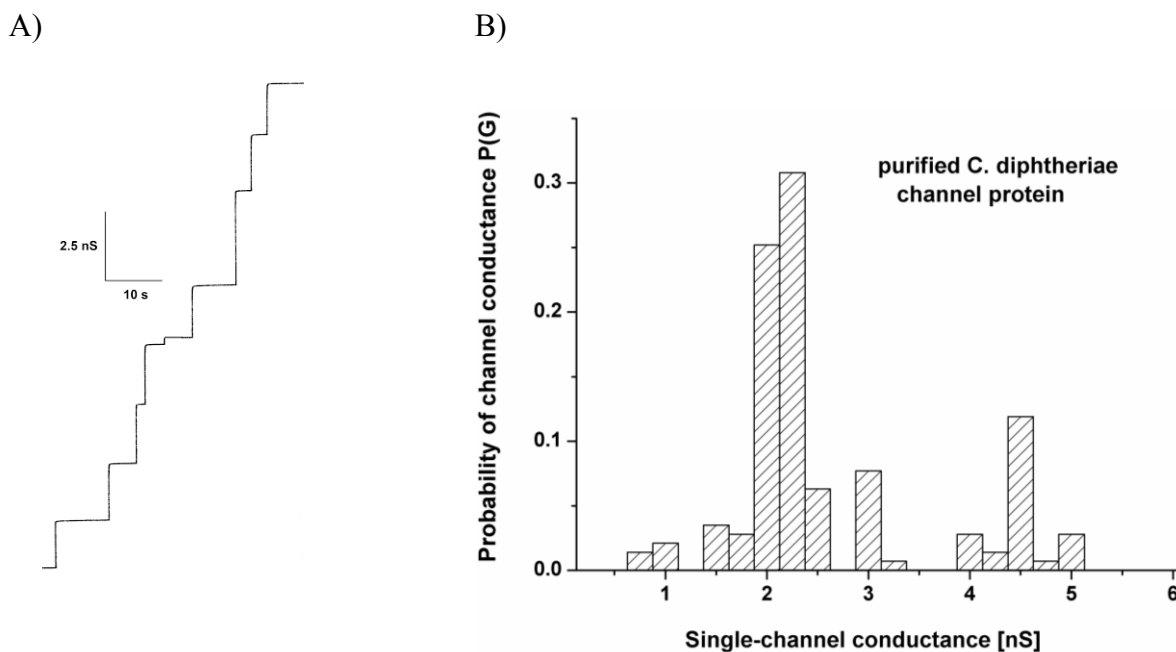
Figure 2.2: (A) Single-channel recording for a PC/*n*-decane membrane in the presence of the channel-forming 5 kDa protein from the cell wall of *C. diphtheriae* ATCC 11913. The aqueous phase contained 1 M KCl buffered with 10 mM Tris-HCl (pH 7) and 10 ng/ml cell wall protein. The applied membrane potential was 20 mV, and the temperature was 20°C. **(B)** Histogram of the probability of the occurrence of a given conductivity observed with membranes formed of PC/*n*-decane in the presence of the cell wall protein of *C. diphtheriae* ATCC 11913. It was calculated by dividing the number of fluctuations with a given conductance rise by the total number of conductance fluctuations. The average single-channel conductance was 2.25 nS for 140 single-channel events. The aqueous phase contained 1 M KCl, 10 mM Tris-HCl (pH 7) and 10 ng/ml of the cell wall protein. The applied membrane potential was 20 mV, and the temperature was 20°C.

Figure 2.2B shows a histogram of the conductance fluctuations observed under the conditions used to obtain Fig. 2.2A (20 mV membrane potential; 1 M KCl, 10 mM Tris-HCl, pH 7). Besides a major conductance step of about 2.25 nS (more than 30% of all conductance fluctuations), channels with a higher single-channel conductance were observed, in particular channels with a single-channel conductance of about 4.5 nS. The latter channels are presumably dimers of the 2.25 nS channel that could not be separated with the time resolution of our experimental setup. All the steps of Fig. 2.2A were directed upwards indicating that under the applied low-voltage conditions the channels were always in the open state. Change of the lipid composition of the membranes from PC to PC/PS (molar ratio 4:1), PC/MA (molar ratio 4:1) or PC/MA/PS (molar ratio 4:4:1) did not influence the single-channel conductance of the *C. diphtheriae* porin.

Insight into the biophysical properties of the cell wall porin of *C. diphtheriae* was acquired by performing single-channel experiments with salts containing other ions than K^+ and Cl^-. The

results summarized in Table 2.2 show that the channel is only moderately selective. This is concluded from experiments in which KCl was replaced by LiCl or KCH$_3$COO. The exchange of the mobile ions K$^+$ and Cl$^-$ by the less mobile ions Li$^+$ and acetate$^-$ showed that cations and anions have a certain permeability through the *C. diphtheriae* channel. The permeability of the cations through the channels followed approximately their mobility sequence in the aqueous phase. This probably means that the cell wall porin is a wide channel, which has only a low field strength inside and no selectivity filter for small molecules (i.e. no binding site), as suggested by the fact that the large organic Tris$^+$ cation could also penetrate the channel.

Salt	Concentration [M]	Single-channel conductance G [nS]
LiCl	1.0	1.25
NaCl	1.0	1.60
KCl	3.0	6.00
	1.0	2.25
	0.6	1.25
	0.3	0.60
	0.1	0.40
	0.03	0.06
CsCl	1.0	2.50
NH$_4$Cl	1.0	2.25
N(CH$_3$)$_4$Cl	1.0	0.80
TrisCl (pH 6)	1.0	0.90
KCH$_3$COO (pH 6)	1.0	1.25

Table 2.2: Average single-channel conductance of the *C. diphtheriae* ATCC 11913 cell wall channel in different salt solutions. The membranes were formed with 1% PC dissolved in *n*-decane. The aqueous solutions were buffered with 10 mM Tris-HCl and had a pH of 7 unless otherwise indicated. The applied voltage was 20 mV, and the temperature was 20°C. The average single-channel conductance was calculated from at least 80 single events derived from measurements of at least four individual membranes.

Table 2.2 also shows the average single-channel conductance studied as a function of the aqueous KCl concentration. The listed single-channel conductance values corresponded to the left-sided maximum in the histograms (i.e., to the 2.25 nS peak in the case of 1 M KCl).

Measurements were performed down to 0.03 M KCl. In contrast to other cell wall channels of the mycolata (Lichtinger *et al.*, 2000; Lichtinger *et al.*, 2001; Riess *et al.*, 2001; Trias & Benz, 1993), a linear relationship between single-channel conductance and KCl concentration was detected. This would only be expected for wide water-filled channels that do not contain point charges similar to those formed by Gram-negative bacterial porins (Benz, 1988; Benz, 1994; Benz, 2003; Weiss *et al.*, 1991). The cell wall channel of *C. diphtheriae* is thus the first described channel amongst members of the mycolata without the presence of positively or negatively charged groups in or near the channel opening influencing the channel properties.

2.4.4   Selectivity of the cell wall channel of *C. diphtheriae*

Zero-current membrane potential measurements were performed to obtain further information on the molecular structure of the *C. diphtheriae* cell wall channel. The experiments were performed as follows: subsequent to the incorporation of 100 to 1000 channels into membranes formed with PC/*n*-decane, the salt concentration was raised fivefold on one side of the membranes beginning from 100 mM. The zero-current potential was measured 5 min after every increase in the salt gradient across the membrane. For KCl and KCH$_3$COO the more diluted side of the membrane (100 mM) always became positive, whereas in the case of LiCl negative membrane potentials were observed (Table 2.3).

Salt	V_m [mV]	Cation/anion permeability ratio
KCl	+ 5.4	1.26
LiCl	- 1.2	0.72
KH$_3$COO	+ 17.5	3.26

Table 2.3: Zero-current membrane potentials of PC/*n*-decane membranes in the presence of the *C. diphtheriae* ATCC 11913 cell wall channel. The potential V_m, measured for a fivefold gradient of different salts, is defined as the difference between the potential on the dilute side and the potential on the concentrated side. The aqueous salt solutions were buffered with 10 mM Tris-HCl (pH 7), and the temperature was 20°C. The cation/anion permeability ratio was calculated from at least 3 individual experiments, as described by Benz *et al.* (1979).

This result indicates that the *C. diphtheriae* channel simply filters the solutes and thus functions as a general diffusion pore, as already known for general diffusion pores of Gram-

negative bacteria (Benz, 2003). Analysis of the membrane potentials using the Goldman-Hodgkin-Katz equation (Benz *et al.*, 1979) confirmed the assumption. According to the determined cation/anion permeability ratios, which were 0.72 (LiCl), 1.26 (KCl) and 3.26 (potassium acetate), both anions and cations are permeable through the channel.

2.4.5   The cell wall channel of *C. diphtheriae* is voltage dependent

Channels of the *C. diphtheriae* cell wall porin occasionally exhibited some flickering in the single-channel recordings at higher voltages, which means that we noticed rapid transitions between an open and closed channel configuration. This observation was studied in separate experiments, as this could have been caused by voltage-dependent closure of the cell wall porin. The channel-forming protein was added in a concentration of 100 ng/ml to one side of a black PC/*n*-decane membrane (the *cis* side). After 30 min the conductance had increased considerably. At this point different positive and negative potentials were applied to the *cis* side of the membrane. For negative and for positive potentials at the *cis* side of the membrane the current decreased in an exponential fashion (data not shown) indicating that the voltage-dependence of the cell wall channel was symmetrical. Addition of the protein to the *trans* side of the membrane or to both sides of the membrane also resulted in a symmetric response to the applied voltage (data not shown).
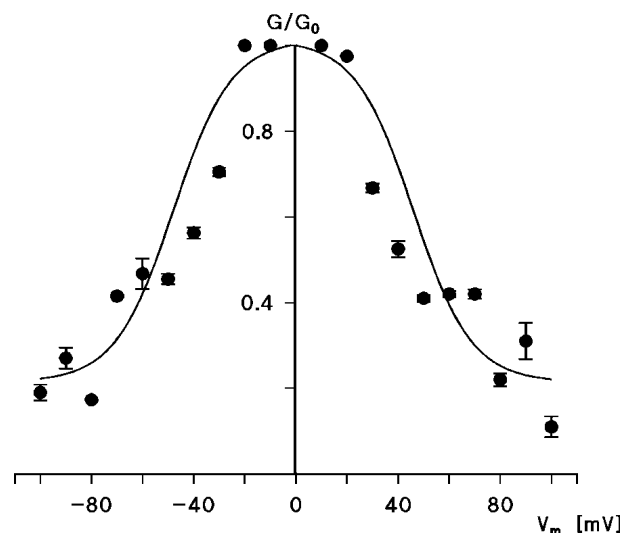
Figure 2.3: Conductance (*G*) at a given membrane potential (*V*$_m$) divided by the conductance at 10 mV (*G*$_0$) shown as a function of the membrane potential. The symbols represent the means of 4 measurements, in which the 5 kDa protein from *C. diphtheriae* ATCC 11913 was added to the *cis* side of membranes. The solid line represents the fit of the experimental data using Equations 2.1 and 2.2 and the parameters *n* = 1, *V*$_0$ = -48 mV (left side of the curve) and *V*$_0$ = 46 mV (right side of the curve). The aqueous phase contained 1 M KCl, 10 mM Tris-HCl (pH 7) and 100 ng/ml porin. The membranes were formed from PC/*n*-decane at a temperature of 20°C.

The data obtained in the experiments were analyzed in the following way: the membrane conductance (G) as a function of voltage (V_m) was measured when the opening and closing of channels reached an equilibrium (i.e., after the exponential decay of the membrane current following the voltage step). G was divided by the initial value of the conductance G_0, (which was a linear function of the voltage) obtained immediately after the onset of the voltage. Figure 2.3 shows the analyzed data of the symmetric and voltage-dependent response of the cell wall porin (mean of four membranes) when the protein was added to the *cis* side (closed circles).

To study the voltage dependence in more detail, the data of Fig. 2.3 were analyzed as described in Ludwig *et al.* (1986) assuming a Boltzmann distribution between the number of open and closed channels, N_O and N_C, respectively (Equation 2.1):

Equation 2.1 $$\frac{N_O}{N_C} = e^{nF(V_m - V_0)/RT}$$

F (= 96500 As/mol), R (= 8.31 J/mol*K) and T are the Faraday constant, gas constant and absolute temperature, respectively. n is the number of charges moving through the entire transmembrane potential gradient for channel gating. V_m equals V_0, is the potential at which 50% of the total number of channels is in the closed configuration. The ratio of open channels to closed channels (N_O/N_C) may be calculated from the data in Fig. 2.3 using Equation 2.2:

Equation 2.2 $$\frac{N_O}{N_C} = \frac{G - G_{min}}{G_0 - G}$$

G in this equation is the conductance at a given membrane potential (V_m). G_0 and G_{min} are the conductance at 10 mV (conductance of the open state) and at very high potentials, respectively. The data of Fig. 2.3 could be fitted with combinations of Equations 2.1 and 2.2. The fit in Fig. 2.3 allowed the calculation of the number of gating charges (n) involved in the gating process and the midpoint potential (V_0) at which the numbers of open and closed channels are identical. The midpoint potential for the addition of the protein to the *cis* side was for applied positive voltages + 46 mV and for applied negative voltages - 48 mV. The gating charge in both cases was close to 1.

2.4.6 Immunological detection of the channel-forming protein of *C. diphtheriae*

Lichtinger *et al.* (1998 & 2001) identified a small-sized, channel-forming peptide in the cell wall of *C. glutamicum*. To check the possible relationship between this peptide and the 5 kDa channel-forming protein of *C. diphtheriae,* we performed Western blot analysis using a polyclonal antibody directed against the porin of *C. glutamicum*. The channel-forming protein of *C. glutamicum* was purified as described previously (Lichtinger *et al.*, 1998) and used as control. Strong cross-reactivity of the antibodies with the 5 kDa channel-forming protein of *C. diphtheriae* and its oligomer was observed (Fig. 2.4), which indicates the presence of highly conserved immunodominant epitopes.
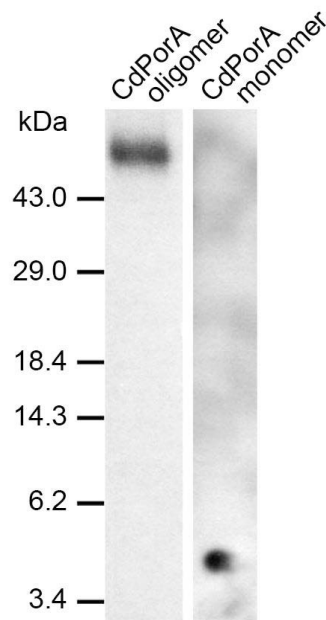
Figure 2.4: Western blot analysis of CdPorA of *C. diphtheriae* ATCC 11913. Tricine-PAGE gels containing CdPorA oligomers and monomers were blotted onto nitrocellulose membranes, which were probed with anti-PorA polyclonal antibodies. Bands were detected using horseradish peroxidase-conjugated antibodies and chloronaphtol-hydrogen peroxide as the substrate. Monomers and oligomers cannot be shown in the same column due to very different blotting times caused by unequal molecular masses.

To confirm the localization of the 5 kDa protein on the surface of *C. diphtheriae* cells, an ELISA test was performed, in which different amounts of whole cells were coupled per well. Experiments with immobilized cells of *C. glutamicum* and *C. diphtheriae* resulted in a very low signal using the preimmunserum, similar to the signals that were detected using immobilized cells treated without any primary antibody (Fig. 2.5). However, usage of the anti-PorA antibody detected immobilized cells of both *C. glutamicum* and of *C. diphtheriae*.
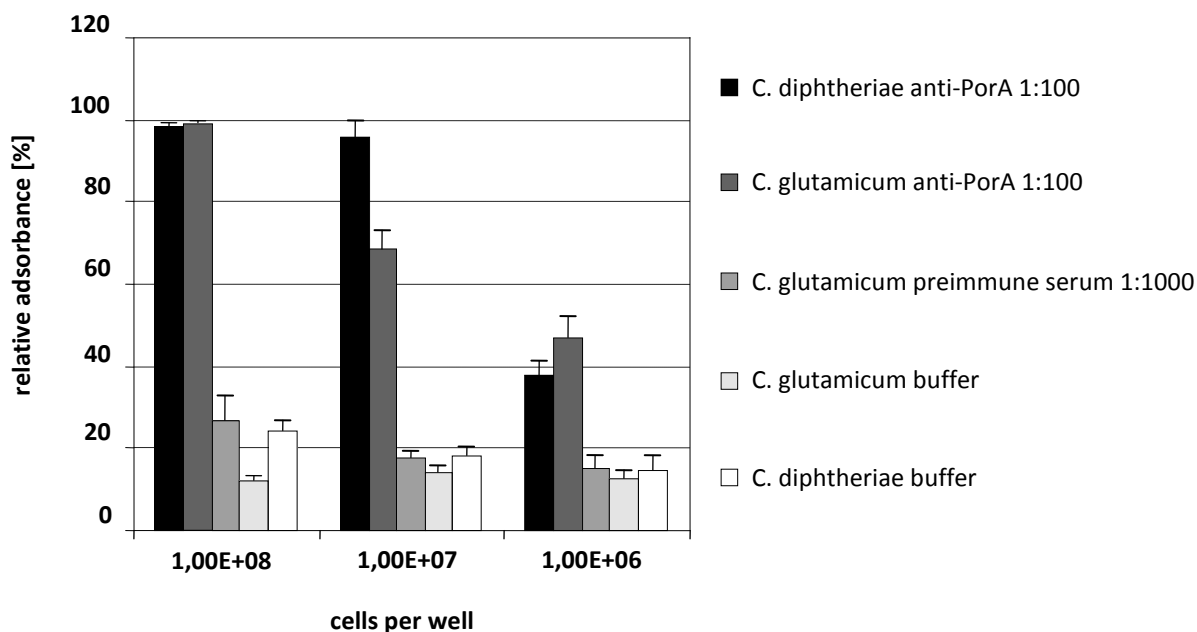
Figure 2.5: Detection of CdPorA of *C. diphtheriae* on the cell wall surface using ELISA. Intact cells of *C. diphtheriae* ATCC 11913 and *C. glutamicum* ATCC 13032 were immobilized and incubated with anti-PorA (dilution 1:100), preimmune serum (dilution 1:1000) and buffer. The maximum binding was defined as 100%. The bars represent the results of at least 8 experiments including the standard deviations. The number of cells per well is indicated.

2.4.7 Identification of the gene coding for the cell wall channel of *C. diphtheriae* ATCC 11913

The observed immunological cross-reactivity between CgPorA of *C. glutamicum* and the cell wall channel of *C. diphtheriae* ATCC 11913 suggested an interesting homology between both proteins. Similarly, Lichtinger *et al.* (2001) previously observed Southern hybridization of the *cgporA* gene with DNA from *C. diphtheriae* suggesting that this organism contains a *porA*-like gene. Search for *cgporA* of *C. glutamicum* in the accessible genome of *C. diphtheriae* NCTC 13129 (Cerdeno-Tarraga *et al.*, 2003) using the NCBI basic local alignment search tool (BLAST) (Altschul *et al.*, 1990) suggested that this genome contained an open reading frame (ORF) that could code for a low-molecular-mass cell wall protein similar to CgPorA (Fig. 2.7). The identified ORF is located between the genes coding for GroEL2 (DIP2020) (Barreiro *et al.*, 2004) and a putative secreted protein (DIP2017), which means that it is localized within a region homologous to the region in the *C. glutamicum* genome containing *cgporA*. Primers were designed to clone the whole region between the two genes DIP2020 (GroEL2) and DIP2017 using chromosomal DNA of *C. diphtheriae* ATCC 11913 as a template (Table 2.1). The PCR product was cloned into the TOPO 2.1 vector and was

sequenced. It contained an ORF which consists of 132 bp and codes for a PorA-like protein that showed only some minor amino acid changes (11 residues) compared with the corresponding protein of *C. diphtheriae* NCTC 13129 (Fig. 2.7). The protein, designated CdPorA (for *C. diphtheriae* pore-forming protein A), is 43 amino acids long (with the inducer methionine) and has a (calculated) molecular mass of 4640 Da. As with CgPorA and CgPorH of *C. glutamicum* (Hünten *et al.*, 2005a; Lichtinger *et al.*, 2001), the cell wall protein of both *C. diphtheriae* strains (ATCC 11913 and NCTC 13129) does not contain a leader sequence.

2.4.8 Expression of CdPorA in *C. glutamicum* ATCC 13032 Δ*porH*Δ*porA* and study of its channel-forming ability

The results of the search for a gene encoding a channel-forming protein in the genome of *C. diphtheriae* NCTC 13129 suggested that CdPorA could be the channel-forming protein in the cell wall.

A)

B)
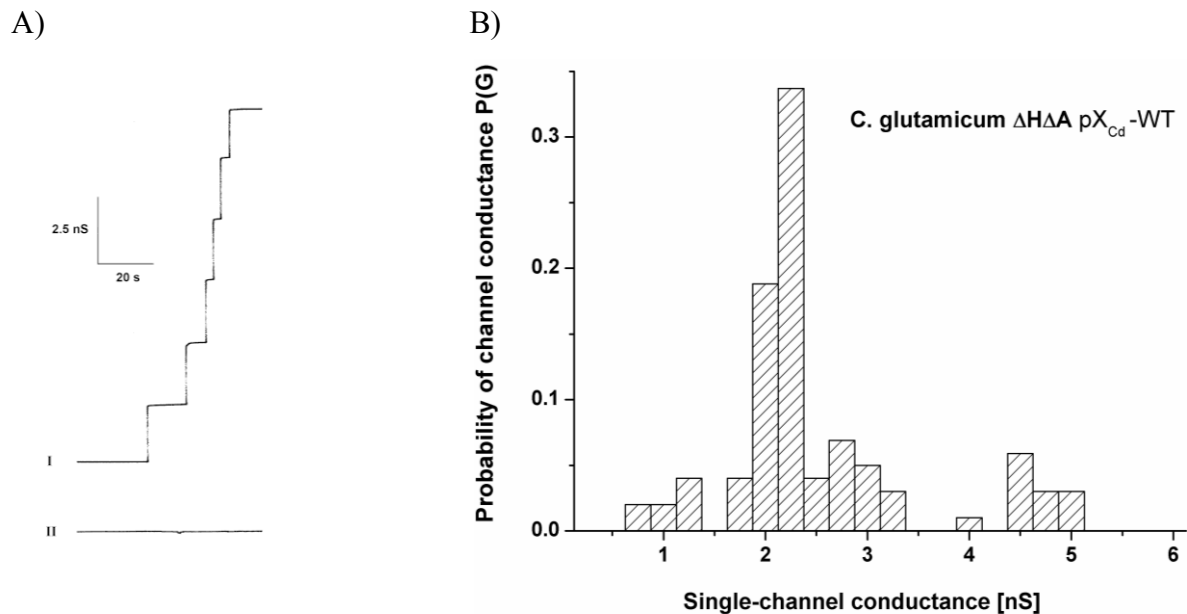
Figure 2.6: (A) Single-channel recording for a PC/*n*-decane membrane in the presence of organic solvent extracts of *C. glutamicum* ATCC 13032 Δ*porH*Δ*porA*. Trace I shows the result for cells transformed with shuttle vector pX$_{Cd}$-WT, in which expression of CdPorA was induced with 1 mM IPTG. Trace II shows the result for a control performed with non-transformed cells of *C. glutamicum* ATCC 13032 Δ*porH*Δ*porA*. The aqueous phase contained 1 M KCl, 10 mM Tris-HCl (pH 7) and 20 ng/ml of the organic solvent extract dissolved in Genapol X-80. The applied membrane potential was 20 mV, and the temperature was 20°C. (B) Histogram of the probability P(G) for the occurrence of a given conductivity unit observed with membranes formed from PC/*n*-decane in the presence of 20 ng/ml of the organic solvent extract of whole *C. glutamicum* ATCC 13032 Δ*porH*Δ*porA* cells transformed with shuttle vector pX$_{Cd}$-WT dissolved in Genapol X-80. The average single-channel conductance was 2.25 nS for 101 single-channel events. The aqueous phase contained 1 M KCl and 10 mM Tris-HCl (pH 7). The applied membrane potential was 20 mV, and the temperature was 20°C.

cdporA (of *C. diphtheriae* ATCC 11913) was expressed in *C. glutamicum* ATCC 13032 Δ*porH*Δ*porA* and whole cells were extracted with organic solvents. The isolated proteins were precipitated with ether in the cold. The precipitate was solved in 1% Genapol X-80, and channel formation was investigated with the lipid bilayer assay using membranes prepared from PC/*n*-decane. The precipitate had high channel-forming activity with a single-channel conductance of 2.25 nS (Fig. 2.6A), i.e. the channels were identical to those of purified CdPorA obtained under the same conditions (Fig. 2.2B, Fig 2.6B). Control experiments with extracts from CgPorA- and CgPorH-deficient *C. glutamicum* cells showed no channel-forming activity.

2.5   Discussion

2.5.1   The cell wall of *C. diphtheriae* contains a channel-forming oligomer

The mycolic acid layer of members of the suprageneric actinomycete taxon mycolata acts as a permeability barrier towards hydrophilic compounds (Jarlier & Nikaido, 1990; Nikaido & Jarlier, 1991; Nikaido *et al.*, 1993). This means that also members of the mycolata need water-filled channels to overcome this barrier, similar to the well known situation in the outer membrane of Gram-negative bacteria (Benz, 1994; Benz, 2003; Nikaido, 2003). Cell wall channels identified in the mycolic acid layer of different members of the suborder *Corynebacterineae* support this assumption (Lichtinger *et al.*, 1998; Niederweis *et al.*, 1999; Riess *et al.*, 2001). The here presented results demonstrate that the cell wall fraction of *C. diphtheriae* also contains a channel-forming protein. With respect to the protein concentration of this fraction, the channel-forming activity was quite high. Moreover, NADH oxidase activity being a marker of the cytoplasmic membrane was rather low for the cell wall fraction. This result ruled out that we were possibly dealing with a contaminant protein responsible for channel formation. In addition, it is clear that the channels can be present only in the cell wall of *C. diphtheriae* and not in the cytoplasmic membrane, because there the presence of these high-conducting channels would result in cell death.

Methodologies previously applied for the isolation of the *C. glutamicum* cell wall channel protein were adopted to purify the *C. diphtheriae* protein; extraction of whole cells with organic solvents was followed by preparative Tricine-PAGE. The results suggested that the

channel-forming protein of *C. diphtheriae* has a low-molecular-mass of about 5 kDa. A polypeptide of this size is certainly not sufficient to form a wide and water-filled channel, as in the case of CgPorA and CgPorH of *C. glutamicum* (Hünten *et al.*, 2005a; Lichtinger *et al.*, 2001). On the other hand, the channel-forming activity of the *C. diphtheriae* protein was smeared over a considerable molecular mass range up to about 70 kDa. Using Western blot analysis we became aware of a possible CdPorA oligomer with a molecular mass of about 66 kDa, when the purified 5 kDa protein was precipitated with ethanol and subjected to Tricine-PAGE without heating. In this respect, it is interesting to note that the 20 kDa molecular mass protein MspA of *Mycobacterium smegmatis* forms an octamer in the cell wall with a molecular mass of 160 kDa (Faller *et al.*, 2004). The smaller size of the CdPorA oligomer compared to that of the MspA octamer may be explained by different cell wall thicknesses of the corresponding bacteria. The corynemycolic acids of corynebacteria are considerably shorter in length (22-38 carbon atoms) than the mycolic acids of other members of the mycolata. This could indicate that the 43 amino acids of CdPorA are sufficient to cross the mycolic acid layer of bacteria belonging to the genus *Corynebacterium*, whereas longer polypeptides are necessary to cross the cell wall of other members of the taxon mycolata. The possibility that glycolipids and corynemycolic acids produced the membrane activity of the detergent and organic solvent cell extracts was ruled out by the disappearance of the channel-forming activity when the *C. diphtheriae* proteins were proteolytically degradated.

2.5.2 The cell wall channel of *C. diphtheriae* is wide and water-filled and does not contain point charges

The conductance of the cell wall channel was a linear function of the bulk aqueous concentration (Table 2.2). Similarly, the selectivity of the CdPorA channel was dependent on the mobility of the ions in the aqueous phase. This represents another indication that it does not contain a binding site or point charges. By sorting the solutes mainly according to their molecular mass, the CdPorA channel functions similar to general diffusion pores in Gram-negative bacteria (Benz, 1994; Benz, 2003). This result is very surprising because to date only cell wall channels in members of the mycolata have been identified that contain charges in or near the channel opening (Table 2.4). The channel presented in this study is the first channel within the *Corynebacterineae* that does not contain point charges, which therefore impedes an estimation of the channel size on basis of the single-channel data, as was the case for other cell wall channels investigated so far (Table 2.4). On the other hand, the size of the CdPorA

channel could be very similar to that formed by CgPorA of *C. glutamicum* because of the sequence homology between both proteins (Fig. 2.7). CgPorA as well as CgPorH of *C. glutamicum* have diameters of about 2.2 nm, so that the CdPorA channel of *C. diphtheriae* could have a similar size.

2.5.3 The cell wall channel of *C. diphtheriae* shows immunological homology with CgPorA of *C. glutamicum*

The immunological results showed that CgPorA of *C. glutamicum* and the 5 kDa protein of *C. diphtheriae* share antigenic structures suggesting some homology between both proteins. In addition to this, the results of the ELISA experiments demonstrated that both proteins are localized on the surface of the cells, which is consistent with their function as channel-tunnels. Moreover, the latter results made us realize that approximately similar amounts of cell wall protein were present on the surface of *C. glutamicum* and of *C. diphtheriae* cells, which means that the cell walls of the two species contain the same number of channels. Control experiments with preimmune serum demonstrated that the antibodies were highly specific for both cell surfaces. Interestingly, in Puech *et al.* (2001) it was reported that the anti-PorA antibodies also reacted with a small-sized cell wall protein of *Corynebacterium pseudodiphtheriticum* whereas no reaction was observed with cell wall proteins of *Corynebacterium amycolatum*; an ambiguous result was obtained for different strains of *Corynebacterium xerosis*. These and our findings suggest that the immune reaction described here was not a nonspecific interaction and that presumably other members (but not all) of the genus *Corynebacterium* also contain PorA-like proteins.

2.5.4 Cloning and sequencing of *cdporA*

Our immunological studies with anti-PorA antibodies and previous Southern hybridization using *cgporA* of *C. glutamicum* (Lichtinger *et al.*, 2001) suggested that *C. diphtheriae* contains a PorA-like protein. A gene encoding a homologous protein was identified by a BLAST search within the known genome sequence of *C. diphtheriae* strain NCTC 13129 that is closely related to the strain used in this study (ATCC 11913). The *cdporA* gene of the *C. diphtheriae* strain NCTC 13129 is localized between the coding DNA sequences of DIP2020 and DIP2017 encoding GroEL2 and a putative secreted protein, respectively. To elucidate the

Cell wall porin	Conductance [nS] in 1 M KCl	Cation/anion permeability ratio in KCl	Point charge at the channel mouth	Channel diameter [nm] estimated by:			Reference(s)
				liposome swelling	single-channel conductance	effect of negative point charges	
C. diphtheriae	2.25	1.26	none				this study
C. glutamicum							
CgPorA	5.5	8.1	-2.0		2.2	2.2	(Lichtinger et al., 1998)
CgPorH	2.5	5.1	-2.0		2.2	2.2	(Hünten et al., 2005a)
CgPorB	0.70	0.12	1.5			1.4	(Costa-Riu et al., 2003b)
R. erythropolis	6.0	11.8	2.7		2.0	2.0	(Lichtinger et al., 2000)
R. equi							
ReqPorA	4.0	9.0	-1.5		1.8	2.0	(Riess et al., 2003)
ReqPorB	0.30	0.16	1.5		1.4	1.4	(Riess et al., 2003)
M. smegmatis							
MspA	4.1	9.7	-4.0		1.8	3.0	(Niederweis et al., 1999; Trias & Benz, 1994)
M. phlei	4.5	14.9	-2.2		1.8	2.0	(Riess et al., 2001)
M. chelonae	2.7	14	2.5	2.2	2.2	2.0	(Trias et al., 1992; Trias & Benz, 1993)
N. farcinica	3.0	8.2	1.3		1.4	1.6	(Riess et al., 1998)

Table 2.4: Comparison of the cell wall channel properties of *C. diphtheriae*, *C. glutamicum*, *Rhodococcus erythropolis*, *Rhodococcus equi*, *M. smegmatis*, *Mycobacterium phlei*, *Mycobacterium chelonae* and *Nocardia farcinica*. The channel diameters were estimated by using the liposome swelling assay, from the single-channel conductance as a function of the hydrated ion radii or from the effect of negative point charges on single-channel conductance.

primary sequence of CdPorA of *C. diphtheriae* ATCC 11913, which was used in this study, the corresponding gene and its flanking regions were cloned and sequenced using the primers Cdiph_XbaI_for/Cdiph_KpnI_rev (derived from the known genome). The result indicated that the ORFs of *cdporA* of strain NCTC 13129 and ATCC 11913 both comprise 132 bp. Although the CdPorA proteins of the two strains are equal in size, they differ by 11 residues and thus show a 74% homology according to their primary peptide sequences (Fig. 2.7). The CdPorA studied here has one more negatively charged amino acid (a total of five glutamates/aspartates, compared to four lysines) than the CdPorA of strain NCTC 13129, which agrees with its small experimentally determined cation selectivity. This is in contrast to the highly cation-selective CgPorA channel of *C. glutamicum* (five negatively charged amino acids, compared with a single lysine) (Lichtinger *et al.*, 1998). Positive and negative amino acids are balanced for CdPorA of the strain NCTC 13129.

```
C. diphtheriae            -    +  -       +-           +-  +  +    -      +
  CdPorA_NCTC 13129   MENINHWVELSS--GKDSIVTVIFGLLKDIAKMGKAIADLIGLAK    43#
                          -         --       -  +  +  +    -      +
  CdPorA_ATCC 11913   MQNIENWVALST--DENSIVTVIFDLLKQVAKMGKAIADLIGLAK    43

C. glutamicum             -    -     -           -     +      -
  CgPorA_ATCC 13032   MENVYEFLGNLDVLSGSGLIGYVFDFLGASSKWAGAVADLIGLLG    45
```

Figure 2.7: Alignment of the PorA amino acid sequences of the strains *C. diphtheriae* NCTC 13129, *C. diphtheriae* ATCC 11913 and *C. glutamicum* ATCC 13032 using Pole Bioinformatique Lyonnaise Network Protein Sequence Analysis (http://npsa-pbil.ibcp.fr). The charged residues of the proteins are indicated at the top. Conserved residues in the three homolog proteins are indicated by shading with yellow (100%) and grey (>50%) colours. [#]indicates the number of amino acids. The sequences of CdPorA from NCTC 13129 and ATCC 11913 have been submitted to the DDBJ/EMBL/GenBank databases under the accession numbers AM689937 and AM690207, respectively.

Inspection of the non-coding regions surrounding the *cdporA* gene of both *C. diphtheriae* strains suggested a putative ribosome binding site (5'-AAAGG-3') that is located eight nucleotides upstream of the start codon of the gene. Furthermore, a stem-loop structure could be identified downstream from the stop codon (TAG) with the tool TransTermHP (http://transterm.cbcb.umd.edu), which is an algorithm to find rho-independent terminators in bacterial genomes (Kingsford *et al.*, 2007). The palindromic sequences of *C. diphtheriae* ATCC 11913 (5'-AAAAGGGCCCGCATCTAAAAGCGGGTCCTTTT-3') and *C. diphtheriae* NCTC 13129 (5'-ATAAGGGCCCGCATCTAAAAGCGGGCCCTTTT-3') have free energy levels of -15.5 and -17.8 kcal/mol, respectively (http://www.genebee.msu.su). This result suggested that these structures are suitable to be putative termination signals of mRNA transcription.

It is worth mentioning that CdPorA of both strains does not contain any C-terminal sorting signal for targeting to the cell wall similar to CgPorA and CgPorH of *C. glutamicum* (Hünten *et al.*, 2005a; Lichtinger *et al.*, 2001). On the other hand, as demonstrated by the ELISA measurements, CdPorA is clearly a protein localized in the cell wall of *C. diphtheriae*. The absence of any obvious signal peptide suggests that its translocation through the cytoplasmic membrane uses an export system different from the Sec system, which is in general responsible for protein sorting and export in Gram-positive bacteria (Freudl, 1992; Navarre & Schneewind, 1999; Peyret *et al.*, 1993; Schneewind *et al.*, 1993).

2.5.5   *CdporA* can be expressed in *C. glutamicum* and complements for CgPorA and CgPorH deficiency

PCR using two primers allowed cloning and sequencing of *cdporA* and its flanking regions. The same DNA sequence was also introduced into the shuttle vector pXMJ19. A CgPorA/CgPorH deficient *C. glutamicum* strain was transformed with the plasmid pX$_{Cd}$-WT. The cells were treated with chloroform/methanol after induction of CdPorA expression. The extract solubilized with Genapol X-80 resulted subsequent to the addition to black lipid membranes in the formation of the same channels as with purified CdPorA protein. This result revealed the close structural and functional relationship between PorA proteins of *C. glutamicum* and *C. diphtheriae*. It is noteworthy that the cell wall porin of *C. diphtheriae* had no properties similar to those of the porins found in the cell walls of other distantly related actinomycetes, which have molecular masses of more than 20 kDa (Niederweis *et al.*, 1999; Riess *et al.*, 1998). A comparison of channels and corresponding properties is provided in Table 2.4 from a variety of different members of the mycolata.

Chapter 3

Study of the major cell wall channel of *Corynebacterium glutamicum*, *Corynebacterium efficiens* and *Corynebacterium diphtheriae* in dependence of PorH and PorA proteins

3.1 Summary

Reconstitution experiments with artificial lipid membranes demonstrated an obligatory dependence of the main cell wall channels of *Corynebacterium glutamicum*, *Corynebacterium efficiens* and *Corynebacterium diphtheriae* on two distinct polypeptides, one of class PorH and one of class PorA. The identification of homologous proteins on the chromosome of *Corynebacterium callunae* suggested a similar result for this strain. In all four strains a heterooligomeric structure composed of PorH and PorA is needed to form the major cell wall channel. This was concluded from complementation experiments using a *porH* and *porA* deficient *C. glutamicum* strain. The strict necessity of proteins of both classes to recover the wild-type channels was demonstrated by black lipid bilayer experiments using detergent or organic solvent extracts of complemented cells. The channel-forming capacity of recombinant expressed, affinity purified PorH and PorA proteins of *C. glutamicum* revealed that the channels consisted solely of these two components. This agreed with results obtained from a transcript encoding for both channel-forming components discovered in *C. glutamicum* by Northern blot and RT-PCR analysis. The transcription start point of the genes was determined by RACE approach, allowing the prediction of the -35 and -10 regions of the promoter. The results demonstrate that the cell wall pore within the suborder *Corynebacterineae* is formed by a two-component oligomer.

3.2 Introduction

Micrococcus glutamicus, first described in 1957 by Kinoshita and coworkers, was isolated from a soil sample at Ueno Zoo (Tokyo) (Kinoshita *et al.*, 2004). In a screening project, the Gram-positive, rod-shaped and non-sporulating species turned out to naturally secrete L-glutamate, the substance responsible for the spicy taste of the Asian cuisine called "umami". Promoted by this finding, *M. glutamicus* (later renamed *Corynebacterium glutamicum*) has made its impact on the fermentative industry and became in the following decades the main producer of the flavour enhancer L-glutamate and the feed additive L-lysine (Georgi *et al.*, 2005; Hermann, 2003; Lakshman & Raghavendra Rao, 1980; Ohnishi *et al.*, 2003). Assisted by the multiple and independent genome decipherment of two *C. glutamicum* species (Ikeda & Nakagawa, 2003; Kalinowski *et al.*, 2003; Yukawa *et al.*, 2007), the research on proteins involved in synthesis and translocation of amino acids was strongly pushed. In recent years, various amino acid exporters, such as LysE, ThrE and BrnFE have been suggested to participate in the flux of lysine, threonine and methionine, respectively (Simic *et al.*, 2001; Trotschel *et al.*, 2005; Vrljic *et al.*, 1996). However, due to the unique composition of the cell wall present in the genus *Corynebacterium*, cytoplasmic membrane-located transporters cannot exclusively account for the overall flux of these and other substances (Eggeling & Sahm, 2001).

The genera *Corynebacterium*, *Mycobacterium*, *Nocardia* and *Rhodococcus* constituting the CMN-group (Ruimy *et al.*, 1994) possess next to the cytoplasma membrane an additional and efficient permeability barrier, the so-called mycolate membrane. This membrane mainly consists of mycolic acids (alpha-branched, beta-hydroxylated fatty acids) covalently attached to an arabinogalactan-peptidoglycan complex and free trehalose derivatives (Daffe & Draper, 1998; Puech *et al.*, 2001; Tropis *et al.*, 2005). Similar to the lipopolysaccharide layer of Gram-negative bacteria, this membrane prevents the passage of hydrophilic and charged compounds (Jarlier & Nikaido, 1990; Nikaido, 2003). In line with the situation in Gram-negative bacteria, it is assumed that in members of the CMN-group the uptake of nutrients and other chemical substances is also facilitated by the presence of specialized water-filled channels. Channel-forming proteins in the cell wall of *Mycobacteria* (Molle *et al.*, 2006; Niederweis *et al.*, 1999), *Corynebacteria* (Costa-Riu *et al.*, 2003b; Hünten *et al.*, 2005a; Lichtinger *et al.*, 1998), *Nocardia* (Riess *et al.*, 1999; Riess & Benz, 2000) and closely related genera support this assumption.

66

In the industry, *Corynebacterium* species used in the fermentative processing of amino acids are nevertheless further permeabilized in order to gain higher productive yields. Methods commonly applied to artificially increase the cell wall permeability include the addition of detergents or chemicals, as well as the limitation of biotin or the upshift of temperature. Although these methods have different points of contact, they all affect the mycolate layer by changing its lipid composition or fluidity which indicates that the corynebacterial outer membrane represents a barrier to the flux of solutes (Gebhardt *et al.*, 2007; Hashimoto *et al.*, 2006; Kumagai *et al.*, 2005; Radmacher *et al.*, 2005). A profound knowledge of porins that establish the natural main passage across the outermost membrane in mycolata could make such treatments unnecessary and could be of great economic advantage. However, this knowledge could also be of great importance for the design of drugs which, in recent years, has become a major challenge to meet the fast emergence of worldwide highly resistant pathogens, such as *Mycobacterium tuberculosis* or *Corynebacterium jeikeium* (Shah *et al.*, 2007; Tauch *et al.*, 2008). For the development of new antimicrobial compounds precisely targeting essential intracellular components, knowledge of the structure of cell wall channels could be of tremendous help.

Here, we report that the main cell wall channel of *C. glutamicum*, its close relative *Corynebacterium efficiens* and a non-pathogenic strain of *Corynebacterium diphtheriae* comprises of two small-sized proteins, designated PorH and PorA. A heterooligomer is thus predicted to form the cell wall channels of these corynebacteria. The thesis was concluded from reconstitution experiments in which the respective main cell wall channels were expressed in a *C. glutamicum* strain deficient of PorH and PorA. The reconstitution of the channels was studied by the black lipid bilayer technique using cell extracts and purified proteins. The report is of further interest because the PorH and PorA homologues of *Corynebacterium callunae*, another prominent amino acid producer, were identified.

3.3   Materials and methods

3.3.1   Bacterial strains and growth conditions

Strains used in this study are summarized in Table 3.1. *C. glutamicum* was grown in brain heart infusion (BHI) medium (Difco Laboratories) or CGXII minimal medium [20 g $(NH_4)_2SO_4$, 5 g urea, 1 g KH_2PO_4, 1 g K_2HPO_4, 0.25 g $MgSO_4 \times 7H_2O$, 42 g MOPS, 10 mg $CaCl_2$, 10 mg $FeSO_4 \times 7H_2O$, 0.2 mg $CuSO_4$, 0.02 mg $NiCl \times 6H_2O$, 10 mg $MnSO_4 \times 2H_2O$, 1 mg $ZnSO_2 \times 7H_2O$, 30 mg protocatechuic acid (3,4-dihydroxybenzoic acid) and 0.2 mg biotin/l distilled water, adjusted with NaOH to pH 7.0] supplemented with 2.5% glucose at 30°C with shaking at 150 rpm or maintained on BHI agar plates. If necessary, agar plates and liquid media were supplemented with 20 or 40 µg/ml chloramphenicol.

Strain	Description	Reference
Corynebacterium glutamicum		
ATCC 13032	wild-type	DSMZ
CglΔA	ATCC 13032 Δ*porA*	(Costa-Riu *et al.*, 2003a)
CglΔHΔA	ATCC 13032 Δ*porH* Δ*porA*	(Schiffler *et al.*, 2007)
Corynebacterium efficiens		
AJ 12310	wild-type	DSMZ
Corynebacterium callunae		
ATCC 15991	wild-type	DSMZ

Table 3.1: Strains used in this study for cloning, RNA isolation and porin complementation. DSMZ stands for Deutsche Sammlung von Mikroorganismen und Zellkulturen (Braunschweig, Germany).

3.3.2   Plasmids and DNA manipulations

The channel-forming capacities of PorH- and PorA like proteins of different *Corynebacterium* strains were studied by cloning the corresponding genes into the multi cloning site of the chloramphenicol resistance conferring expression vector pXMJ19 (Schäfer *et al.*, 1994). All plasmids were sequenced (Seqlab, Germany) prior to their transformation into the channel deficient *C. glutamicum* Δ*porH*Δ*porA* mutant according to a slightly modified standard electro-transformation method (van der Rest *et al.*, 1999). Protein expression was always

induced overnight in liquid cultures at the mid-exponential growth phase by the addition of 1 mM isopropyl-β-D-thiogalactopyranoside (IPTG).

3.3.2.1 Cloning of *C. glutamicum* porins

From chromosomal *C. glutamicum* DNA the individual gene *cgporH* (i), *cgporA* (ii) and a fragment comprising both genes (iii) were PCR amplified including small flanking regions (Fig. 3.1). The 50 µl PCR reactions contained 1 × Taq buffer, 0.2 mM dNTPs, 3 mM $MgCl_2$, 1 U Taq DNA polymerase (Fermentas, St. Leon-Rot, Germany) and 0.4 µM primers in the following combination: FP Cg_HA_XbaI/RP Cg_H_BamHI (i), FP Cg_A_XbaI/RP Cg_HA_BamHI (ii) and FP Cg_HA_XbaI/RP Cg_HA_BamHI (iii) (Table 3.2). Corresponding PCR conditions were: initial denaturing at 95°C for 5 min, 25 cycles at 95°C for 1 min, 45°C for 1 min, 72°C for 30 [(i), (ii)] or 60 sec (iii) and a final extension at 72°C for 10 min. The PCR products were digested with *Bam*HI, *Xba*I and ligated with the similarly cut plasmid pXMJ19 using T4 DNA Ligase (Fermentas). The resulting plasmids were designated pX_{Cg}-H (i), pX_{Cg}-A (ii) and pX_{Cg}-HA (iii).

In this study, PorH and PorA proteins of *C. glutamicum* were purified by immobilized metal ion affinity chromatography (IMAC). Histidine residues required for purification of the proteins were factor Xa cleavable attached either to the 3' end of *cgporH* or to the 5' end of *cgporA*. This was performed in a nested PCR approach using plasmid pX_{Cg}-HA as template (Fig. 3.1), buffer D and the Failsafe polymerase of the FailSafe PCR system (Biozym Scientific, Oldendorf, Germany) as described by the manufacturer. 25 PCR cycles were performed with conditions as follows: 95°C for 1 min, 45°C for 1 min and 72°C for 45 sec. The PCR products obtained with primers FP Seq/RP Cg_H_CHisXa_NheI and FP Cg_H_CHisXa_NheI/RP Insert (both used to construct the fragment H_{CHis}A), as well as the products of FP Seq/RP Cg_A_NHisXa_NheI and FP Cg_A_ NHisXa_NheI/RP Insert (both used to construct the fragment HA_{NHis}) were digested by the *Nhe*I enzyme. Matching fragments were ligated and subjected to a further PCR making use of the flanking primers FP Seq/RP Insert. This time elongation was prolonged to 1 min at 72°C. Subsequent to *Hind*III-*Eco*RI double digestion amplificates were ligated in a similarly cut pXMJ19 vector resulting in pX_{Cg}-H_{CHis}A and pX_{Cg}-HA_{NHis}.

The genes *cgporH*_{CHis} and *cgporA*_{NHis} were PCR-amplified from pX_{Cg}-HCHisA and pX_{Cg}-HA_{NHis}, respectively. Apart from the primers used, both PCR reactions were performed according to the protocol described above (i). *cgporH*_{CHis} was cloned with primers FP Seq/RP Cg_H_EcoRI and the amplificate was inserted in *Hind*III, *Eco*RI cleaved pXMJ19 vector leading to pX_{Cg}-H_{CHis}. *cgporA*_{NHis} was isolated with primers FP Cg_A_XbaI/RP Insert. The PCR product and plasmid pXMJ19 were *Xba*I, *Eco*RI digested and ligated to obtain pX_{Cg}-A_{NHis}.

3.3.2.2 Cloning of *C. efficiens* porins

Genomic DNA of *C. efficiens* was used for PCR amplification of chromosomal stretches that were slightly larger than the individual gene of *ceporH* (I), *ceporA* (II) and a fragment carrying both genes (III) (Hünten *et al.*, 2005b). PCR reactions and conditions used were identical to those described for the PCR isolation of the homologous *C. glutamicum* genes (see i to iii), differing only in the applied template and primers (Table 3.2). The PCR products of FP Ce_A_XbaI/RP Ce_HA_EcoRI (II) and FP Ce_HA_XbaI/RP Ce_HA_EcoRI (III) were *Xba*I-*Eco*RI double-digested and ligated in the backbone of similarly cut pXMJ19 vector resulting in pX_{Ce}-A (II) and pX_{Ce}-HA (III). The amplificate of FP Ce_HA_XbaI/RP Ce_H_BamHI (I) was subsequent to *Xba*I and *Bam*HI cleavage inserted into suitably digested pXMJ19 vector, designated pX_{Ce}-H.

3.3.2.3 Cloning of *C. diphtheriae* porins

The plasmid pX_{Cd}-WT corresponds to the expression plasmid described by Schiffler *et al.* (2007). It contains a PCR-amplified genomic fragment from *C. diphtheriae* ATCC 11913 that complemented the channel deficiency of the *C. glutamicum* Δ*porH*Δ*porA* mutant. Site-directed mutagenesis was used to study the participation of fragment-encoded polypeptides involved in the process of channel formation. For this purpose, the TOPO 2.1 vector with the original PCR amplicon of strain ATCC 11913 (Schiffler *et al.*, 2007) was subjected to quick change (QC) PCR using Pfu DNA polymerase (Fermentas) and QC primers of Table 3.2 (e.g. FP Cd_WTQC1/RP Cd_WTQC1) as described by the manufacturers. Subsequently, the plasmid with the parental template was digested with *Dpn*I (Fermentas) to select for mutation-containing plasmids, which were then transformed in One Shot Top10 F' cells. Plasmid mini-

Section of the *C. glutamicum* chromosome
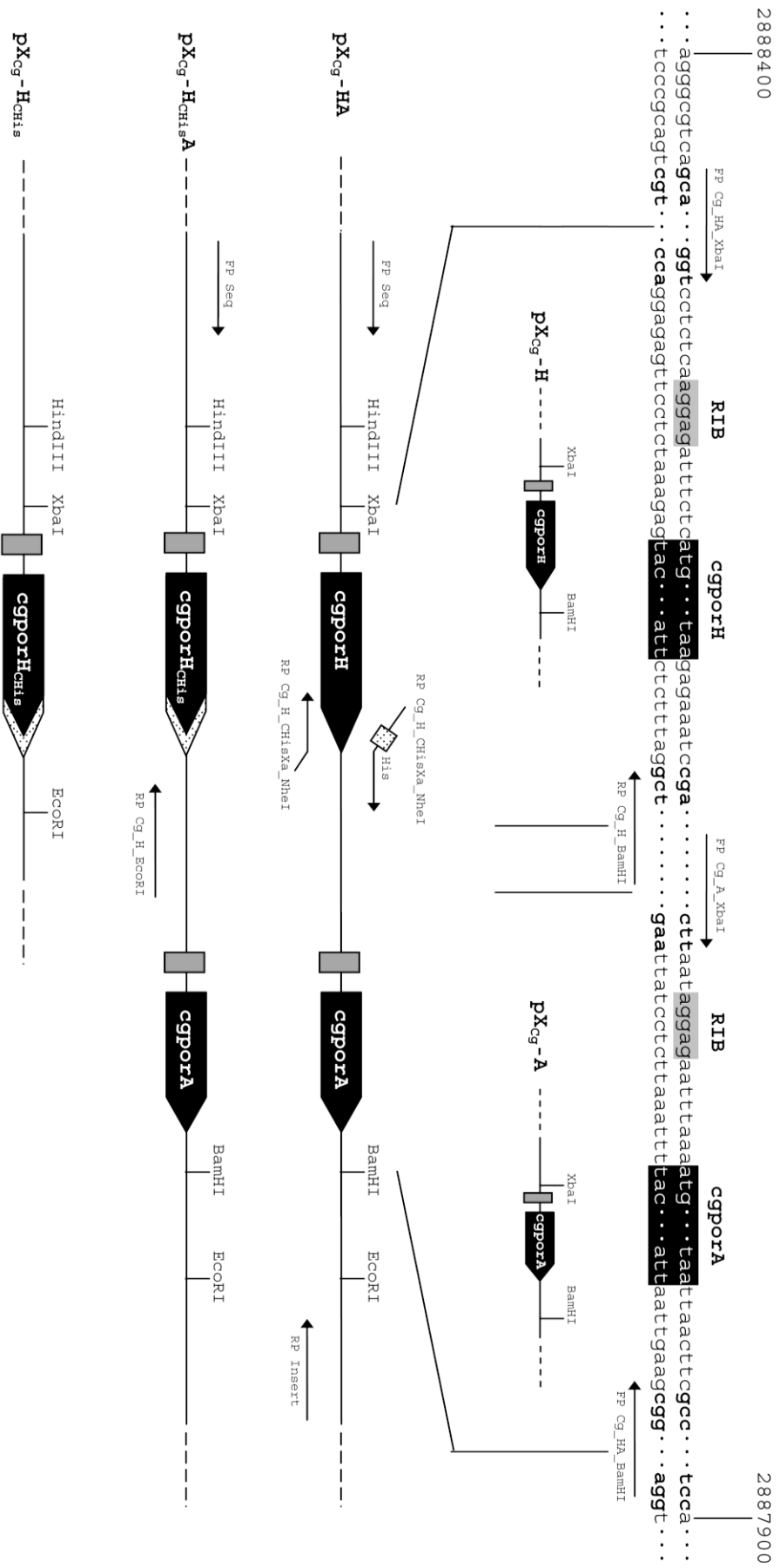
Figure 3.1: Illustration of the cloning strategy to obtain complementation plasmids with mono- and bicistronic porin sequences of *C. glutamicum*. Putative ribosome binding sites (RIB) are shaded in grey; porin genes *cgporH* and *cgporA* are shaded in black. Boldface letters next to arrows indicate partial primer sequences according to Table 3.2.

Oligonucleotides	Sequence 5' → 3'	Position
FP Cg_HA_XbaI	GCAAACTGGCAACCATC<u>TCTAGA</u>TTTCTTTGCTGGT	2888391-2888356†
RP Cg_HA_BamHI	GGATCAGAGTTTTT<u>GGATCC</u>TTTGCCCGTGGGC	2887933-2887901†
FP Cg_A_XbaI	CACAGCCTTCCCC<u>TCTAGA</u>CCTCATCTCAACTCTT	2888130-2888096†
RP Cg_H_BamHI	GGAAGGCTGT<u>GGATCC</u>TAGCCAATCAGCCAAATCG	2888154-2888119†
RP Cg_H_EcoRI	GGAAGGCTGT<u>GAATTC</u>TAGCCAATCAGCCAAATCG	2888154-2888119†
FP Seq	GTGAGCGGATAACAATTTCAC	-
RP Insert	CTCTCATCCGCCAAAACAGC	-
FP A_NHisXa_NheI	AGAATTTAAAATG<u>GCTAGC</u>CGCGGATCCCATCACCATCACCATCACCATCACATCGAAGGCCGCGAAAACGTTTACGAGTTCCTTGGA	-
RP A_NHisXa_NheI	GATGGGATCCGCG<u>GCTAGC</u>CATTTTAAATTCTCCTATTAAGAGTTGAGATGAG	-
FP H_CHisXa_NheI	ATCGAAGGCCGC<u>GCTAGC</u>CGCGGATCCCATCACCATCACCATCACTAAGAGAAATCCGATTTGGCTGATTGGCTA	-
RP H_CHisXa_NheI	GGATCCGCG<u>GCTAGC</u>GCGGCCTTCGATGGAAGAGAAGTTATCCAGATTCTCGCC	-
FP Ce_HA_XbaI	CAAACTGGCAACCATC<u>TCTAGA</u>TTATTTGCTGGTCC	2727847-2727882‡
RP Ce_HA_EcoRI	GGACGGGAGCT<u>GAATTC</u>TACGCCGGAGCG	2727431-2727403‡
FP Ce_A_XbaI	CCTAGAAGCTGAGAT<u>TCTAGA</u>CTTTTTCTTAATCTC	2727628-2727593‡
RP Ce_H_BamHI	CAGCTTCTAGGT<u>GGATCC</u>CCTAGCAGCAAGA	2727648-2727618‡
FP Cd_WTQC1	GCTATTCACAATAGGATATTTTTGTAGTGCTCTTGCGGC	
RP Cd_WTQC1	GCCGCAAGAGCACTACAAAAATATCCTATTGTGAATAGC	
FP Cd_WTQC2	CTCAAGGAGGAAGATTAGGACATTCAGTTCA	
RP Cd_WTQC2	TGAACTGAATGTCCTAATCTTCCTCCTTGAG	
FP Cd_WTQC3	GAAAGGGGTTAAATTAGCAGAACATTGAGA	
RP Cd_WTQC3	TCTCAATGTTCTGCTAATTTAACCCCTTTC	
FP Cg_KO_HA_CHECK2	ACATGCACGGCAACCTTCCGTTAAC	2888780-2888756†
RP Cg_OPERON_1_5	CTTCAGCAGCTCGATCGGAG	2887621-2887601†
FP Cg_H	ATGGATCTTTCCCTTCTCAAGG	2888336-2888315†
RP Cg_H	TTAGGAAGAGAAGTTATCCAGA	2888184-2888163†
RP Cg_A	TTAGCCAAGCAGACCGATGAG	2887942-2888308†
RP Cg_Extension2	CACCGAAGGTCTCGTAGTTGCCGA	2888285-2888308†
FP Cc_HA1	GACCACTGAGGCTGTCGTTGCTGACAAG	2888961-2888988†
RP Cc_HA3	TTGAAGCGCTTAATGGTGCCACCCTTACC	2887506-2887534†

Table 3.2: Oligonucleotides of the study. Primer binding positions in the chromosomes of the accessible genomes of *C. glutamicum* ATCC 13032 (Ref.Seq. NC_003450 †) and *C. efficiens* AJ 12310 (NC_004369 ‡) are provided. Recognition sites of restriction enzymes are underlined.

prep of *Escherichia coli* cells was used for sequencing (Seqlab) mutated amplicons with primers M13 forward and reverse (Invitrogen). Amplicons with the intended mutations were *EcoR*I and *Xba*I cut from the TOPO 2.1 plasmid and inserted into the backbone of pXMJ19. The resulting vectors were designated pX$_{Cd}$-WTQC1, pX$_{Cd}$-WTQC2 and pX$_{Cd}$-WTQC3.

3.3.2.4   Cloning of the porin domain of *C. callunae*

The region harbouring the genes that encode the PorH and PorA homologues of *C. callunae* was cloned with the FailSafe PCR system. Amplification of this region was performed in a 50 µl reaction using chromosomal DNA of the *C. callunae* strain ATCC 15991 as template, primers FP Cc_HA1/RP Cc_HA3 (Table 3.2), Failsafe polymerase and buffer E according to the manufacturer's advice. PCR conditions were: initial denaturing at 95°C for 5 min, 30 cycles at 95°C for 1 min, 45°C for 1 min, 72°C for 3 min and a final extension at 72°C for 10 min. The reaction was loaded on a 0.8% agarose gel and compared to a 1 kb ladder (GeneRuler, Fermentas). The PCR product was cut out of the gel, ligated in the TOPO 2.1 cloning vector (Invitrogen) and transformed in One Shot Top10 F' cells. Minipreped plasmids of the *E. coli* cells were used for sequencing the amplicon with primers M13 forward and reverse.

3.3.3   Extraction of RNA

Total bacterial RNA (tRNA) was extracted by use of the RNeasy Mini Kit (Qiagen, Hilden, Germany) as described by the supplier with minor modifications. The bacterial pellet of 10 ml of a *C. glutamicum* culture, which was grown to an OD$_{600}$ of about 3, was resuspended in 700 µl RLT (lysis buffer) supplemented with β-mercaptoethanol and transferred to a 2 ml screw-cap tube containing 300 mg glass beats. The sample was homogenized in a Fastprep120 cell disrupter (ThermoSavant) at maximum speed for 45 sec at 4°C. Glass beats and cell wall debris were removed by centrifugation (13000 rpm, 1 min, RT), and the supernatant was mixed with 500 µl ethanol before it was loaded onto a RNeasy column. RNA isolation was then performed as described in the supplier's protocol. Concentration of the eluted RNA was determined by measuring the absorbance at 260 nm. When the 260/280 absorbance ratio was to exceed 1.9, the RNA eluate was considered to be pure. For downstream applications, such as Northern blotting, RNA integrity was checked visually by denaturing formaldehyde

agarose gel electrophoresis combined with ethidium bromide staining of 16S and 23S ribosomal RNA bands.

3.3.4 DIG-labelled DNA probes

DNA probes, used for transcript analysis, were complementary to the *cgporH* and *cgporA* RNA sequences of *C. glutamicum*. The design of probe_porH (5'-TCCAGATTCTCG CCGGTGGTGTCAGCGAGA-3') and probe_porA (5'-CCGATGAGGTCAGCAACTGCGC CAGCCCAC-3') was based on non-homologous gene stretches. Both probes were received as 3' digoxygenin (DIG) labelled oligonucleotides from MWG Biotech (Ebersberg, Germany). Prior to hybridization, the probes were denatured by incubation at 95°C for 10 min.

3.3.5 Northern blot analysis

For the purpose of performing a Northern blot analysis, 5 µg of *C. glutamicum* tRNA isolated from the wild-type strain and the Δ*porA* mutant was fractionated on a denaturing agarose gel (2% agarose, 1 × morpholinepropanesulfonic acid [MOPS], [1 × MOPS is 20 mM MOPS, 5 mM sodium acetate, 2 mM EDTA (pH 7)], 2% formaldehyde). The size-separated tRNA was then transferred to a Nytran N membrane (Schleicher&Schuell, Germany) overnight by capillary transfer (Sambrook & Russell, 2001) with 20 × SSC (3 M NaCl, 300 mM sodium citrate, pH 7) and fixed by ultraviolet cross-linking (Stratalinker UV Crosslinker 2400, Stratagene). Reactive membrane binding sites were blocked through prehybridization in DIG Easy Hyb (Roche Applied Science, Mannheim, Germany) for 45 min at 45°C on a rotary shaker. Hybridization with probes (50 ng/ml) was performed overnight in the same solution at 50°C. Subsequent to the removal of the hybridization solution, membranes were first washed twice for 10 min in 2 × SSC/0.1% (w/v) SDS at room temperature, and then twice for 15 min in 0.1 × SSC/0.1% (w/v) SDS at 50°C. Bound DIG-labelled probes were detected by use of the DIG Luminescent Detection Kit (Roche Applied Science), with CSPD (provided with the kit) as the alkaline phosphatase substrate, according to the instructions of the manufacturer. Developed blots were exposed to autoradiography film (HyperfilmMP, GE Healthcare, UK) for 30 to 60 min. Determination of the size of the detected signals was performed based on 16S and 23S ribosomal RNA bands (1.5 and 2.9 kbp, respectively), stained with ethidium bromide.

3.3.6   Reverse transcription

Trace elements of contaminating chromosomal DNA in a tRNA eluate were eliminated by DNaseI (Turbo DNA, Ambion, Foster City, CA) digestion. Subsequently, the added enzyme was removed with the Ambion DNase Inactivation Reagent. Reverse transcription was performed with minor variations according to the supplied two step protocol of the used Enhanced Avian RT-PCR Kit (Sigma-Aldrich, Munich, Germany). In the first step, 1.5 µg tRNA was reverse transcribed into single-stranded cDNA. The 20 µl reaction contained 1 × AMV-RT buffer, 250 µM dNTPs, 1.25 µM random nonamers, 20 U RNase inhibitor and 20 U AMV reverse transcriptase. The reaction was incubated 15 min at 25°C and additional 50 min at 45°C. In the second step, a target of the cDNA was amplified by PCR in a 25 µl reaction containing 3 µl of the cDNA, 1 × AccuTaq buffer, 200 µM dNTPs, 1.25 U AccuTaq LA DNA polymerase mix and 0.4 µM primers (see *Results*). Identical PCR reactions were setup with not reverse transcribed tRNA used as template to exclude false positive results.

3.3.7   5' Rapid amplification of cDNA ends

The transcription start point (TSP) was determined using the rapid amplification of cDNA ends (RACE) method. Following the protocol supplied with the chosen 5'/3' RACE Kit (Roche Applied Science), 1.3 µg of DNaseI-treated *C. glutamicum* tRNA (see section RT-PCR) were reverse-transcribed into first strand cDNA in a 20 µl reaction. The reaction included 1 × cDNA synthesis buffer, 1 mM dNTPs, 12 U RNase inhibitor, 25 U Transcriptor reverse transcriptase and 1.5 µM of the gene-specific primer RP Cg_H (Table 3.2, Fig. 3.2). It was incubated for 60 min at 55°C. The produced cDNA was purified with the High Pure PCR Product Kit (Roche Applied Science) and poly(A)-tailed by a terminal transferase at its 3' end. This modified cDNA was subsequently PCR-amplified in a 50 µl reaction making use of Taq DNA polymerase (Fermentas) and primers Oligo dT-Anchor (Roche)/RP Cg_Extension2 (Table 3.2). The PCR conditions were: initial denaturing at 95°C for 5 min, 35 cycles at 95°C for 1 min, 52°C for 1 min, 72°C for 45 sec and final extension at 72°C for 10 min. The PCR product was gel-purified and subjected to a second PCR with the nested primers PCR Anchor (Roche)/RP Cg_Extension2. This amplificate, again gel-purified, was sequenced with primer RP Cg_Extention2 (Seqlab). The transcription start point was identified due to its direct localization next to the poly(A) tail.

mRNA   5' ⌇⌇⌇⌇⌇ [cgporH] ⌇⌇⌇ → 3'   synthesis of the first strand cDNA with primer RP Cg_H

RP Cg_H

cDNA   3' ⋯⋯⋯⋯ 3'   degradation of the mRNA template by RNase H activity of the reverse transcriptase

poly (A)-cDNA   3' $(A)_n$AAA ———— 5'   tailing of the cDNA by a terminal transferase

Oligo dT-Anchor

$(T)_n$TTTV
$(A)_n$AAAA ————

RP Cg_Extension2   first PCR amplification of the tailed cDNA by using Oligo (dT)-Anchor and RP Cg_Extension2

PCR Anchor   second PCR amplification with PCR Anchor and RP Cg_Extension2

RP Cg_Extension2

gel purification and sequencing

V = A, C or G

Figure 3.2: Illustration of the RACE method used for determination of the transcription start point heading the messenger RNA of the co-transcribed porin genes from *C. glutamicum* (*cgporA* is not shown).

3.3.8   Isolation of the channel-forming proteins

For the isolation of the channel-forming proteins a method was used that has previously been introduced by Lichtinger *et al*. (1998). It is based on the extraction of whole cells with detergents or organic solvents and avoids the substantial loss of material caused by sucrose density centrifugation of the cell envelope to separate the cytoplasmic membrane from the cell wall fraction. Cells of a 100 ml overnight BHI culture of *C. glutamicum*, grown to an OD_{600} of about 6, were harvested by centrifugation (5000 rpm for 10 min in Heraeus Minifuge RF centrifuge). The bacterial pellet was washed twice with 1/10 culture volume of Tris-buffer (10 mM Tris, pH 8). One part of the cells (0.3 g wet weight of the bacterial pellet) was resuspended in five parts detergent (1.5 ml 1% LDAO, 10 mM Tris, pH 8) or organic solution (1.5 ml of chloroform/methanol at a [v/v] ratio of 1:2). The cell suspension was then agitated in a closed tube for 3 h at RT. As the channel-forming proteins were expected to be in the supernatant (Hünten *et al*., 2005a; Hünten *et al*., 2005b; Lichtinger *et al*., 1998), cells were pelleted using a table top centrifuge (10000 rpm for 10 min at 4°C) and discarded. Proteins isolated with organic solvents were precipitated overnight at -20°C by adding to the chloroform-methanol solution a volume of ice-cold diethyl ether that was 9-fold greater than the volume of the solution. The resultant (protein) pellet was resolved in detergent (0.4 to 1%

LDAO, 10 mM Tris, pH 8). Organic solvent extraction and detergent extraction were both applied for the isolation of cell wall proteins. The cell preparations were investigated for the presence of channel-forming proteins using artificial black lipid membranes.

3.3.9   Affinity purification with immobilized Ni^{2+}-ions

The proteins $CgPorH_{CHis}$ and $CgPorA_{NHis}$ were purified to homogeneity from pX_{Cg}-H_{CHis} or pX_{Cg}-A_{NHis} complemented and overnight IPTG-induced $\Delta porH\Delta porA$ cells of *C. glutamicum*. Whole cells were extracted with detergent buffer (1% LDAO, 20 mM Tris, pH 8) as described above. The supernatant was loaded onto Ni-NTA spin columns (Qiagen, Hilden, Germany) pre-equilibrated with buffer 1 (20 mM Tris-HCl, pH 8). Proteins that have interacted with the Ni^{2+}-matrix were washed 10 × with 650 µl of buffer 2 (0.4% LDAO, 50 mM NaCl, 20 mM Tris-HCl (pH 8), 50 mM imidazol). Bound protein was eluted with 2 × 200 µl of buffer 3 (buffer 2 supplemented with 250 mM imidazol). All centrifugation steps were done at RT in a table top centrifuge at 2000 rpm.

3.3.10   Digestion with Factor Xa protease

When necessary, the histidine tag of IMAC purified proteins was removed by Factor Xa treatment. For this purpose, the eluate containing the purified protein was dialysed against Xa buffer (0.4% LDAO, 1 mM $CaCl_2$, 50 mM NaCl, 20 mM Tris-HCl, pH 6.5) using the Spectra/Por Micro DispoDialyser (Carl-Roth, Karlsruhe, Germany) for at least 3 h. The cleavage was performed overnight with 4 units Factor Xa.

3.3.11   Protein electrophoresis, immunoblotting and antibodies

Protein samples were size-separated by Tris-Tricine 12% or 16.5% polyacrylamide gel electrophoresis (PAGE) (Schägger & von Jagow, 1987). For protein visualization, the gels were either stained with Coomassie brilliant blue, silver stain (Blum *et al.*, 1987) or immunoblotted (Towbin *et al.*, 1979). In the case of the latter method, proteins were at first transferred to a 0.1 µm nitrocellulose membrane (Protran, BA79, Whatman) using a wet tank blot system with Towbin buffer (25 mM Tris, 192 mM glycine, 20% methanol). Because of

the low-molecular-mass of the porin proteins, the blotting time was 4 min at 350 mA current. Reactive binding sites on the membrane were blocked with 5% skimmed milk in TBS-T buffer (0.1% Tween, 0.01 M NaCl, 20 mM Tris-HCl, pH 7.5). As primary antibodies, we used polyclonal rabbit anti-PorH antibodies (Hünten *et al.*, 2005a), polyclonal rabbit anti-PorA antibodies (Lichtinger *et al.*, 1998) or monoclonal mouse anti-His antibody (Amersham Biosciences, UK) at dilutions of 1:2500, 1:8000 and 1:5000, respectively, to detect porin proteins of *C. glutamicum* (i.e., CgPorH, CgPorA, CgPorH$_{CHis}$, or CgPorA$_{NHis}$). As secondary antibodies, we applied peroxidase-conjugated anti-Rabbit or anti-Mouse antibodies (DAKO, Denmark) at a dilution of 1:5000. For visualization of detected proteins the enhanced chemiluminescent Western blot detection system (GE Healthcare, UK) and autoradiography film (HyperfilmMP, GE Healthcare, UK) were used according to the manufacturer's instructions. The exposure time that was necessary until an observable signal appeared varied between 20 seconds up to a couple of minutes, as required by the sample.

3.3.12 Black lipid bilayer assay

The principles used for the lipid bilayer experiments have been described previously in detail (Benz *et al.*, 1978; Benz, 2003). The core of the experiment is a Teflon chamber which is divided into two aqueous compartments. Both aqueous compartments are connected by a small circular hole with a surface area of about 0.2 mm^2. Artificial lipid bilayers were formed by painting onto the hole a 1% (w/v) solution of diphytanoyl phosphatidylcholine (PC) (Avanti Polar Lipids, Alabaster) in *n*-decane. For the electrical measurements two Ag/AgCl electrodes are submerged to each compartment. One electrode is joined to a voltage source and allows the application of defined membrane potentials on the *cis* side of the membrane. The resulting current through the membrane was detected by the second electrode on the *trans* side, which was connected to a current-to-voltage converter made from a Burr Brown operational amplifier. The amplified signal was monitored on a digital oscilloscope and recorded with a strip chart recorder. KCl was obtained at analytical grade from Merck (Darmstadt, Germany) and used unbuffered. During all experiments, the temperature was maintained at 20°C.

3.4   Results

3.4.1   Northern analysis of the genes *porH* and *porA* of *C. glutamicum* show a bicistronic transcript

A previous study (Hünten *et al.*, 2005a) suggested that the genes *porH* and *porA* of *C. glutamicum* could belong to a transcriptional unit consisting of up to 13 coding DNA sequences (CDS). Putative transcriptional terminators within this gene cluster indicate, however, the possibility of different sized transcripts. We thus performed Northern blot experiments to identify the transcripts of *cgporH* and *cgporA* of *C. glutamicum* because the gene products of both genes were shown to possess channel-forming activity in previous studies (Hünten *et al.*, 2005a; Lichtinger *et al.*, 1998). *C. glutamicum* was cultured in BHI as well as in CGXII media. The Δ*porA* strain of *C. glutamicum* served to exclude unspecific binding of applied DNA probes where possible. Cells of the wild-type and the *porA* ⁻ strain were harvested at the mid-exponential growth phase by centrifugation and the bacterial pellets were used for tRNA isolation.

Figure 3.3A shows a Northern blot of the transcripts of *cgporH* and *cgporA* of *C. glutamicum*. The same amounts of tRNA of BHI-cultured *C. glutamicum* and Δ*porA* cells were blotted onto a nylon membrane after size separation. Transcripts of *cgporH* (probe_porH) and *cgporA* (probe_porA) were detected by DIG-labelled DNA probes derived from non-homologous regions of the genes. For probe detection anti-DIG Fab fragments conjugated to alkaline phosphatase were applied and chemiluminescent signals were recorded. In slots with tRNA of the wild-type strain probe_porH as well as probe_porA resulted in detection of single bands with comparable sizes. No band was observed in slots with tRNA of the *porA* ⁻ strain. In case of cells cultured in minimal medium a similar result was obtained (data not shown). This means that the transcription of both porin genes occurred independent of the culture medium. Lack of the probe_porH signal in the slot of the mutant strain indicated that the *cgporH* transcript is somehow affected by the deletion of *cgporA* (see *Discussion*).

A)

B)
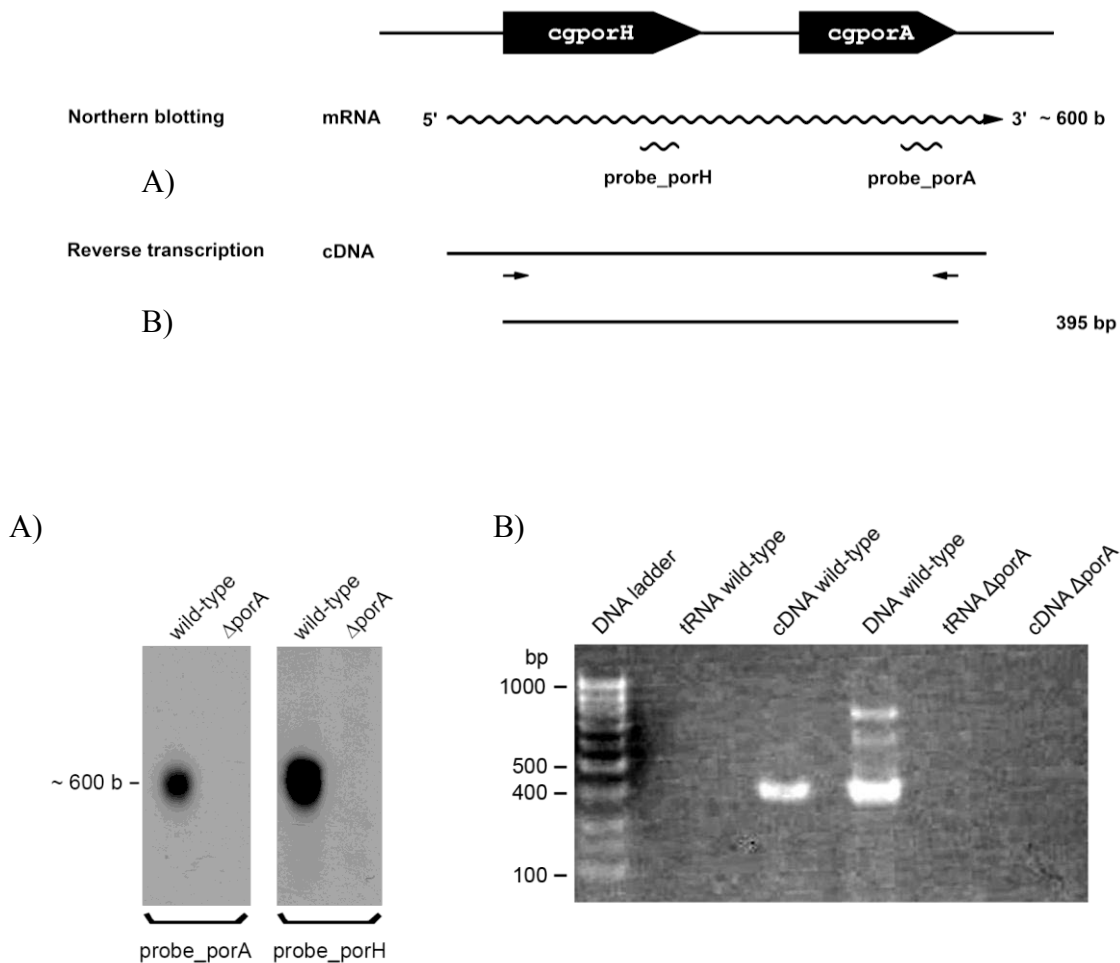
Figure 3.3: Transcript analysis of *porH* and *porA* of *C. glutamicum*. Total RNA was isolated from the wild-type and a mutant strain deficient of *porA* (Costa-Riu *et al.*, 2003a). (A) shows Northern blots of a single membrane in which 5 µg tRNA of *C. glutamicum* cells grown in BHI medium were probed with either a *porH* or a *porA* probe. A co-transcript of approximately 600 b was detected. (B) depicts an agarose (1.5%) gel with a comparable sized co-transcript obtained by RT-PCR from a *porH* and a *porA* specific primer. A lacking PCR product in the control agreed with the *porA* deficiency of the mutant cells. The cells in this experiment were grown in BHI medium.

The bands in Fig. 3.3A had sizes of about 600 bases. The ORFs of *cgporH* (174 bp) or *cgporA* (138 bp) are obviously undersized to match the bands. According to the deposited genome data of *C. glutamicum* (GenBank Accession number NC_003450) direct neighbours of *cgporH* are NCgl2621 (ORF 1647 bp) (Barreiro *et al.*, 2004) and *cgporA* followed by NCgl2620 (ORF 921 bp) (Lindner *et al.*, 2007). Because of the size of the four genes we deduced absence of NCgl2621 and NCgl2620 as part of the detected transcripts. Only a transcriptional unit of *cgporH* and *cgporA* (taking into account 83 bases of the region between both genes) could nearly account for the observed Northern blot signals.

3.4.2 RT-PCR analysis confirms the bicistronic transcript in *C. glutamicum*

Total RNA of both the wild-type and the *porA*⁻ strain of *C. glutamicum* were transcribed by reverse transcription into cDNA using random nonamers. Subsequently, the obtained cDNA was PCR-amplified using *cgporH* and *cgporA* specific primers (FP Cg_H and RP Cg_A). As shown in Fig. 3.3B, the RT-PCR resulted in the amplification of a wild-type DNA fragment with a size of about 400 bp. No PCR product could be obtained in control experiments where cDNA of the *porA*⁻ strain was used as template. The chromosomal template DNA of the wild-type strain was used as positive control and further resulted in minor unspecific PCR products. RT-PCRs intended to connect the coding sequences of NCgl2620 and NCgl2621 to the bicistronic porin transcript in an approach similar to Fig. 3.3B resulted negative (data not shown).

3.4.3 The transcription start point of the *porH-porA* transcript of *C. glutamicum*

C. glutamicum cultured in BHI was used for analysis of the 5' TSP of the porin co-transcript as described in the section *Material & Methods* of this chapter. Data of the sequenced PCR product determined guanine as TSP. This point was located 75 bases upstream of the inducer methionine of CgPorH (Fig. 3.4). In comparison to canonical hexamers TTGACA and TATAAT of *E. coli* and *Bacillus subtilis* (Harley & Reynolds, 1987; Helmann, 1995), promoter sequences of *Corynebacterium* species are less well conserved. An analysis of the region in front of the TSP suggested a putative promoter corresponding to the transcript. The associated -10 TTGAAT and -35 TTGACG hexamers of the porin promoter (Fig. 3.4) show homology to the consensus sequences -10 tgngnTA(c/t)aaTgg and -35 TTGGCA suggested for vegetative genes (Patek *et al.*, 2003; Vasicova *et al.*, 1999).

3.4.4 Transcriptional terminators flank the *porH-porA* region in *C. glutamicum*

With the aid of the tool TransTermHP (Kingsford *et al.*, 2007), the non-coding region between NCgl2621 and NCgl2620 was searched for inverted repeat sequences that may form stem and loop structures. Two distinctive rho-independent terminators were predicted within the region (Fig. 3.4). The first structure (5'-GCCCTCCCGCACGCTTTGCGGGAGGGC-3') is located downstream of NCgl2621, whereas the second structure (5'-AAAAACTCTGA

TCCATATGGATCAGAGTTTTT-3') is positioned downstream of *cgporA*. Both sequences presumably form hairpins with free energy levels of -21.8 and -15.7 kcal/mol, respectively (http://www.genebee.msu.su). Noteworthy, no terminator was found within the intergenic region between *cgporH* and *cgporA*.

3.4.5   Genotype and phenotype of the used *C. glutamicum* expression strain

The cell wall of *C. glutamicum* contains two prominent channel-forming units of large ion conductance. These units have previously been proposed to be formed by separate CgPorH and CgPorA proteins (Hünten *et al.*, 2005a; Lichtinger *et al.*, 2001). Northern blot analysis shown above, demonstrated that the corresponding genes constituted for a transcriptional unit. Even though this observation was not necessarily in conflict with the previous assumptions of individual channels, it was in line with rather than excluding an interaction of both proteins. We clarified the question by taking advantage of the channel deficiency of a *porH* and *porA* knock-out mutant of *C. glutamicum* to reconstitute the wild-type pores. The chromosomally deleted region (Schiffler *et al.*, 2007) of the double porin mutant is shown in Fig. 3.4 in comparison to the wild-type strain. Importantly, both detergent and organic solvent preparations of the PorH- and PorA-deficient strain produced in lipid membranes no longer large ion-conducting channels, as it has already been shown previously (Schiffler *et al.*, 2007).

3.4.6   Functional analysis of the bicistronic porin transcript of *C. glutamicum*

Plasmid complementation was used to answer the question if the PorH and PorA proteins form alone or together the channels in the cell wall of *C. glutamicum*. This was done by restoring either one or both gene defects of the Δ*porH*Δ*porA* mutant by using different constructs coding for CgPorH or CgPorA or for both. Cells of the mutant were electrotransformed with plasmid pX$_{Cg}$-H, pX$_{Cg}$-A, or pX$_{Cg}$-HA. Expression of the porin proteins was in each plasmid-complemented strain induced overnight by IPTG addition. Extraction with organic solvents was used to isolate the expressed porin proteins from harvested cells. Chloroform-methanol extracts were precipitated with ether in the cold, and the precipitate was resolved in 1% LDAO detergent. Channel-forming activity of all precipitates was studied using a 1 M KCl solution that bathed black lipid membranes formed

```
                              NCgl2621 (GroEL)
Cgl WT   GACGAGATGGGCGGCATGGGCGGCTTCTAAGCCCCTCATTCGCGCACCTC   2888875
                              hairpin
Cgl WT   AATTGCCCTCCCGCACGCTTTGCGGGAGGGCTTTTGCGTGTCAAAAGATA   2888825
Cgl WT   TTGCTTTTCGACGTCTCCCCACACCTTCGGAGGGGCGTAAGGTGACATGC   2888775
Cgl WT   ACGGCAACCTTCCGTTAACCTGCTAGACATCTCAAATCTTGATAAAAAAG   2888725
Cgl WT   ACTAACTCCACACCTTTTTTCGACCACCCCACTTAGCCAATGGTGTAAAT   2888675
Cgl WT   TACCCCCATATTAGGGTGTGTATGACAATCGCTTTTTTAAAGTTTCGCTT   2888625
Cgl WT   TAATCGAGCCGTTGTTAAGTAGTGTTACACCTTCATGGGGTTTAGCTGGA   2888575
Cgl WT   AAGTTTTCTCCCTGTTCACTTAAATATCTAACATTTCTGCAGGTCAAGAT   2888525
Cgl WT   ATATTTACGGGAAAAATCGTCAAATAATTCTTTGCTGAGTTTGGTTGAAA   2888475
                                            -35
Cgl WT   AGCACGCTGGGAAACTTTCCTGATTCGCCTTGACGTGTTGTCAAAATGTG   2888425
              -10            ⌐→TSP
Cgl WT   ATTGAATAATTGAGTGACGTCCTGAGGGCGTCAGCAAACTGGCAACCATC   2888375
CglΔHΔA   ATTGAATAATTGAGTGACGTCCTGAGGGCCC------------------
                              RBS          cgporH
Cgl WT   ACCAGCTTTCTTTGCTGGTCCTCTCAAGGAGATTTCTCATGGATCTTTCC   2888325
CglΔHΔA   --------------------------------------------------
Cgl WT   CTTCTCAAGGAAACCCTCGGCAACTACGAGACCTTCGGTGGCAACATCGG   2888275
CglΔHΔA   --------------------------------------------------
Cgl WT   TACCGCTCTTCAGAGCATCCCAACCCTGCTCGATTCCATCCTTAACTTCT   2888225
CglΔHΔA   --------------------------------------------------
Cgl WT   TCGACAACTTCGGAGATCTCGCTGACACCACCGGCGAGAATCTGGATAAC   2888175
CglΔHΔA   --------------------------------------------------
Cgl WT   TTCTCTTCCTAAGAGAAATCCGATTTGGCTGATTGGCTAAAATCCACAGC   2888125
CglΔHΔA   --------------------------------------------------
                              RBS          cgporA
Cgl WT   CTTCCCCCTTCCCCCTCATCTCAACTCTTAATAGGAGAATTTAAAATGGA   2888075
CglΔHΔA   --------------------------------------------------
Cgl WT   AAACGTTTACGAGTTCCTTGGAAACCTTGATGTCCTTTCCGGCTCCGGCC   2888025
CglΔHΔA   --------------------------------------------------
Cgl WT   TCATCGGCTACGTCTTCGACTTCCTCGGCGCTTCCAGCAAGTGGGCTGGC   2887975
CglΔHΔA   --------------------------------------------------
Cgl WT   GCAGTTGCTGACCTCATCGGTCTGCTTGGCTAATTAACTTCGCCCACGGG   2887925
CglΔHΔA   --------------------------------------------------
                              hairpin
Cgl WT   CAAAGTTTTCAAAAACTCTGATCCATATGGATCAGAGTTTTTTCGTATCT   2887875
CglΔHΔA   ---AGTTTTCAAAAACTCTGATCCATATGGATCAGAGTTTTTTCGTATCT
Cgl WT   GCCACCAGAAAGACGCCCCTTTGGCACGCCGAATTAGTCAATGGTGGGTA   2887825
                           NCgl2620(PPK2B)
Cgl WT   AACTTCCCATCATGGCTGAAACCAACGAAAATGATCTTCCAGTTATCGAC   2887775
```

Figure 3.4: Comparison of the genotypes of *C. glutamicum* wild-type and Δ*porH*Δ*porA* mutant strains. The sequence of the mutant strain used for the alignment with the wild-type sequence is deduced from a sequenced PCR product obtained with primers FP Cg_KO_HA_CHECK2/RP Cg_OPERON_1_5 (Table 3.2) and template DNA of *C. glutamicum* Δ*porH*Δ*porA* (not shown). The deleted region comprises 472 bp, including both genes *porH* and *porA* (black highlighted) coding for the components of the main cell wall channel of *C. glutamicum*. The boldface type indicates CDSs adjacent to the porins. The TSP of the *porH-porA* co-transcript is marked by a broken arrow. Putative -10 and -35 boxes are shown by underlined italics. Boldface italics sign putative ribosome binding sites (RBS) whereas double underlined letters indicate rho-independent hairpin terminators (Kingsford *et al.*, 2007). The numbers to the right of the nucleotide sequence correspond to the position in the genome of *C. glutamicum* with the GenBank Accession number NC_003450.

83

from PC/*n*-decane. The precipitate of *cgporH* and *cgporA* complemented mutant cells (using plasmid pX$_{Cg}$-HA matching the wild-type genotype) showed high channel-forming activity (data not shown). Addition of the precipitate to the aqueous phase (about 10 ng/ml) of a black membrane resulted with a few minutes delay in a step-wise increase of ion conductance. The recorded single-channel events had a long-lifetime and were comparable to the prominent 2.5 and 5.5 nS channels of the *C. glutamicum* wild-type strain, as described previously by Lichtinger *et al*. (1998) and Hünten *et al*. (2005a). Surprisingly, no channels were recorded from precipitates of mutant cells complemented solely for the defect of *cgporH* (pX$_{Cg}$-H) and *cgporA* (pX$_{Cg}$-A), respectively.

3.4.7   Validation of the expression of CgPorH and CgPorA proteins

Expression failure could be the cause of the absent channel activity in mutant cells transformed with pX$_{Cg}$-H or pX$_{Cg}$-A. To check for this possibility, we subjected these and other organic solvent precipitates to SDS-PAGE containing tricine. Coomassie stain of the gel (Fig. 3.5A) revealed identical protein patterns. That means that bands of the porin proteins (about 5 kDa in size, Table 3.3) were overlaid by other low-molecular-mass protein bands. As a consequence, size-separated precipitates were immunoblotted either with anti-PorH or anti-PorA antibodies.
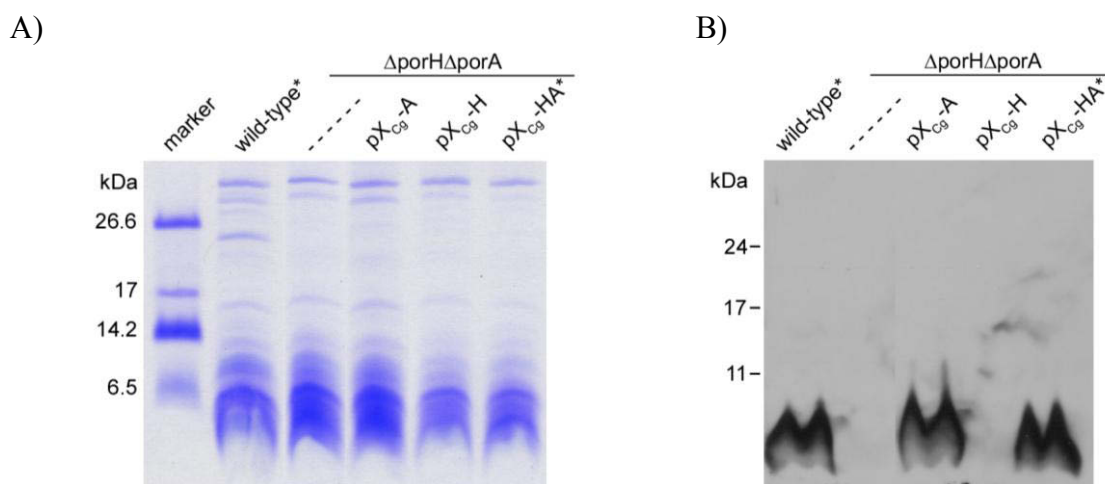
Figure 3.5: Protein pattern of organic solvent extracted *C. glutamicum* cells. The relevant genotypes are indicated above each lane. Dashed lines represent extracts of non -complemented *porH* and *porA* deficient *C. glutamicum* cells. (A) Tricine (12%)-PAGE of 50 µl ether-precipitated cell extracts dissolved in 15 µl sample buffer. (B) Western blot analysis of an identical loaded Tricine (12%)-PAGE gel probed with anti-PorA antibodies. Asterisks highlight samples showing channel-forming activity in the black lipid bilayer assay. Samples of either tricine-containing SDS-PAGE were treated for 5 min at 95°C prior to electrophoresis.

Figure 3.5B shows the chemiluminescent signals of a blot probed with anti-PorA immunoglobulins. The 5 kDa PorA protein was expressed in the wild-type but not in the *porH⁻* and *porA⁻* strain of *C. glutamicum*. An identical CgPorA-signal (expected because of channel activity) arose from the precipitate of mutant cells complemented with pX$_{Cg}$-HA. Astonishingly, also the non-pore-forming precipitate of cells transformed with pX$_{Cg}$-A resulted in an equally strong signal. Expression failure and lack of CgPorA was therefore excluded as cause of missing channel activity. Immunoblots with anti-PorH antibodies showed unfortunately unspecific binding in the low-molecular-mass region (data not shown). It seemed that one of the detected bands could correlate with the expression of the 6 kDa CgPorH monomer in respective precipitates. A missing PorH channel activity in the precipitate of pX$_{Cg}$-H complemented cells was thus not understandable, similarly as in the case of cells complemented with pX$_{Cg}$-A if both proteins formed homooligomeric channels. Inspired by the Western blot results, we mixed the precipitates from the mutant cells complemented either by pX$_{Cg}$-H or by pX$_{Cg}$-A. Interestingly, the mixture showed the same pore-forming activity in the lipid bilayer assay as the precipitate of the mutant strain complemented with pX$_{Cg}$-HA, which agreed again with the assumption that the major cell wall channel in *C. glutamicum* is formed by a combination of PorA and PorH.

3.4.8   Applicability of histidine fusion tags attached to CgPorH and CgPorA

A common method used for purification of proteins is to attach a histidine tag although the tag could influence or impede the function of the recombinant protein. To overcome this problem protease Xa cleavable histidine tags were attached to the N-terminus (NHis) or the C-terminus (CHis) of the two porin proteins coded by the plasmid pX$_{Cg}$-HA. The resultant plasmids pX$_{Cg}$-H$_{CHis}$A (coding for PorH$_{CHis}$/PorA channels) and pX$_{Cg}$-HA$_{NHis}$ (coding for PorH/PorA$_{NHis}$ channels) were transformed into cells of the Δ*porH* and Δ*porA* mutant of *C. glutamicum*. Organic solvent preparations of IPTG induced cells were precipitated with ether in the cold. Protein expression and translocation of the recombinant proteins into the cell wall of the *C. glutamicum* mutant, as judged by Western analysis using anti-His antibody, were very similar to those of the native proteins (not shown, compare Fig. 3.6A). Moreover, precipitates (solved in 1% LDAO) of organic solvent extracted plasmid-complemented strains showed in black lipid membranes the same channel-units as the native proteins from the wild-type strain (Hünten *et al.*, 2005a; Lichtinger *et al.*, 1998). This means that the histidine tag of

the recombinant protein (i.e., PorH$_{CHis}$ or PorA$_{NHis}$) caused no apparent change of the channel conductance indicating that the His-tags could not be localized in or close to the channel lumen. However, single-channel events of the PorH/PorA$_{NHis}$ type were clearly less frequent observed than channel events of the PorH$_{CHis}$/PorA type. The channel activity of the latter type was comparable to the activity of the native channel type. Protease Xa treatment of the precipitate of the mutant strain complemented with pX$_{Cg}$-HA$_{NHis}$ strongly increased the channel-forming activity.

3.4.9   Purification of recombinant CgPorH$_{CHis}$ and CgPorA$_{NHis}$ proteins

The described reconstitution experiments did not provide any indication that other proteins besides PorH and PorA were involved in the formation of the *C. glutamicum* major cell wall channel. However, we could not completely exclude such a possibility (Fig. 3.5A) and studied this question in more detail. PorH and PorA were expressed in the Δ*porH* and Δ*porA* mutant of *C. glutamicum* using the plasmids pX$_{Cg}$-H$_{CHis}$ and pX$_{Cg}$-A$_{NHis}$, respectively. This means that the cell wall of the mutant contained either the recombinant protein CgPorH$_{CHis}$ or CgPorA$_{NHis}$ after IPTG induction. The cells were extracted by detergent buffer, and the proteins were purified to homogeneity using Ni^{2+}-affinity chromatography.
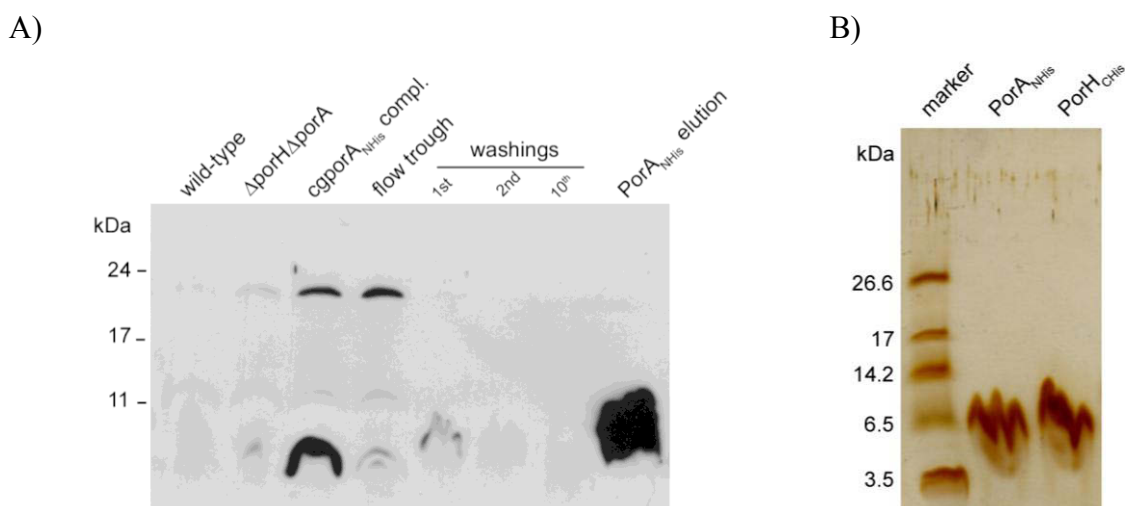
Figure 3.6: Analysis of the affinity purification of recombinant porin protein on a Ni-NTA column. Histidine-tagged proteins were concentrated from plasmid-complemented and detergent extracted *C. glutamicum* Δ*porH*Δ*porA* cells. (A) IMAC purification of PorA$_{NHis}$ is shown. Indicated fractions were separated by Tricine (12%)-PAGE, blotted onto a nitrocellulose membrane and probed with anti-His antibody. (B) Silver stain of IMAC purified PorA$_{NHis}$ and PorH$_{CHis}$ proteins separated in a 12% tricine SDS-PAGE.

Figure 3.6 shows the different purification steps of the Ni^{2+}-affinity chromatography yielding an eluate enriched in $CgPorA_{NHis}$. The purified proteins were subjected to Western blotting using anti-His antibody as primary immunoglobulin and were found to be pure (Fig. 3.6A). Similarly, the two proteins were free of contaminants according to an overloaded and silver-stained tricine-containing SDS-PAGE of both purified proteins (Fig. 3.6B).

3.4.10 The cell wall channel of *C. glutamicum* is exclusively composed of PorH and PorA proteins

Above we could demonstrate that the combinations $PorH/PorA_{NHis}$ and $PorH_{CHis}/PorA$ were able to form channels in reconstitution experiments, indicating that one His-tag attached to PorA or PorH did not inhibit channel formation. However, when PorA and PorH contained His-tags, i.e. when the combination $PorH_{CHis}/PorA_{NHis}$ was used in the reconstitution experiments, it was not possible to observe any channel-forming activity in the lipid bilayers.

A)

B)
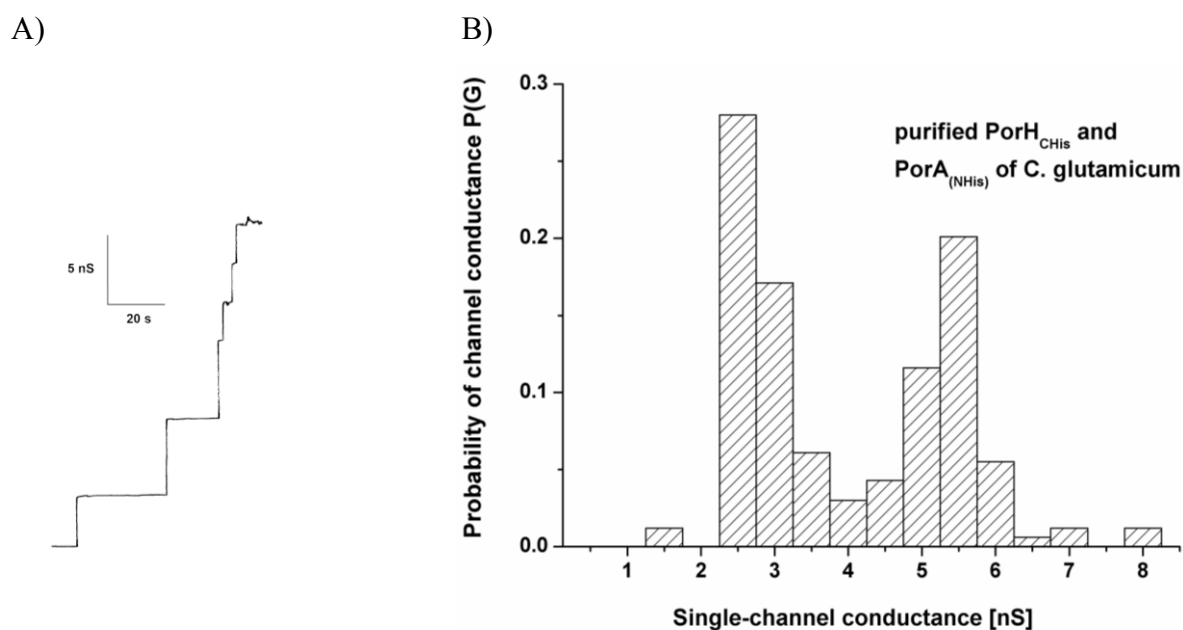
Figure 3.7: (A) Single-channel recording of a PC/*n*-decane membrane in presence of purified PorH$_{CHis}$ and factor Xa treated PorA$_{(NHis)}$ proteins of *C. glutamicum*. About 10 min after the formation of the membrane, 20 ng/ml of a 1:1 protein mixture was added to the aqueous phase on both sides of the membrane. The aqueous phase contained 1 M KCl. The applied membrane potential was 20 mV, and the temperature was 20°C. (B) Histogram of the probability P(G) for the occurrence of a given conductivity unit observed with membranes formed from PC/*n*-decane in the presence of 20 ng/ml of a 1:1 protein mixture of purified PorH$_{CHis}$ and factor Xa treated PorA$_{(NHis)}$ proteins of *C. glutamicum*. The most frequent single-channel conductances were 2.5 (left-side maximum) and 5.5 nS (right-side maximum) for a total of 164 single-channel events. The data were collected from more than 3 individual membranes. The aqueous phase contained 1 M KCl. The applied membrane potential was 20 mV, and the temperature was 20°C.

Obviously it was not possible to obtain membrane channels in such a case. To overcome this problem PorA$_{NHis}$ was treated with factor Xa to remove the His-tag. Interestingly, the mixture of pure PorH$_{CHis}$ and PorA added to lipid bilayers caused again a stepwise increase of conductance similar to the PorH/PorA wildtype combination as shown in Fig. 3.7A. In this experiment approximately 20 ng/ml 1:1 protein mixture of pure PorH$_{CHis}$ and pure PorA was added to a black membrane formed from PC/*n*-decane bathed in 1 M KCl. Statistical analysis of 164 recorded single-channel events collected from more than 3 individual membranes suggested that prominent conductive units had 2.5 and 5.5 nS (Fig. 3.7B). This means that channels formed by the purified PorH$_{CHis}$ and PorA monomers matched units of previously examined whole cell preparations. No pore was recorded in control experiments when only detergent or a single component of the *C. glutamicum* channel was added to lipid membranes (not shown). These important results indicate that the main cell wall channel of *C. glutamicum* is exclusively formed by PorH and PorA monomers.

3.4.11 Heterologous expression of PorH and PorA homologues of *C. efficiens* and study of their channel-forming capacities

The major cell wall channel of *C. efficiens* was previously isolated and characterized in lipid bilayers (Hünten *et al.*, 2005b). The slightly anion-selective channel was proposed to be formed by an oligomer of the 6 kDa CePorH protein, which is homologous to the CgPorH protein of *C. glutamicum* (Table 3.3). Its gene *ceporH* is located in close vicinity to *ceporA* (Hünten *et al.*, 2005b), the predicted homologous gene to *cgporA* of *C. glutamicum* (Schiffler *et al.*, 2007). Both *Corynebacterium* species are close relatives (Fudou *et al.*, 2002), which means that it is possible that the major cell wall channel of *C. efficiens* is also a heterooligomer formed by the combination of CePorH and CePorA, similar to the situation in *C. glutamicum*. This question was addressed by heterologous expression of CePorH and CePorA in the *C. glutamicum* Δ*porH*Δ*porA* mutant using the plasmids pX$_{Ce}$-H and pX$_{Ce}$-A containing the genes *ceporH* and *ceporA*, respectively, of *C. efficiens*. The plasmid pX$_{Ce}$-HA harboured both genes together, *ceporH* and *ceporA*. Expression of the *C. efficiens* proteins was carried out overnight by IPTG induction. Cells were harvested, and the bacterial pellets were separately extracted with organic solvents. Proteins within the organic solvent extracts were precipitated with ether in the cold. The precipitates (dissolved in 1% LDAO detergent) were inspected for their channel-forming capacity by the black lipid bilayer assay.

The precipitate of the *C. glutamicum* mutant complemented with *ceporH* showed no channel-forming activity. The same result was observed when CePorA was expressed in another experiment. A mixture of these non-channel-forming precipitates (in 1:1 molar ratio), however, yielded high channel-forming activity and single-channel events comparable to Fig. 3.8. Similarly, the expression of both proteins in the *C. glutamicum* Δ*porH*Δ*porA* mutant using the plasmid pX$_{Ce}$-HA resulted in an organic solvent precipitate that formed the major cell wall channels of *C. efficiens* in a PC/*n*-decane membrane bathed in 1 M KCl when about 20 ng/ml precipitate was added to lipid bilayer membranes (see Fig. 3.8).

A)

B)
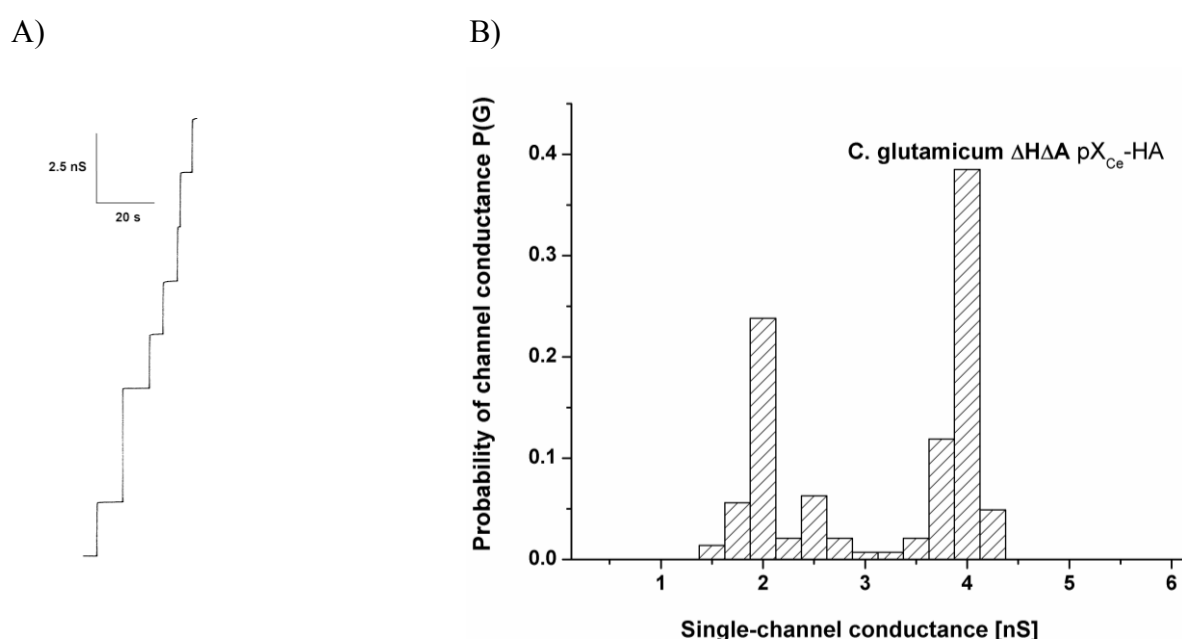
Figure 3.8: Single-channel analysis of porin proteins of *C. efficiens* expressed by plasmid pX$_{Ce}$-HA in the *C. glutamicum* Δ*porH*Δ*porA* mutant. (A) Single-channel recording of a PC/*n*-decane membrane in the presence of PorH and PorA proteins of *C. efficiens*. About 20 ng/ml of ether-precipitated organic solvent extract of whole *C. glutamicum* Δ*porH*Δ*porA* cells transformed with plasmid pX$_{Ce}$-HA was added to the aqueous phase on both sides of the membrane. The aqueous phase contained 1 M KCl. The applied membrane potential was 20 mV, and the temperature was 20°C. (B) Histogram of the probability P(G) for the occurrence of a given conductivity unit observed with membranes formed from PC/*n*-decane in the presence of 20 ng/ml of ether-precipitated organic solvent extract of whole *C. glutamicum* Δ*porH*Δ*porA* cells transformed with plasmid pX$_{Ce}$-HA. The most frequent single-channel conductances were 2.0 (left-side maximum) and 4.0 nS (right-side maximum) for a total of 143 single-channel events. The data were collected from more than 3 individual membranes. The aqueous phase contained 1 M KCl. The applied membrane potential was 20 mV, and the temperature was 20°C.

Most steps (about 60% of all conductance fluctuations) in the experiment had a conductance of 2.0 and 4.0 nS (Fig. 3.8B). The latter step represented presumably dimers of the 2.0 nS channel that could not be separated with the time resolution of our experimental setup. It is noteworthy that the results are in good agreement with the previous study of the major cell

wall channel of *C. efficiens* (purified from strain AJ 12310) where an average single-channel conductance of 2.3 ± 0.3 nS was obtained (Hünten *et al.*, 2005b). However, it is clear from this study that the major cell wall channel of *C. efficiens* is not formed by CePorH alone but needs also the presence of CePorA indicating the channel-forming unit is a heterooligomer formed by CePorH and CePorA (see also Table 3.3).

3.4.12 Identification of a *porH*-like open reading frame in close proximity to the gene *porA* of *C. diphtheriae*

A lipid bilayer study of the major cell wall channel of the *C. diphtheriae* strain ATCC 11913 suggested that the major cell wall channel of this strain is wide and water-filled and has a slight selectivity for cations (Puech *et al.*, 2001; Schiffler *et al.*, 2007). The channel-forming protein could be PorA (CdPorA) from *C. diphtheriae*, a protein homologous to CgPorA of *C. glutamicum* and the corresponding proteins from *C. efficiens* (CePorA) and *C. callunae* (CcPorA). This was judged from the expression of a cloned chromosomal fragment (cloned in vector pX$_{Cd}$-WT, harbouring *cdporA*) of strain ATCC 11913 in the *C. glutamicum* Δ*porH*Δ*porA* mutant strain (Schiffler *et al.*, 2007). In this study we became interested in the question if the cloned *C. diphtheriae* segment (of plasmid pX$_{Cd}$-WT) codes also for other proteins than CdPorA. Figure 3.9 demonstrates that the *C. diphtheriae* fragment indeed coded for three putative ORF including a PorH homologous protein (localized on the same strand as *cdporA*). These ORFs differed only in the start codon while sharing a common stop codon (TAG) and their genes were localized near *cdporA*, similar to the conditions in the genomes of *C. glutamicum* and *C. efficiens* where *porA* and *porH* are obviously co-transcribed. To study the function of gene products in more detail, these four genes were inactivated by point-mutating respective translational initiation sites. Figure 3.9 shows the sequence changes in comparison to plasmid pX$_{Cd}$-WT, which was used in our previous study.

3.4.13 Reconstitution of the major cell wall channel of *C. diphtheriae* requires the presence of PorH and PorA homologues of this bacterium

To identify the proteins involved in the formation of the major cell wall channel of *C. diphtheriae*, we transformed the *C. glutamicum* Δ*porH*Δ*porA* mutant strain with the plasmids pX$_{Cd}$-WT, pX$_{Cd}$-WTQC1, pX$_{Cd}$-WTQC2 and pX$_{Cd}$-WTQC3 (Fig. 3.9), respectively. Protein
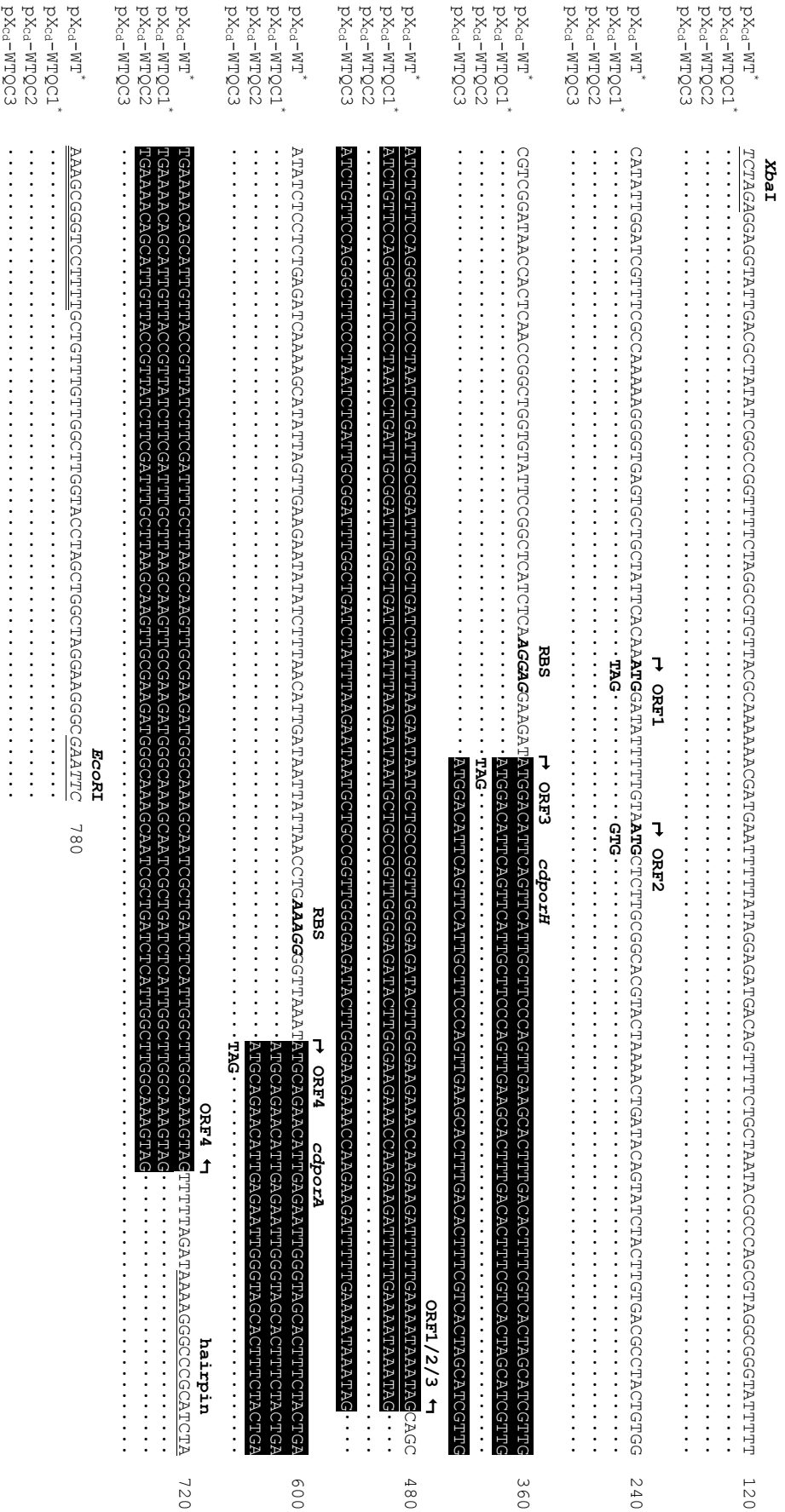
Figure 3.9: Open reading frame analyses of a plasmid-embedded *C. diphtheriae* fragment. Depicted is the fragment of strain *C. diphtheriae* ATCC 11913, which is integral part of plasmid pX_cd_-WT. The fragment of this plasmid complements the channel deficiency of the *C. glutamicum* Δ*porH*Δ*porA* mutant (Schiffler *et al.*, 2007). Gene silencing disclosed the 59 AS small protein CdPorH together with CdPorA accounted for the channel activity. The genes *cdporH* and *cdporA* of *C. diphtheriae* are highlighted in black. Dots below the provided sequence of the cloned *C. diphtheriae* fragment indicate identical nucleotides, whereas mutations are specified in boldface type. Boldface italics show putative RBS in front of each porin gene. Underlined italics mark *XbaI* and *EcoRI* sites used for cloning. A transcriptional terminator is specified by double-underlined letters (Schiffler *et al.*, 2007). The numbers behind the DNA sequence give the specific size of the fragment in the plasmid. * specifies plasmids with a functional *C. diphtheriae* channel domain.

shows 20 and 24% identity to the PorH protein of *C. efficiens* and *C. glutamicum*, respectively. The genes *cdporH* and *cdporA* of *C. diphtheriae* are highlighted in black.

expression was performed similar to the experiment described by Schiffler *et al.* (2007), which means that protein expression was induced overnight with IPTG. Whole cells were extracted with organic solvents; proteins of the extract were precipitated with ether in the cold and dissolved in 1% LDAO. The presence of pore-forming units in each precipitate was investigated with black lipid bilayers formed in a 1 M KCl solution. The precipitate of pX_{Cd}-WT transformed mutant cells showed high channel-forming activity with a major conductance step of about 2.25 nS (Schiffler *et al.*, 2007). Results from mutant cells harbouring pX_{Cd}-WTQC1 were similar (not shown). However, neither pX_{Cd}-WTQC2 (expression of CdPorA) nor pX_{Cd}-WTQC3 (expression of CdPorH) provided protein precipitates that were active in the lipid bilayer assay. Activity was only observed when CdPorH and CdPorA were expressed together in the *C. glutamicum* Δ*porH*Δ*porA* mutant strain (see Fig. 3.9). BLAST result of the CdPorH protein sequence to the non-redundant GenBank database (6970043 sequences, 06/08, National Center for Biotechnology Information) found only two matches; a significant match to DIP2019 (a putative transposase) of *C. diphtheriae* NCTC 13129, and a match to cgR_2618 (hypothetical protein) of *C. glutamicum* R. The protein of the latter CDS is no doubt the homologue of PorH of *C. glutamicum* ATCC 13032 and also of *C. efficiens* AJ 12310 (see Table 3.3) (Hünten *et al.*, 2005a; Hünten *et al.*, 2005b). The CdPorH polypeptide of strain ATCC 11913 is 59 amino acids long (with the inducer methionine) and has a (calculated) molecular mass of 6781 Da. Nine aspartates and glutamates compared to five lysines and a single histidine give the protein an acidic character (Table 3.3). The PorH homologue of *C. diphtheriae* NCTC 13129 is part of DIP2019. Similarly, *cdporH* and *cdporA* of strain NCTC 13129 (GenBank Accession number NC_002935) are direct neighbours in the chromosome of this strain (see Fig. 3.9). *cdporH* of strain NCTC 13129 is 177 bp long and it codes for a 58 AS polypeptide with a (calculated) molecular mass of 6567 Da. Six aspartates and glutamates compared to five lysines result in an almost balanced protein (Table 3.3). Taken together, a homooligomeric (CdPorA) channel in *C. diphtheriae* is excluded in favour of a functional heterooligomeric channel composed of CdPorH and CdPorA subunits.

3.4.14 Cloning of the prospective channel domain of *C. callunae*

To date, the *C. callunae* strain ATCC 15991 is the fourth species among the genus *Corynebacterium* with a well-studied cell wall channel (Hünten *et al.*, 2005b). The cation-selective pore is associated with a low-molecular-mass protein. The sequence of the *C.*

callunae protein is only partially known, but it is clearly a homologue of PorH of *C. glutamicum* and *C. efficiens* (Hünten *et al.*, 2005b). When the results of the study with *C. glutamicum*, *C. efficiens* and *C. diphtheriae* are considered (see above), it is clear that the major cell wall channel of *C. callunae* is presumably also formed by two proteins, a PorA homologue and a PorH homologue. The genome of *C. callunae* is not yet known to allow a clear judgment. However, the close relationship between *C. glutamicum* and *C. callunae* (Fudou *et al.*, 2002; Ruimy *et al.*, 1995) let us believe that the *porH* and *porA* genes of the latter strain are localized in a chromosomal region that is similar to the region of the other strains investigated here. To decide this question we cloned the presumably homologous region of the genome of *C. callunae* using the primers FP Cc_HA1/RP Cc_HA3 (Table 3.2), which were derived from the CDS of NCgl2620 and NCgl2621 (in *C. glutamicum*; see Fig. 3.4). For the design of the primers we took also the homologous CDS of *C. efficiens* (CE2558 and CE2561, respectively) and *C. diphtheriae* (DIP2016 and DIP2020, respectively) into consideration, which have a high degree of conservation. Using these primers we obtained a single PCR product from genomic *C. callunae* DNA as a template, which was comparable in size to the PCR product of *C. glutamicum* template (Fig. 3.10). About 1500 bp in size, the *C. callunae* amplicon was cut out of the gel, cloned into the TOPO 2.1 vector and sequenced with primers M13 forward and reverse. The sequence of the PCR product is provided in Fig. 3.11.
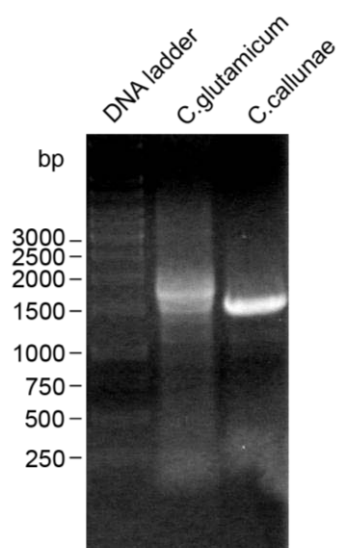
Figure 3.10: Agarose (0.8%) gel from PCR-amplified homologous porin regions of *C. glutamicum* and *C. callunae*. Amplicons were obtained with primers FP Cc_HA1 and RP Cc_HA3 using chromosomal DNA of both strains as template. The sequence of the *C. callunae* PCR product is shown in Fig. 3.11.

```
                 FP Cc_HA1                          ccgroEL
Ccal    GACCACTGAGGCTGTCGTTGCTGACAAGCCACAGCCAGCAGGTGCCGCAA     50
              (homolog of NCgl2621,CE2561,DIP2020)
Ccal    TGCCAGGCGCTGATGAGATGGGTGGCATGGGCGGCTTCTAAGCCTTCTAA    100
                               hairpin
Ccal    CCTCTCATACCGATAAGCTCCTCCCGCTTCTTGCGGGAGGAGCTTATTTG    150
        GCGTTTTAGGGCGCTTTTCGACGATTTCCTGGCCACCGTAGCATTAGAGG    200
Ccal    TGATCTCTTAATTACCGCCGGGTGGGTTAAGATTTTCACCACTTACCCTC    250
Ccal    TGATGGGGGTGGGTAAAAATGATCCTATCAAGTTGTGTGGCCTTAATCGC    300
Ccal    AGCCTTGTAAATTCTTGTTACATGTTTTGATAGTTATATAGAAAGTTTT     350
Ccal    CCTTAAGTTAGCCTTAAAAATCCACATATCCCCAGTTCAAGCTAAAATAC    400
Ccal    TTGGCAATTTTATTTATGAAAAATTAATAAATTAGAGCTTGATGGAAGAT    450
Ccal    AAAAAACTTTGCAAATCGTCTTGGCGGTTGTCAAAAATGTGATTGAATGT    500
Ccal    GTGAGTGACGTCCTGAGGACGTTAGCAAACTGGCAACCTTCACCAGCTCC    550
                 RBS         ccporH
Ccal    TTGCTGGTCCTCTTAAGGAGATTTCTCATGGATCTTTCCCTTCTCGCAGA    600
Ccal    CAACCTTGACGATTACTCCACCTTTGGTGGCAACATCGGCACCGCTCTTA    650
Ccal    CCATGATCCCTGATCTACTCAAGGGCATCATCGCGTTCTTCGAGAACTTC    700
Ccal    GGTGACAACGCTGACGCAACCAGCGCTGCTTTCGAAGGCCTCTCCTCTTA    750
Ccal    ATTTTCAATATGGCTGTTAGGTAAGTGCCTAGAAGCCTTTTCCCTTCACC    800
                 RBS         ccporA
Ccal    CGTATTTAAAATTCTCTAAAGGAGATTAAAAATGGACAACTTTGTTGAAT    850
Ccal    TCCTCGACAACGTAAACACCCTTTCTTCCACCGGCCTCGTTGCTGAGCTT    900
Ccal    CTTGATTTCTTTACTGCTTCCGGCAAGTGGGCTGGCGCAGTTGCTGACCT    950
Ccal    CCTCGGACTGGTTAAGTAATTTAAACCCTTAGGTTTAAATCCTTAAAGCT   1000
             hairpin
Ccal    CCGATCCTTAACAGGATCGGAGATTTTTGTTGTGAGCACTACATTAAATA   1050
                         cc_hypothetical_gene
Ccal    CGCTACACATCGCGCCTAATGTGCGGGAGGTAGGTATGATTTTCAGCATG   1100
              (homolog of NCgl2620,CE2558,DIP2016)
Ccal    GCTAATACCAACGATAATGATCTCCCCGTCATCGATCTTGCAAAGATTGA   1150
Ccal    AGGCTATGTAGTTGATGATTCAGACGAGGATGATCCGGTACTCCTGCGTC   1200
Ccal    CAGATGGCACAGCCATTGAAACCTGGAGGGAAAACTATCCTTATCAAGAG   1250
Ccal    CGCGTTAACCGCGAGGACTATGAAAAGGTCAAGCGTTCCTTACAGATCGA   1300
Ccal    ACTGCTGAAGTGGCAGAACTGGACCAAGGAAACTGGCCAGCGCCACATCA   1350
                                   RP Cc_HA3
Ccal    TCCTCTTTGAAGGCCGCGATGCTGCTGGTAAGGGTGGCACCATTAAGCGC   1400
Ccal    TTCAA                                              1405
```

Figure 3.11: Analysis of the *C. callunae* porin domain. The amplicon of Fig. 3.10 was cloned into the TOPO 2.1 vector and sequenced. Primers used for cloning of the *C. callunae* region are marked by underlined italics. The boldface type represents the *C. callunae* homologues of, e.g., NCgl2620 and NCgl2621 of *C. glutamicum* ATCC 13032. The identified *C. callunae ccporH* and *ccporA* genes (black highlighted) share the same chromosomal localization as *porH* and *porA* genes of other in this study investigated corynebacteria. As with *C. glutamicum*, a putative RBS shown in boldface italics attends each porin gene. Moreover, both genes are surrounded by distinct hairpin structures marked as double-underlined letters. Numbers behind the DNA sequence display the specific size of the PCR product inserted into the TOPO 2.1 vector.

3.4.15 Identification of the genes coding for the PorH and PorA homologues of *C. callunae*

Two small-sized coding sequences, each with a putative ribosome binding site (5'-AGGAG-3'), were disclosed by search of the sequence shown in Fig. 3.11 for ORFs. The protein sequence derived from the first CDS (*ccporH*) corresponded (with minor variations) to the partial amino acid stretches of the directly sequenced CcPorH protein (Hünten *et al.*, 2005b). The mature CcPorH protein is 57 amino acids long and has a calculated molecular mass of 5963 Da. Nine aspartates and glutamates, compared to one lysine, give the polypeptide an overall negative charge (Table 3.3). Only 80 bp downstream of *ccporH* is the localization of the second CDS. The deduced polypeptide sequence comprises 45 amino acids (with the inducer methionine) and shows about 24 to 53% identity to PorA of *C. diphtheriae*, *C. efficiens* and *C. glutamicum* (Table 3.3). In analogy to the other components of the corynebacterial cell wall channels, we assumed that the second CDS encodes the PorA protein of *C. callunae* and named it *ccporA* (for *C. callunae* pore forming gene A). CcPorA has a calculated molecular mass of 4790 Da and is overall negatively charged (six glutamates and aspartates, compared to two lysines). Considering the results of other investigated *Corynebacterium* species, it is clear that the major cell wall channel of *C. callunae* is presumably also a heterooligomer of CcPorH and CcPorA. In this respect it is interesting that acidic characters of both proteins agree well with the cation selectivity of the *C. callunae* cell wall channel (Hünten *et al.*, 2005b).

3.4.16 Transcriptional terminators flank the *porH-porA* region in *C. callunae*

An analysis of inverted repeat sequences that likely form stem-loop structures revealed that there is one transcriptional terminator in the non-coding region downstream of *ccgroEL* and a second terminator behind the *ccporA* gene (Fig. 3.11); the free energy levels of the 5'-ATA AGCTCCTCCCGCTTCTTGCGGGAGGAGCTTAT-3' and the 5'-AAAGCTCCGATCCTT AACAGGATCGGAGCTTT-3' sequences are -25.7 and -25.9 kcal/mol, respectively (http://www.genebee.msu.su). As no distinct rho-dependent terminator is spotted between *ccporH* and *ccporA,* we believe that these genes form a transcriptional unit responsible for the main cell wall channel of *C. callunae* similarly to the situation in the genomes of the other *Corynebacterium* species studied here.

3.5 Discussion

3.5.1 The genes *porH-porA* structure a porin operon in *C. glutamicum*

In this study we investigated the transcriptional analysis of the genes *cgporH* and *cgporA* of *C. glutamicum*. The products of these genes have been associated in the past (seemingly wrong) with individual channel-forming units in the cell wall of *C. glutamicum*, i.e. it was assumed that CgPorA and CgPorH formed homooligomeric channels (Hünten *et al.*, 2005a; Lichtinger *et al.*, 2001). A 600 bp transcript was found in Northern blot experiments (Fig. 3.3A) that suggested that both genes were co-transcribed. This co-transcript was observed for *C. glutamicum* grown under rich and minimal media conditions, which means that both proteins are expressed under all conditions. This co-transcript is responsible for a coordinated expression of PorH and PorA in equimolecular amounts to form channels of the CgPorH/CgPorA type in the cell wall. Another indication that both transcripts were necessary for channel formation came from the observation that the *C. glutamicum* Δ*porA* strain did not contain the major cell wall channel (Costa-Riu *et al.*, 2003a). Other Northern experiments were performed with the *C. glutamicum* Δ*porA* strain to study the *cgporH* transcript. Interestingly, this transcript was not observed in the *C. glutamicum* Δ*porA* strain although there was no obvious reason for this. RT-PCR experiments using primers directed against *cgporH* (FP Cg_H/RP Cg_H) produced a very faint amplificate for the *C. glutamicum* Δ*porA* strain (data not shown) suggesting that the gene is transcribed. The *cgporA* deletion presumably affects the stability and causes fast degradation of the residual *cgporH* transcript in the mutant strain. On the other hand, RT-PCR primers annealing to the 5' end of *cgporH* and to the 3' end of *cgporA* yielded a PCR product, which covered both genes but did not consider non-coding flanking regions (Fig. 3.3B).

The transcription start point of the *cgporH-cgporA* transcript was determined by RACE analysis. This enabled to postulate the -10 box. Corynebacterial promoters often show a considerable variation of nucleotides in this conserved region, which has the extended consensus sequence tgngnTA(c/t)aaTgg (capital letter mark residues with a high degree of conservation) (Patek *et al.*, 2003). In seven positions the postulated -10 box (Fig. 3.4) agrees with the shown sequence of vegetative promoters. The -35 box of the promoter of the PorH/PorA operon has four nucleotides identical to the -35 consensus region for vegetative *C.*

glutamicum promoters (Vasicova *et al.*, 1999). Sequence analysis of the flanking regions of the porin operon discovered two inverted repeats; the potential terminator of the bicistronic porin transcript and the potential terminator of NCgl2621, which represents the shock-regulated GroEL chaperon (Barreiro *et al.*, 2004). This means that separate *groEL* and *porH-porA* transcripts existed. It is noteworthy that elements of the *C. glutamicum cgporH-cgporA* operon were also found in the homologous region of the *C. callunae* (Fig. 3.10), *C. diphtheriae* (Fig. 3.9) and *C. efficiens* (Hünten *et al.*, 2005b) chromosome. Inverted repeat structures flank the proximate *porH/porA* genes of these species in a similar way, which suggests that these porin genes are also co-transcribed.

3.5.2 The oligomeric major cell wall channels of *C. glutamicum* and its close relatives consist of homologous PorH and PorA subunits

The results of the transcriptional analysis suggested that the large cell wall pores of *C. glutamicum* represent oligomers composed of two proteins, CgPorH and CgPorA. Pore-forming activity in a *porH⁻* and *porA⁻ C. glutamicum* strain was only observed when both proteins were expressed, similar as in the fully complemented *C. glutamicum ΔporH ΔporA* mutant or the wild-type strain of *C. glutamicum*. In addition, recombinant expressed and affinity-purified proteins were only active in the lipid bilayer assay, when both proteins were present. There is no chance that a further protein is involved in channel formation. It is noteworthy that this observation is consistent with the results of the transcriptional analysis showing a bicistronic porin transcript for *C. glutamicum*. Consideration of the bilayer results obtained from the reconstitution experiments of PorH and PorA from the *C. glutamicum* channel allowed also the reconstruction of the PorH/PorA cell wall pore of *C. efficiens* and *C. diphtheriae* in *C. glutamicum* by heterologous expression. Similar as in the case of *C. glutamicum*, functional channels could only be observed in these cases when both PorH and PorA of these strains were expressed in *C. glutamicum*. The knowledge of the location of the *porA* and *porH* genes in the genomes of *C. efficiens*, *C. diphtheriae* and *C. glutamicum* allowed also the cloning and sequencing of the complete porin region of *C. callunae* strain ATCC 15991. Oligomeric channels are not rare within the taxon mycolata; MspA of *Mycobacterium smegmatis* and PorB of *C. glutamicum* form also oligomeric channel structures; MspA is an octamer, whereas PorB could be a pentamer (Faller *et al.*, 2004; Ziegler *et al.*, 2008). Because of their small sizes, PorH and PorA proteins presumably contain only one single membrane-spanning domain. This means that the higher structured

heterooligomer is needed to form the stable, large ion-conducting channels in the mycolic acid layer and artificial lipid membranes.

In previous reports we favoured the view that *C. glutamicum*, *C. callunae* and *C. efficiens* contained two major cell wall channels formed by oligomers of PorA and oligomers of PorH (Costa-Riu *et al.*, 2003a; Hünten *et al.*, 2005a; Hünten *et al.*, 2005b; Lichtinger *et al.*, 2001). This clearly contradicts the results of this study; the architecture of the major cell wall channels of all these bacteria including that of *C. diphtheriae* is formed by a heterooligomer of PorA and PorH (Table 3.3) (Schiffler *et al.*, 2007). PorA or PorH alone cannot form a cell wall channel. The previous misinterpretation of the results was presumably caused by incomplete separation of the PorA and the PorH proteins of *C. glutamicum*, *C. callunae* and *C. efficiens* because of their low molecular mass. Small amounts of PorH in PorA or vice versa are sufficient for the reconstitution of active channels in the lipid bilayer assay.

For *C. glutamicum*, previous reconstitution experiments with artificial lipid membranes revealed a prominent single-channel conductance of about 5.5 nS in 1 M KCl (Lichtinger *et al.*, 1998; Niederweis *et al.*, 1995). A significant but lower amount of recorded channels had in these experiments a conductance of 2.5 nS. This study revealed a comparable result but the 2.5 nS channel unit appeared to be more frequent (Fig. 3.7). This means that it could be possible that the smaller conductive unit corresponded to a single *C. glutamicum* cell wall channel, whereas the larger conductance (5.5 nS) was most likely caused by the incorporation of two channels at once. This could be concluded from other studies with corynebacterial PorH/PorA cell wall channels. For instance, the single-channel conductance of PorH/PorA channels of *C. diphtheriae* (Schiffler *et al.*, 2007) and *C. efficiens* (Hünten *et al.*, 2005b) was only about 2.3 nS. Protein sequences as well as other intrinsic properties of PorH and PorA proteins aligned in Table 3.3 suggest that their structures should be very similar, which supports the view that their conductance should also be similar, i.e. close to 2.5 nS in 1 M KCl and not 5.5 nS.

Channel components	Sequence alignment	N	MW	pI	Reference(s)
PorA homologs					
C. glutamicum CgPorA_ATCC 13032	MENVYEFLGNLDVLSGSGLIGYVFDFLGASSKWAGAVADLIGLLG	45	4.7	3.8	(Lichtinger *et al.*, 2001)
hyp_CgPorA_R	MENVTTFLDNLGILSTTGLFGDAFSFLAASGNWADAVAKIIGLL-	44	4.6	3.8	This study
C. efficiens CePorA AJ 12310	MESITDFLANVSNLSSTGLVGTVEFGLLKTAGDWADNVAKILGLLG	45	4.6	4.2	This study
C. callunae hyp_CcPorA_ATCC 15991	MDNFVEFLDNVNTLSSTGLVAELLDFFTASGKWAGAVADLLGLVK	45	4.8	4.0	This study
C. diphtheriae CdPorA_NCTC 13129	MENINHWVE-LSS-GKDSIVTVIFGLLKDIAKMGKAIADLIGLAK	43	4.6	6.5	(Schiffler *et al.*, 2007)
CdPorA_ATCC 11913	MQNIENWVA-LST-DENSIVTVIFDLLKQVAKMGKAIADIIGLAK	43	4.7	4.9	This study
PorH homologs					
C. glutamicum CgPorH_ATCC 13032	MDLSLLKETIGNYETFGGNIGTALQSIPTLLDSILNFFDN----FGDLADTTGENLDNFSS	57	6.2	3.5	(Hünten *et al.*, 2005a)
hyp_CgPorH_R	MDLSLLKDNISDYATFGKNIGTALQSIPTVLNSILDFFTG----FGDNADTTGKAFENLSS	57	6.1	4.0	This study
C. efficiens CePorH_AJ 12310	MDLSLLKDSISDFATLGKNLGPALQGIPTLLNSIIAFFQN----FGDLAETTGDAAGNLSS	57	5.9	3.9	(Hünten *et al.*, 2005b)
C. callunae CcPorH_ATCC 15991	MDLSLLADNTDDYSTFGGNIGTALTMIPDLLKGIIAFFEN----FGDNADATSAAFEGLSS	57	6.0	3.4	This study
C. diphtheriae CdPorH_ATCC 11913	MDIQFIASQIKHFDTFVTSIVDLFQGFPNLIADLADLFKNNAAGWGDTWEETKKIFENK--	59	6.8	4.5	This study
CdPorH_NCTC 13129	MDPQFIASQIKNFETFVTNIATLFEGFPQLIKQLAGLFNNGAEGWGKAWESTKKIFEN---	58	6.6	5.1	This study

Table 3.3: Alignment of PorH and PorA amino acid sequences of the strains *C. glutamicum* ATCC 13032, *C. glutamicum* R, *C. efficiens* AJ 12310, *C. callunae* ATCC 15991, *C. diphtheriae* NCTC 13129 and *C. diphtheriae* ATCC 11913 using ClustalW2 at the European Bioinformatics Institute. Residues conserved in homologous proteins are highlighted by yellow (100%) and grey (>50%) shading. The charged residues of the proteins are indicated at the top. N, MW and pI correspond to the calculated number of amino acids, the molecular mass and the isoelectric point of the proteins, respectively (http://www.expasy.org/tools/pi_tool.html).

Chapter 4

Corynebacterium jeikeium jk0268 constitutes for CjPorA, which forms a homooligomeric and anion-selective cell wall channel

4.1 Summary

Corynebacterium jeikeium, a resident of human skin, is often associated with multidrug resistant nosocomial infections in immunocomprised patients. *C. jeikeium* K411 belongs to mycolic acid-containing actinomycetes, the mycolata, and contains a channel-forming protein as judged from reconstitution experiments with artificial lipid bilayer experiments. The channel-forming protein was present in detergent treated whole cell extracts. A gene coding for a 40 AS protein possibly responsible for the pore-forming activity was identified in the known genome of *C. jeikeium* by its similar chromosomal localization to known *porH* and *porA* genes of other corynebacteria. The gene *jk0268* was expressed in a porin deficient *C. glutamicum* strain. For purification temporarily histidine-tailed, the homogeneous protein caused channel-forming activity with an average conductance of 1.25 nS in 1 M KCl identical to the channels formed by the detergent extracts. Zero-current membrane potential measurements of the voltage dependent channel implied selectivity for anions. This preference is according to single-channel analysis caused by some excess of cationic charges located in the channel lumen. The channel has a suggested diameter of 1.4 nm as judged from the permeability of different sized hydrated anions using the Renkin correction factor. Surprisingly, the genome of *C. jeikeium* contained only one gene coding for a cell wall channel of the PorA/PorH type found in other corynebacteria. The possible evolutionary relationship between the heterooligomeric channels formed by certain strains and the homooligomeric pore of *C. jeikeium* is discussed.

4.2 Introduction

Corynebacterium jeikeium is generally regarded as a lipophilic and extremely drug-resistant bacterial species that initially was detected in human blood cultures and is associated with severe endocarditis following cardiac surgery (Jackman *et al.*, 1987; Johnson & Kaye, 1970; Mookadam *et al.*, 2006). Subsequent medical studies clearly established that *C. jeikeium* can be considered as part of the normal human skin flora, but it can also be detected in the inanimate hospital environment (Funke *et al.*, 1997). Clinical isolates of *C. jeikeium* were implicated as a cause of a variety of nosocomial infections, including prosthetic and native heart valve endocarditis, bacteraemia, septicaemia, meningitis and osteomyelitis (Funke *et al.*, 1997). *C. jeikeium* is taxonomically referred to as lipophilic species due to the strict requirement of exogenous fatty acids for growth on synthetic culture media (McGinley *et al.*, 1985). Antimicrobial susceptibility assays revealed that only glycopeptides, i.e. vancomycin and teicoplanin, remain universally active against *C. jeikeium* (Funke *et al.*, 1997).

Today the knowledge on the complete genome sequence of *C. jeikeium* K411 provides the basis for an in-depth understanding of the physiology of this medically important bacterium (Tauch *et al.*, 2005). The chromosome of *C. jeikeium* K411 has a size of 2.46 Mbp and comprises 2104 predicted coding regions, of which 68 most likely represent pseudogenes. The chromosomal architecture of *C. jeikeium* K411 revealed a moderate number of genomic rearrangements when compared to other sequenced corynebacterial genomes (Tauch *et al.*, 2005). These structural differences of the chromosome have been attributed very recently to the phylogenetic position of *C. jeikeium* within the taxonomic tree of the genus *Corynebacterium* (Tauch *et al.*, 2008). Annotation of the genomic data revealed that the lipophilic phenotype of *C. jeikeium* is caused by the absence of a gene coding for a fatty acid synthase and linked to pathogenicity, and that events of horizontal gene transfer are responsible for multidrug resistance (Tauch *et al.*, 2005). The annotated genome sequence can be regarded as starting point for comprehensive post-genomic studies at the transcriptomic and proteomic levels (Brune *et al.*, 2006; Hansmeier *et al.*, 2007), but also for the detailed functional analysis of predicted coding regions, for instance the putative porin gene locus of *C. jeikeium* K411.

Commonly, porins are crucial components in the outermost membrane of Gram-negative bacteria (Benz, 1994; Nikaido & Jarlier, 1991; Nikaido *et al.*, 1993) but they were also found

in a variety of mycolic acid-containing actinomycetes, the mycolata, which include *Corynebacteria*, *Mycobacteria*, *Nocardia*, *Rhodococci* and closely related genera. These bacteria share an unusual cell envelope composition and architecture (Daffe & Draper, 1998) by having a thick peptidoglycan layer, covered by lipids in form of mycolic acids and other lipids (Barksdale, 1981; Nikaido *et al.*, 1993). This means that the cell wall of the mycolata forms a permeability barrier and probably has the same function as the outer membrane of Gram-negative bacteria. Latter membranes contain channel-forming proteins for the passage of hydrophilic solutes (Benz, 2003; Jarlier & Nikaido, 1990; Nikaido, 2003). Similarly, channels are present in the mycolic acid layer of the mycobacterial cell wall (Trias *et al.*, 1992; Trias & Benz, 1993) and the cell walls of a variety of *Corynebacteria* species, such as *Corynebacterium glutamicum* (Costa-Riu *et al.*, 2003b; Hünten *et al.*, 2005a; Lichtinger *et al.*, 2001), *Corynebacterium efficiens* (Hünten *et al.*, 2005b), *Corynebacterium callunae* and *Corynebacterium diphtheriae* (Schiffler *et al.*, 2007). In all these cases it seems conceivable that PorA and PorH proteins form heterooligomers responsible for the mostly cation-selective major cell wall channel besides a smaller anion-selective channel (Costa-Riu *et al.*, 2003b). Similar as has been found in recent years by the investigation of cell wall channels in different members of the mycolata (Lichtinger *et al.*, 1998; Lichtinger *et al.*, 1999; Lichtinger *et al.*, 2000; Riess *et al.*, 1998; Riess & Benz, 2000; Riess *et al.*, 2001), cell wall channels on the surface of corynebacteria define the mycolic acid layer as a permeability barrier.

In this study, we extended the search for cell wall channels to the *C. jeikeium* strain K411, which is a clinical isolate originally recovered from the axilla of a bone marrow transplant patient. Using lipid bilayer experiments we could demonstrate that the extracts of whole *C. jeikeium* cells contain a protein that forms wide and water-filled channels similar to the porins found in Gram-negative bacteria and in other corynebacteria (Benz, 1988; Benz, 1994; Benz, 2003). The channel-forming protein, named CjPorA, was identified within the accessible genome of *C. jeikeium* K411 by suspecting its localization is homologous to CgPorH and CgPorA of *C. glutamicum*. CjPorA was expressed in a CgPorA/CgPorH-deficient strain of *C. glutamicum* (Hünten *et al.*, 2005a; Lichtinger *et al.*, 2001; Schiffler *et al.*, 2007) and purified to homogeneity. The protein is active as a homooligomer in contrast to PorA/PorH of most *Corynebacteria* species, which form heteromeric channels. We present in this study the characterization of the first homooligomeric channel-forming protein of a strain within the genus *Corynebacterium*.

4.3   Materials and methods

4.3.1   Bacterial strains and growth conditions

The corynebacterial strains *C. glutamicum* ATCC 13032 and *C. jeikeium* K411 were grown in 1000 ml baffled Erlenmeyer flasks containing 250 ml of brain heart infusion (BHI) medium (Difco Laboratories) and 250 ml Erlenmeyer flasks containing 25 ml BYT medium (Tauch *et al.*, 2004). The former cultures were stirred on a rotary shaker at 140 rpm and 30°C, the latter ones at 280 rpm and 37°C. *Escherichia coli* NEB5α (New England Biolabs, Frankfurt, Germany), used for cloning, was grown under standard conditions in Luria broth (LB). If necessary, agar plates and liquid media were supplemented with 20 and 40 µg/ml chloramphenicol, respectively.

4.3.2   Cloning and expression

The gene *jk0268* and its putative ribosome binding site was PCR amplified from genomic *C. jeikeium* DNA. It was isolated in a 50 µl reaction volume containing 1× Taq buffer, 0.2 mM dNTPs, 3 mM $MgCl_2$, 1 U Taq DNA polymerase (Fermentas, St. Leon-Rot, Germany) and 0.4 µM primers FP JK0268XbaI/RP JK0268EcoRI (Table 4.1). Used PCR conditions were: initial denaturation at 95°C for 5 min, 30 cycles at 95°C for 1 min, 45°C for 1 min, 72°C for 1 min and a final extension at 72°C for 10 min. After agarose gel size separation, a PCR product of about 200 bp was cut out, ligated into the TOPO2.1 vector (Invitrogen, Karlsruhe, Germany) and heat-shock transformed into *E. coli* NEB5α cells according to the instructions of the manufacturers. One plasmid that contained the amplicon was *Eco*RI and *Xba*I (Fermentas) digested, and the 200 bp fragment was ligated in the backbone of *Eco*RI and *Xba*I linearised vector pXMJ19 (Schäfer *et al.*, 1994) eventually resulting in the expression plasmid pXJK0268.

For immobilized metal ion affinity purification (IMAC) the vector pXMJ19 was upgraded by introduction of a DNA cassette coding for a C-terminal factor Xa (Ile-Glu-Gly-Arg) linked octa-histidine tag. Therefore, the single-stranded oligonucleotides FP KpnIXa8HisEcoRI and RP KpnIXa8HisEcoRI were first 5' phosphorylated, then annealed by a temperature gradient step to provide double-stranded DNA with *Kpn*I and *Eco*RI overhangs and finally ligated in

104

*Kpn*I and *Eco*RI cut pXMJ19 vector with T4 DNA Ligase (Fermentas). The resulting plasmid was designated pXHis.

Oligonucleotides	Sequence 5'→ 3'	Position
FP JK0268XbaI	GGAACCTGGCGC<u>TCTAGA</u>TCTCTTAAGAGGA	329071-329101
RP JK0268EcoRI	GAAGCCGGGGTTT<u>GAATTC</u>TTAAGCGGAAGC	329232-329262
RP JK0268KpnI	TAAGCGGA<u>GGTACC</u>CTTAGCAGCGGTCCACTTAACG	-
FP KpnIXa8HisEcoRI	CATCGAGGGCCGCGGCGGCCACCACCACCACCACCACCACTAATAGG	-
RP KpnIXa8HisEcoRI	<u>AATTC</u>CTATTAGTGGTGGTGGTGGTGGTGGTGGTGGCCGCCGCGGCCCTCGATG<u>GTAC</u>	-
FP pXMJ19Seq	GTGAGCGGATAACAATTTCAC	-
RP pXMJ19Insert	CTCTCATCCGCCAAAACAGC	-

Table 4.1: Oligonucleotides used in this study. The sequences of the primers were derived from the prospective gene *jk0628* of the cell wall channel and its flanking regions taken from the genome of *C. jeikeium* K411 (Tauch *et al.*, 2005). Primer binding positions in the accessible chromosome of this strain are provided (reference sequence NC_007164).

To apply the C-terminal tag of plasmid pXHis to *jk0268* the native stop codon of the gene was mutated by PCR amplification. Using PCR conditions mentioned before, primers FP pXMJ19Seq/RP JK0268KpnI and template pXJK0268 (pXMJ19 equipped with *jk0268*) provided an about 250 bp fragment. This fragment as well as plasmid pXHis were *Xba*I and *Kpn*I digested, overnight ligated (16°C) and named pXJK0268His.

The sequences of all expression vectors were verified by sequencing (Seqlab, Germany) prior to transformation of the plasmids into the porin deficient *C. glutamicum* ATCC 13032 Δ*porH* Δ*porA* strain (Schiffler *et al.*, 2007). Transformation was performed using a slightly modified standard electro-transformation method (van der Rest *et al.*, 1999). Heterologous expression of the proteins was induced by addition of 1 mM isopropyl-β-D-thiogalactopyranoside (IPTG) to a liquid culture at the mid-exponential growth phase.

4.3.3 Isolation of cell wall proteins

Cell wall-associated proteins were isolated by methods described in detail previously (Lichtinger *et al.*, 1998; Lichtinger *et al.*, 2000). Cells of *C. jeikeium* or *C. glutamicum* were harvested from liquid cultures by centrifugation (6000 rpm, 15 min and 4°C in Heraeus Minifuge RF centrifuge). The cell pellet was washed twice with 10% culture volume (10 mM Tris, pH 8) before cell wall proteins were extracted either by shaking the cells in detergent or a 1:2 (v/v) mixture of the organic solvents chloroform and methanol. For both extraction methods one part cells (0.3 g wet weight bacterial pellet) was resuspended in five parts detergent solution (1.5 ml 1% lauryldimethylamine-oxid (LDAO), 10 mM Tris, pH 8) or organic solvent (1.5 ml chloroform/methanol). After 3h of agitation at RT, cells were sedimented in a table top centrifuge (10000 rpm, 10 min and 4°C) and the pellet was discarded. The detergent supernatant was subjected to Ni^{2+}-affinity purification or tested for channel-forming activity using the lipid bilayer assay. The chloroform-methanol mixture was first precipitated overnight with 9 times the volume of ice-cold diethyl ether (-20°C) before the obtained pellet was solved either in detergent solution (1% LDAO, 10 mM Tris, pH 8) or Redmix buffer for gel electrophoresis.

4.3.4 IMAC purification

Histidine-tailed *C. jeikeium* proteins were purified to homogeneity utilizing the affinity of the recombinant polypeptide to immobilized Ni^{2+}-ions. From detergent treated *C. glutamicum* cells, 5 ml of the 1% LDAO supernatant were loaded on Ni-NTA spin columns (Qiagen, Hilden, Germany) pre-equilibrated with buffer 1 (0.4% LDAO, 50 mM NaCl, 20 mM Tris, pH 8). After ten washing steps each with 650 µl of buffer 2 (= buffer1 supplemented with 10 mM imidazol) bound protein was eluted from the column with 200 µl buffer 3 (= buffer 1 supplemented with 300 mM imidazol).

4.3.5 Protease Xa cleavage

Subsequent to IMAC purification the eluate contained high imidazol concentrations which strongly inhibit protease Xa (Qiagen) activity. Removal of imidazol was performed by dialysing the protein solution overnight against cleavage buffer (0.4% LDAO, 1 mM $CaCl_2$,

50 mM NaCl, 20 mM Tris, pH 6.5) using a cellulose membrane with a molecular weight cut-off of 2 kDa (Spectra/Por 6, Carl Roth, Karlsruhe, Germany). To cleave the poly-histidine tag 4 units protease Xa (Qiagen) were added overnight to the dialysed sample (37°C). The enzyme was removed with the factor Xa removal Kit according to Qiagen's instructions. A second Ni-NTA column passage separated the cleaved JK0268 (CjPorA) protein from uncleaved and cut histidine-peptides.

4.3.6   Protein electrophoresis and immunoblotting

Protein samples were size separated subsequent to a denaturation step (5 min, 95°C) by 12% or 16.5% Tris-Tricine polyacrylamide gel electrophoresis (PAGE) (Schägger & von Jagow, 1987). Afterwards, proteins were either stained with Coomassie brilliant blue, silver stain (Blum *et al.*, 1987) or electroblotted (Towbin *et al.*, 1979). In the latter case, proteins were transferred to a 0.1 μm nitrocellulose membrane (Protran, BA79, Whatman). The blotting was performed for 4 to 5 min in a wet tank blot system (Biorad) with Towbin buffer (20% methanol, 192 mM glycine, 25 mM Tris) at 350 mA current. Reactive binding sites on the membrane were blocked with 5% skimmed milk in TBS-T buffer (0.1% Tween, 0.01 M NaCl, 20 mM Tris, pH 7.5) before probing with the first 1:5000 diluted monoclonal mouse anti-His antibody (Amersham Biosciences, UK). Subsequent to multiple TBS-T washing steps the second peroxidase-conjugated anti-Mouse antibodies (DAKO, Denmark) were added at the same dilution. Attending to the manufacturer's instructions, application of the ECL Western blot detection system (GE Healthcare, UK) resulted in light emission that was recorded on autoradiography films (HyperfilmMP, GE Healthcare, UK). Dot blot immunodetection was carried out identically to Western blot immunodetection without prior Tricine-PAGE. Exposure times varied between 10 seconds to 5 minutes, as required by the sample.

### 4.3.7   Black lipid bilayer membranes

The methods used for the lipid bilayer experiments have been previously described in detail (Benz *et al.*, 1978). In the experimental setup two compartments of a Teflon cell filled with electrolyte solution were connected by a small circular hole that had about 0.2 mm^2 area. The black lipid membrane was made by painting a 1% (w/v) diphytanoyl phosphatidylcholine

(PC)/*n*-decane solution (Avanti Polar Lipids, USA) across the hole. Ag/AgCl electrodes were used connected in series to a voltage source and a home-made current-to-voltage converter for the electrical measurements. The amplified signal was recorded with a strip chart recorder. Depending on the experiment applied potentials varied from ± 10 to 100 mV. All salts were obtained from Merck (Germany) or Sigma-Aldrich (Germany) at analytical grade. The aqueous salt solutions were unbuffered and, if not explicitly mentioned, had a pH of around 6. The temperature during all experiments was maintained at 20°C. The zero-current membrane potential measurements were performed as it has been described earlier (Benz *et al.*, 1979) by establishing a fivefold salt gradient across membranes containing 10 to 1000 cell wall channels. Zero-current potentials were measured with a high impedance electrometer (Keithley 617).

4.4   Results

4.4.1   Cell wall proteins of *C. jeikeium* K411 affect the conductance of lipid bilayer membranes

Cells of an overnight grown *C. jeikeium* culture were extracted with 1% LDAO. A few microlitres of the crude cell wall extract were tested in the lipid bilayer assay for pore-forming activity (Fig. 4.1A). Irrespective, if added to one or both sides of the lipid membranes two discrete conductance steps with 1.25 and 2.75 nS were observed in 1 M KCl solution at 20 mV applied membrane potential (Fig. 4.1B). Channel formation by the cell wall extract of *C. jeikeium* was not a rare event. Addition of higher amounts of the extract to the lipid membranes resulted in a strong increase of the conductance indicating the formation of many channels of the same conductance. The conductance increase caused by the detergent extract was not sudden but it was a function of time after the addition of the sample to membranes in the black state. Within circa 20 to 30 min the membrane conductance increased by several orders of magnitude above that of membranes without the extract (from about 0.05 μS/cm^2 to 150 μS/cm^2). After that time, only a small further increase compared with the initial one occurred. Control experiments performed only with LDAO at the same concentration as in the experiments with the cell extract demonstrated that the conductance increase was caused by the presence of the cell extract and not by the detergent. This result indicated that channel-forming proteins were present in the detergent extract of whole *C. jeikeium* cells.

A)   B)
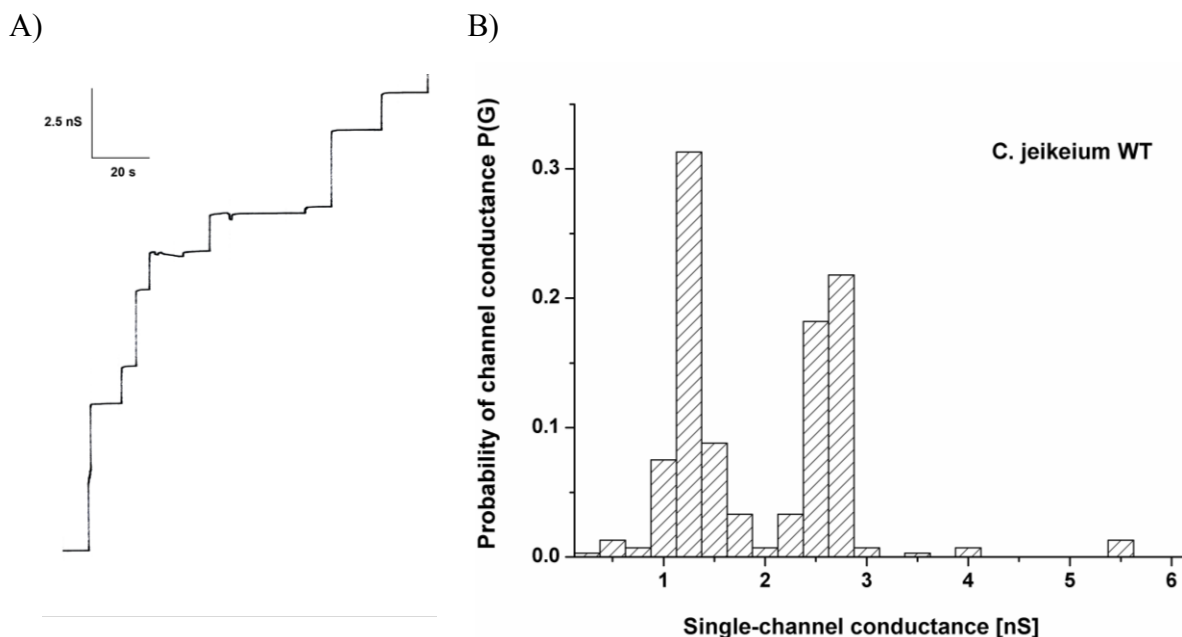
Figure 4.1: (A) Single-channel recording of a 1% PC/*n*-decane membrane in the presence of the detergent extract of whole *C. jeikeium* K411 cells. The aqueous phase contained 1 M KCl and 50 ng/ml protein extract. The applied membrane potential was 20 mV and the temperature was 20°C. (B) Histogram of the probability P(G) for the occurrence of a given conductivity unit observed with membranes formed with 1% PC/*n*-decane. It was calculated by dividing the number of fluctuations with a given conductance rise by the total number of conductance fluctuations in the presence of the detergent extract of whole *C. jeikeium* K411 cells. Two frequent conductive units were observed for 307 single events taken from 13 individual membranes. The average conductance of the steps corresponding to the left-side maximum was 1.25 nS and that of the right-side maximum was 2.75 nS. The aqueous phase contained 1 M KCl and 50 ng/ml protein extract. The applied membrane potential was 20 mV, and the temperature was 20°C.

4.4.2   Identification of the gene coding for the cell wall channel of *C. jeikeium* K411

The *C. jeikeium* cell extract was subjected to preparative Tricine-PAGE and gel bands at different molecular masses were excised and extracted with 1% LDAO detergent. The highest channel activity was observed in the low-molecular-mass region of the gel, especially in the region of about 5 kDa, but it was impossible to relate a single band to the channel-forming activity. This means that for *C. jeikeium* a protein of similar size as the pore-forming proteins CgPorH and CgPorA of *C. glutamicum* (Hünten *et al.*, 2005a; Hünten *et al.*, 2005b; Lichtinger *et al.*, 2001) was responsible for the membrane activity in lipid bilayer experiments (Fig. 4.1A). Previously, we could identify CdPorA of *C. diphtheriae* based on its homology with CgPorA of *C. glutamicum* and other corynebacteria (Lichtinger *et al.*, 2001; Schiffler *et al.*, 2007). Using PorH and PorA porin sequences, the genome of *C. jeikeium* K411 (Tauch *et al.*, 2005) was searched for known protein and gene sequences with the basic local alignment search tool (BLAST) (Altschul *et al.*, 1997), but we did not obtain a significant hit. Therefore, we compared the chromosomal localizations of to date known *porH* and *porA* genes of the

different corynebacteria (Fig. 4.2). Our analysis suggested that these genes are located in a conserved chromosomal region framed by genes encoding a chaperonin (GroEL2) and a poly-phosphate kinase (PPK2). This result applied to the annotated *C. jeikeium* genome yielded a region that contained an open reading frame (*jk0268*) between the homologous genes *jk0267* (GroEL2) and *jk0269* (PPK2) that could code for a low-molecular-mass cell wall protein (Fig. 4.2).
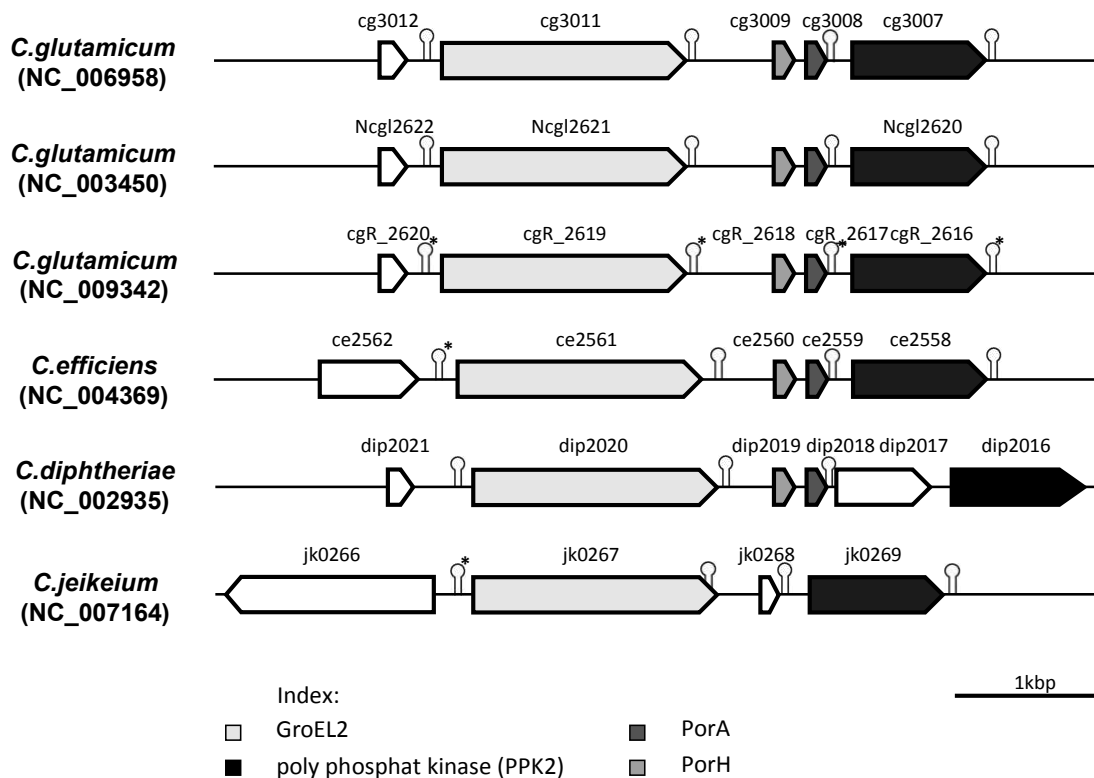
Figure 4.2: Analysis of the accessible genomes from species of *C. glutamicum*, *C. efficiens, C. diphtheriae and C. jeikeium*. The homolog genes of the chaperonin GroEL2 and a poly-phosphate kinase PPK2 enclose a presumed conserved porin domain. The operon covering the genes *cgporH* (cg3009) and *cgporA* (3008) whose proteins build the bicomponental main cell wall channel of *C. glutamicum* is inferred to exist in all strains except for *C. jeikeium*. Possible terminator sequences of mRNA transcripts were predicted with TransTermHP (Kingsford *et al.*, 2007) (indicated by hairpins; or identified manually (marked by asterisk) by comparative analysis).

Primers were designed to clone the region between the two genes *jk0267* (GROEL2) and *jk0269* (poly-phosphate kinase) using DNA of *C. jeikeium* as a template (Table 4.1). The PCR-product was cloned into the TOPO 2.1 vector and was sequenced. It contained *jk0268* that could code for a small cell wall channel.

The involvement of JK0268 in the observed channel formation of *C. jeikeium* extracts was

examined by expressing the corresponding gene *jk0268* in a *C. glutamicum* mutant deficient of its main cell wall channel (Schiffler *et al.*, 2007).
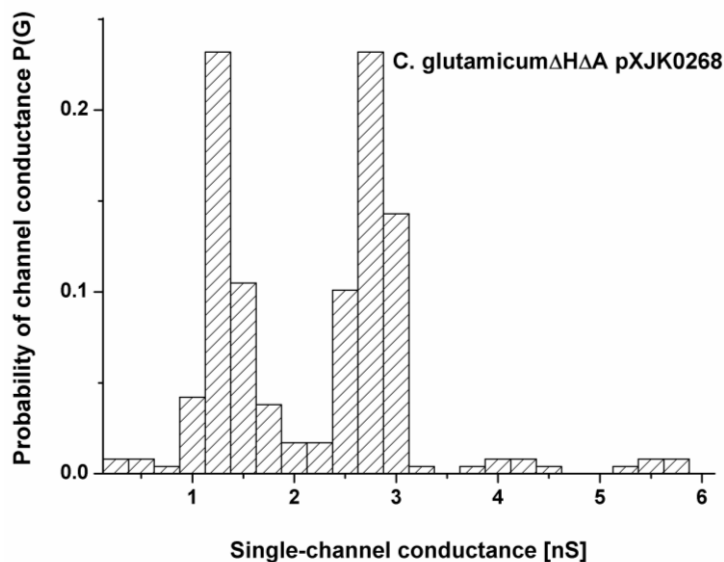
Figure 4.3: Histogram of the probability P(G) for the occurrence of a given conductivity unit observed with membranes formed with 1% PC/*n*-decane in the presence of 50 ng/ml of the detergent extract of whole *C. glutamicum ΔporHΔporA* mutant cells expressing JK0268. Two frequent conductive units were observed for 230 single events taken from 7 individual membranes. The average conductance of the steps corresponding to the left-side maximum was 1.25 nS and that of the right-side maximum was 2.75 nS. The aqueous phase contained 1 M KCl, the applied membrane potential was 20 mV, and the temperature was 20°C.

Whereas in terms of identical treatment cell wall samples of the *C. glutamicum* mutant did not produce any channels in black lipid membranes, samples of pXJK0268 transformed and IPTG induced mutant cells caused well-defined and step-wise channel events that were similar to those shown in Fig. 4.1A. Statistical analysis of the observed single-channel events (Fig. 4.3) further supported the conclusion that these channels were identical to those of the *C. jeikeium* extract showing two maxima of 1.25 and 2.75 nS in 1 M KCl. This result implied that JK0268 (named in the following CjPorA for *C. jeikeium* PorA) is the main cell wall channel of *C. jeikeium*.

4.4.3   Comparison of CjPorA with PorA and PorH of other corynebacteria

Figure 4.4 shows a comparison of the sequences of the cell wall proteins PorA and PorH of different corynebacteria with that of CjPorA derived with AliBee (www.genebee.msu.su).

A)

```
PorA_Cglut1   M-ENVYEFLGNLDV-LSGSG-LIGYVFDFLGASSKWAGAVADLIGLLG   45#   C.glutamicum ATCC 13032
PorA_Cglut2   M-ENVTTFLDNLGI-LSTTG-LFGDAFSFLAASGNWADAVAKLIGLL-   44    C.glutamicum R
PorA_Ceff     M-ESITDFIANVSN-LSSTG-LVGTVFGLIKTAGDWADNVAKLIGLLG   45    C.efficiens AJ 12310
PorA_Ccall    M-DNFVEFLDNVNT-LSSTG-LVAELLDFFTASGKWAGAVADLLGLVK   45    C.callunae ATCC 15991
PorA_Cdiph1   M-QNIENWVA-LST--DENS-IVTVIFDLLKQVAKMGKAIADLIGLAK   43    C.diphtheriae ATCC 11913
PorA_Cdiph2   M-ENINHWVE-LSS--GKDS-IVTVIFGLLKDIAKMGKAIADLIGLAK   43    C.diphtheriae NCTC 13129

PorA_Cjei     MIDQITEIFGQLGTFLGGFGNIFKGLKDVIETIVKW--TAAK------   40    C.jeikeium K411
```

B)

```
PorH_Cglut1   MDLSLLKETLGNYETFGGNIGTALQSIPTLLDSILNFFDNFGDLADTTGE------NLDNFSS   57    C.glutamicum ATCC 13032
PorH_Cglut2   MDLSLLKDNLSDYATFGKNIGTALQSIPTVLNSILDFFTGFGDNADTTGK------AFENLSS   57    C.glutamicum R
PorH_Ceff     MDLSLLKDSLSDFATLGKNLGPALQGIPTLLNSIIAFFQNFGDLAETTGD------AAGNLSS   57    C.efficiens AJ 12310
PorH_Ccall    MDLSLLADNLDDYSTFGGNIGTALTMIPDLLKGIIAFFENFGDNADATSA------AFEGLSS   57    C.callunae ATCC 15991
PorH_Cdiph1   MDIQFIASQLKHFDTFVTSIVDLFQGFPNLIADLADLFKN---NAAGWGDTWEETKKIFENK---   59    C.diphtheriae ATCC 11913
PorH_Cdiph2   MDPQFIASQLKNFETFVTNIATLFEGFPQLIKQLAGLFNN-G--AEGWGKAWESTKKIFEN---   58    C.diphtheriae NCTC 13129

PorA_Cjei     M-IDQITEIFGQLGTFLGGFGNIFKGLKDVIETIVKWTAAK----------------   40    C.jeikeium K411
```
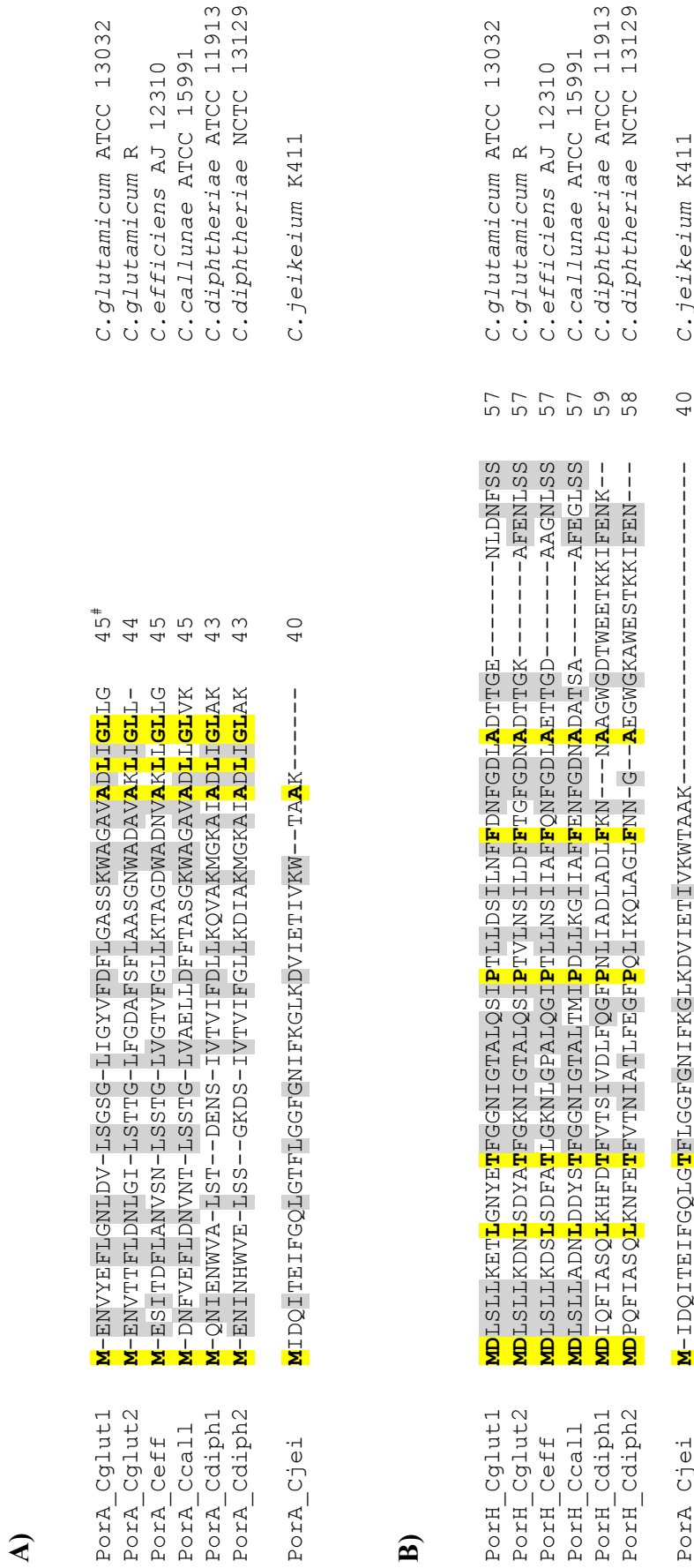
Figure 4.4: Protein alignment of CjPorA against the class of PorA (A) and PorH (B) porins identified in *C. glutamicum*, *C. efficiens*, *C. callunae* and *C. diphtheriae*. The comparison was made with AliBee (www.genebee.msu.su) using default parameters. Residues with total or > 50% conservation are shaded by yellow or grey colours. #indicates the number of amino acids.

The protein has similar to PorA and PorH known to date only the inducer methionine but no presequence similar to CgPorA and CgPorH of *C. glutamicum* (Hünten *et al.*, 2005a; Lichtinger *et al.*, 2001), which means that the proteins are exported to the cell wall by a not yet identified mechanism. Similar is also the length of CjPorA (40 amino acids) as compared to that of the different PorA (on average 43 amino acids) and PorH (57 amino acids) proteins. But apart from that, the homology is rather poor because in comparison to PorH only a small number of amino acids are conserved. Nevertheless, it is clear that the sequences of the different proteins are related, which means that they are presumably descendents of a common ancestor protein (see *Discussion*).

4.4.4 Heterologous expression and purification of the C-terminal tagged channel-forming protein CjPorA

Cell wall preparations either taken from *C. jeikeium* or *C. glutamicum* expressing CjPorA indicated a significant contribution of this protein to the noticed channels. For purification of the protein we used a PCR based mutagenesis approach to introduce a DNA sequence coding a protease Xa cleavable, 8 histidine residues comprising protein tail. This tail was added to the C-terminus of the wild-type gene. The constructed DNA cassette, accounting for the *C. glutamicum* codon usage frequencies (Hallin & Ussery, 2004), was introduced in the pXMJ19 expression vector and the stop codon (TAA) of *jk0268* was substituted (GGT) to fuse the peptide tail.

From IPTG-induced and detergent-extracted *C. glutamicum* cells expressing CjPorA we could not directly notice expression of neither the wild-type nor the modified *C. jeikeium* protein in SDS-PAGE gels. Only higher concentrated samples of chloroform/methanol precipitates combined with immunoassay using an anti-His antibody revealed expression of a small-sized protein, as shown by Western blots with detergent and organic solvent extracts of induced and not induced cells (Fig. 4.5). The molecular mass of this protein matched well with the calculated MW of CjPorA-His (6.2 kDa). It was therefore purified and enriched from detergent extracts by Ni^{2+}-affinity chromatography (Fig. 4.5).

The pure and still histidine-tailed protein was capable of forming channels after trace amounts were added to the aqueous phase in the lipid bilayer setup (not studied in detail). However, in
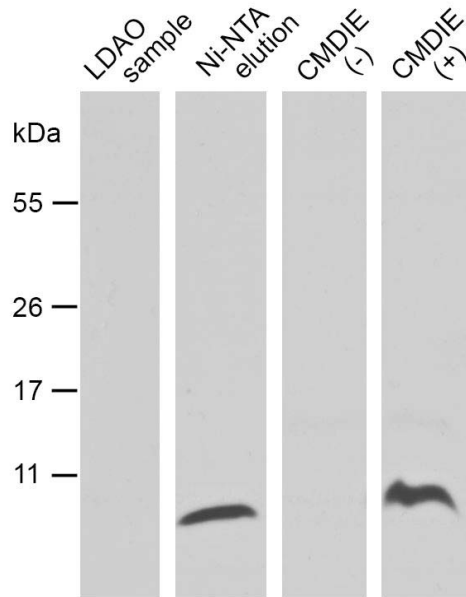
Figure 4.5: Western blot analysis of IMAC purified his-tagged CjPorA protein. The protein was expressed in *C. glutamicum* Δ*porH*Δ*porA* and purified by Ni^{2+}-affinity from the supernatant of detergent prepared whole cells. CMDIE represents chloroform-methanol extracted cells of pXJK0268His transformed (+) or non-transformed (-) *C. glutamicum* Δ*porH*Δ*porA* cells in which the crude protein content was concentrated around 8-fold by diethyl-ether precipitation. Subsequent to Tricine (12%)-PAGE the gel was blotted onto a nitrocellulose membrane and CjPorA-His was visualized by anti-His antibody and a chemiluminescent reaction. All samples were boiled for 5 min in Redmix before loading.
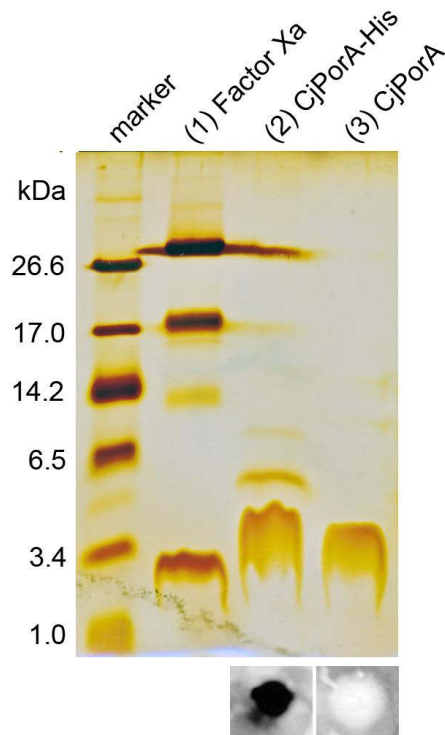
Figure 4.6: Silver-stained Tricine (16.5%)-PAGE gel of Ni^{2+}-purified and factor Xa digested CjPorA protein. Lanes: 1, 3 units of protease Xa (control); 2, 10 µl of three pooled Ni-NTA elutions containing CjPorA-His; 3, 10 µl of protease Xa treated and purified CjPorA protein (for details see text). The dot blot immunoassay pictures underneath lanes 2 and 3 show cleavage of the histidine tail using anti-His antibody and 5 µl of corresponding samples. Before loading all samples were boiled for 5 min in Redmix.

order to approach the situation of the native protein the His-tag was cleaved with protease Xa and the truncated CjPorA protein (containing the C-terminal linker residues Gly-Thr-Ile-Glu-Gly-Arg) was again purified to homogeneity (Fig. 4.6). All further biophysical measurements were performed with pure CjPorA obtained in this way.

4.4.5   Pore conductance analysis of CjPorA

Addition of small amounts of the purified *C. jeikeium* cell wall protein (about 10 ng/ml) to one or both sides of a black lipid membrane resulted after a few minutes delay in observation of step-like conductance increases. These channels had the same size as described above for detergent-solubilised material from *C. jeikeium* and *C. glutamicum* pXJK0268. Further, the channels were stable and had a long lifetime leading to superposition of the steps (Fig. 4.7A). Most of the steps were directed upwards indicating that the channels were for long time in an open state under low voltage conditions (20 mV).

A)   B)
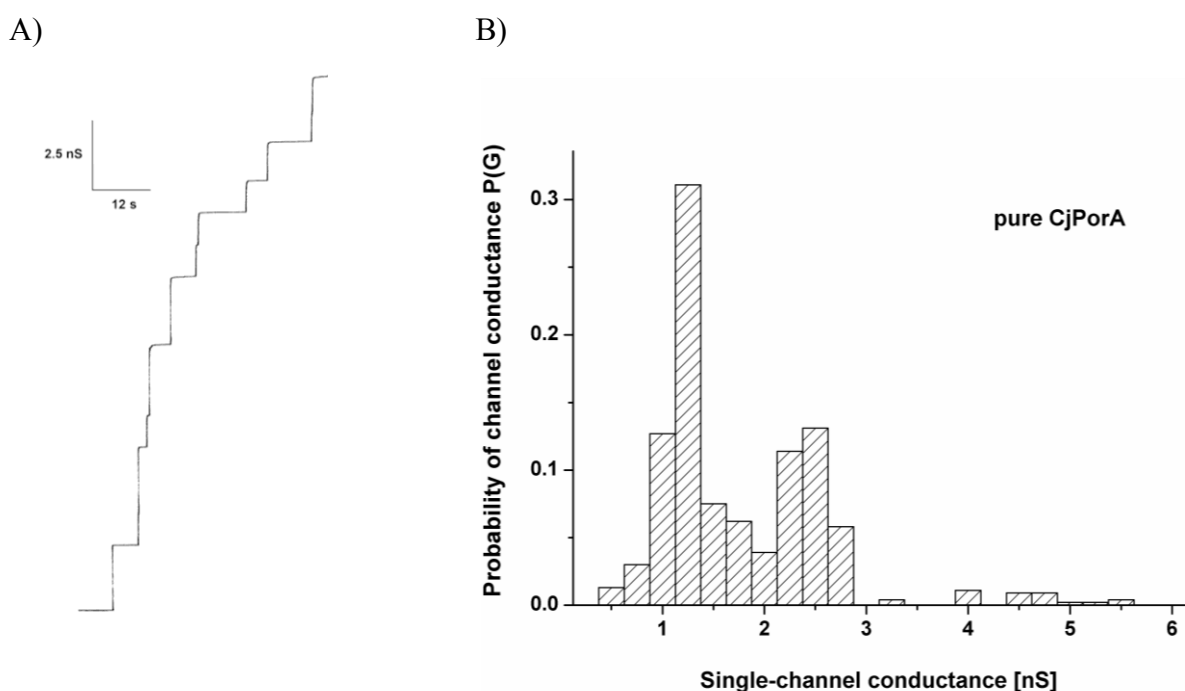
Figure 4.7: (A) Single-channel recording for a PC/*n*-decane membrane in the presence of pure CjPorA protein. The aqueous phase contained 1 M KCl and 10 ng/ml protein extract. The applied membrane potential was 20 mV and the temperature was 20°C. (B) Histogram of the probability P(G) for the occurrence of a given conductivity unit observed with membranes formed of 1% PC/*n*-decane in the presence of pure CjPorA protein. Two frequent conductive units were observed for 460 single events taken from 18 individual membranes. The average conductance of the steps corresponding to the left-side maximum was 1.25 nS and that of the right-side maximum was 2.5 nS. The aqueous phase contained 1 M KCl and 10 ng/ml protein. The applied membrane potential was 20 mV, and the temperature was 20°C.

Only a few channels showed some flickering pointing towards transitions between open and closed states. The statistical analysis (Fig. 4.7B) being similar to those shown in Fig. 4.1B and Fig. 4.3 indicated that most of the channels (more than 40% of all fluctuations) caused conductivity steps with 1.25 or 2.5 nS in 1 M KCl (20 mV applied membrane potential). This means that beside a major conductance step of about 1.25 nS we observed also channels with a higher single-channel conductance, in particular channels with a single-channel conductance of about 2.5 nS. The latter channels are presumably dimers of the 1.25 nS channel that could not be separated within the time resolution of our experimental setup. It is also possible that the two different channels represent two different arrangements of the CjPorA monomers. However, this is rather unlikely because under all conditions used here we found a 1:2 relationship for the two maxima within the histograms, which were denoted there as left-side and right-side maximum.

In order to obtain some information on the biophysical properties of the *C. jeikeium* cell wall channel we expanded the pore conductance analysis to other salts than KCl and different molarities. According to the results shown in Table 4.2, the channel seemed to be moderately selective for anions. This is concluded from experiments in which KCl was replaced by LiCl or KCH_3COO. The exchange of the mobile ions K^+ or Cl^- by the less mobile ions Li^+ or CH_3COO^- revealed that cations and anions can permeate through the *C. jeikeium* channel. However, the effect of anions on the single-channel conductance was more substantial. The permeability of the ions through the channels followed approximately their mobility sequence in the aqueous phase. This indicates that the channels formed by CjPorA are wide and water-filled and have only a small field strength inside and no small selectivity filter (i.e. no binding site) as is suggested by the fact that also large organic anions could penetrate the channel.

Table 4.2 also contains the average single-channel conductance values of the *C. jeikeium* channel obtained from KCl measurements performed down to 0.01 M. The values for G always corresponded to those of the two maxima in the histograms, i.e. to the 1.25 and 2.5 nS peaks in the case of 1 M KCl. For the *C. jeikeium* channel, we observed a linear relationship between single-channel conductance and KCl concentration, as it is shown in Fig. 4.8 exemplary for the left-side maximum of the single-channel conductance (filled squares). This result excluded both point charges at the channel mouth attracting ions under low salt concentrations and the presence of an ion binding site in the channel, as no saturation under

Salt	Concentration [M]	Single-channel conductance G [pS]	
		maximum	
		left-side	right-side
KCl	3.0	3.250	6.500
	1.0	1.250	2.500
	0.3	350	750
	0.1	175	325
	0.03	50	120
	0.01	33	70
LiCl	1.0	1.000	2.000
KCH_3COO	1.0	500	1.100
	0.1[a]	50	115
KBr	0.1	170	340
KNO_3	0.1	140	260
$KClO_3$	0.1	115	235
KF	0.1	70	180
KCHOO	0.1[a]	65	155

Table 4.2: Average single-channel conductance G of pure CjPorA cell wall protein in different salt solutions. For determination of the pore diameter on basis of the Renkin formalism the data of 0.1 M potassium saline were used. The membranes were formed with 1% PC/_n_-decane. The aqueous solutions were unbuffered and had a pH of around 6 ([a] pH was around 7.4). The applied voltage was 20 mV, and the temperature 20°C. The table shows the mean of at least 100 single-channel events.
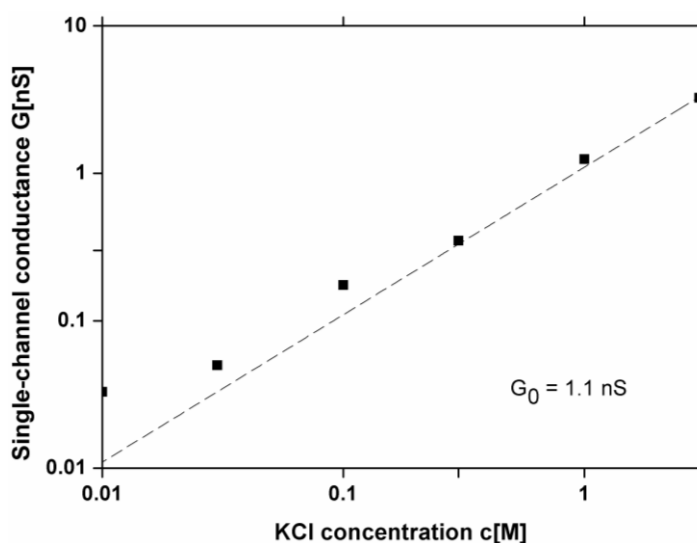
Figure 4.8: Single-channel conductance of the CjPorA cell wall protein expressed as a function of the aqueous KCl concentration. Squares symbolise the data of the left-side maximum taken from Table 4.2. The dashed line is the single-channel conductance of the cell wall channel in absence of point net charges and corresponds to a linear function between channel conductance and bulk aqueous concentration. G_0 represents the single-channel conductance excluding point net charges in 1 M KCl.

high salt concentrations occurred. This means that the cell wall channels of *C. jeikeium* showed characteristics of wide and water-filled channels similar to those found in Gram-negative bacteria (Benz, 2003). Thus, the channels of *C. jeikeium* are together with those of *C. diphtheriae* the first ones without point charge effects on the channel properties within the suborder *Corynebacterineae* (Schiffler *et al.*, 2007) (see *Discussion*).

4.4.6   Zero-current membrane potential measurements of CjPorA

Zero-current membrane potential measurements were performed to obtain further information on the structure of the *C. jeikeium* cell wall channel. The experiments were performed in the following way. After the incorporation of 10 to 1000 channels into the PC membranes bathed in 100 mM salt solution, the salt concentration on one side of the membranes was raised fivefold beginning from 100 mM and the zero-current potentials were measured 5 min after every increase of the salt gradient across the membrane. For KCl, LiCl and KCH$_3$COO the more diluted side of the membrane (100 mM) always became negative, which indicated for all three salts preferential movement of the anions. This result indicates that the channel functions as a general diffusion pore for negative solutes. Analysis of the membrane potential using the Goldman-Hodgkin-Katz equation (Benz *et al.*, 1979) confirmed the assumption that anions and cations are permeable through the channel (Table 4.3). The calculated cation/anion permeability ratios were 0.34 (KCl), 0.25 (LiCl) and 0.40 (potassium acetate), which means that the selectivity followed the mobility sequence of anions and cations in the aqueous phase, i.e. the *C. jeikeium* channel is indeed water-filled.

Salt	V$_m$ [mV]	Cation/anion permeability ratio
KCl	- 15.7	0.34
LiCl	- 22.1	0.25
KCH$_3$COO	- 13.4	0.40

Table 4.3: Zero-current membrane potentials of PC/*n*-decane membranes in the presence of pure CjPorA cell wall protein measured for a fivefold gradient of different salts. V$_m$ is defined as the difference between the potential at the dilute side (100 mM) and the potential at the concentrated side (500 mM). The pH of the aqueous salt solutions was around 6, and the temperature was 20°C. The cation/anion permeability ratio was calculated from at least 3 individual experiments using the Goldman-Hodgkin-Katz equation (Benz *et al.*, 1979).

4.4.7 Investigation of the voltage dependence of CjPorA

In single-channel recordings the cell wall porin showed only occasionally rapid transitions between open and closed configurations at low applied membrane voltages (20 mV). The frequency of closed configurations increased considerably at higher voltages. This could be caused by voltage-dependent closure of CjPorA pores, so this was studied in detail. For this purpose, multi-channel experiments were performed in which CjPorA was added in concentrations of 100 ng/ml to one side of a black membrane (the *cis* side). After the conductance reached a stationary state, increasing positive and negative potentials were applied to the *cis* side of the membrane (beginning with 10 mV), and the change in conductance was recorded as a function of time.
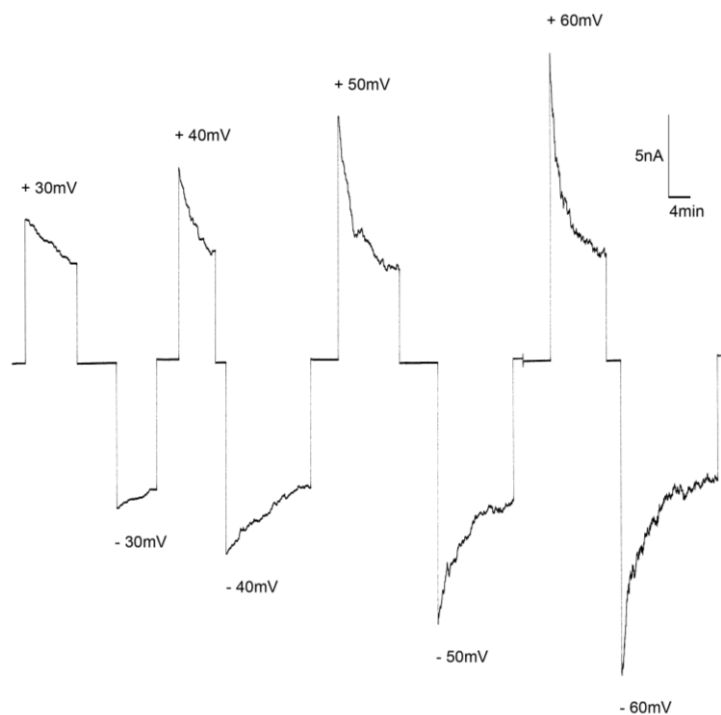
Figure 4.9: Investigation of the voltage-dependence of CjPorA in a multi-channel experiment. The purified protein was added to the *cis* side of a PC/*n*-decane membrane (100 ng/ml) and reconstitution of channels was followed until equilibrium. Then, positive (upper traces) and negative voltages (lower traces) were increasingly applied to the *cis* side of the membrane and the membrane current was measured as a function of time. The aqueous phase contained 1 M KCl, and the temperature was 20°C.

As shown in Fig. 4.9 for voltages between ±30 and ±60 mV, the current decreased in an exponential fashion following the application of negative as well as positive potentials at the *cis* side of the membrane. This result indicated symmetrical voltage-dependence of the *C. jeikeium* cell wall channel. A similar result was obtained for CjPorA added to the *trans* side or to both sides of the membrane (data not shown). Taken together, these results indicated either

symmetric orientation of the cell wall channel in lipid bilayer membranes or symmetrical response of the channel to the applied potential.

The data of the experiments were analyzed as follows: the membrane conductance (G) as a function of the applied voltage (V_m) was measured when the opening and closing of channels reached an equilibrium (i.e., after the exponential decay of the membrane current following the voltage step V_m). G was divided by the initial value of the conductance G_0, which was obtained directly after the onset of the voltage and which was a linear function of the voltage. The data of Fig. 4.10 correspond to the symmetric voltage-dependence of the *C. jeikeium* cell wall channel (mean of six membranes) when CjPorA was added to the *cis* side of the lipid membranes (closed squares).
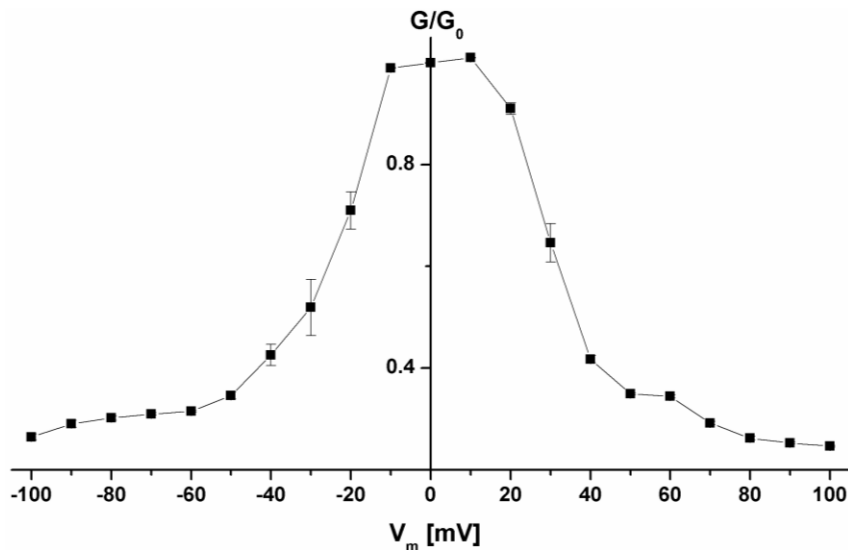
Figure 4.10: Conductance (G) at a given membrane potential (V_m) divided by the conductance at 10 mV (G_0) expressed as a function of the membrane potential. The symbols represent the mean of six measurements, in which the pure CjPorA protein was added to the *cis* side of the membranes. The aqueous phase contained 1 M KCl and 100 ng/ml porin. The membranes were formed from PC/*n*-decane at a temperature of 20°C.

In order to study the voltage dependence in more detail, the data of Fig. 4.10 were analyzed by applying Equation 4.1 assuming a Boltzmann distribution between the numbers of opens (N_O) and closed (N_C) channels (Ludwig *et al.*, 1986) and Equation 4.2 that builds the bridge to the conductance data.

Equation 4.1
$$\frac{N_O}{N_C} = e^{nF(V_m - V_0)/RT}$$

n in this equation represents the number of charges moving due to the applied external transmembrane potential leading to the observed channel gating. V_0 is the midpoint potential (potential at which $N_O/N_C = 1$). F (= 96500 As/mol), R (= 8.31 J/mol*K), T are Faraday constant, gas constant and temperature, respectively.

Equation 4.2 $$\frac{N_O}{N_C} = \frac{G - G_{min}}{G_0 - G}$$

G in this equation is the conductance at a given membrane potential (V_m). G_0 and G_{min} are the conductance at 10 mV (conductance of the open state) and very high potentials, respectively.

Figure 4.11 shows the semi-logarithmic plot of the ratio of open channels to closed channels (N_O/N_C) as a function of the voltage (V_m). The results (closed circles) could be fitted into strait lines which allowed the calculation of the midpoint potential (V_0) (at which 50% of the total number of channels is in the closed configuration) and the number of gating charges (n) involved in the gating process. The midpoint potential for the addition of the protein to the *cis* side was for applied positive voltages + 24.6 mV and for applied negative voltages – 24.0 mV. The gating charge in both cases was 1.9.
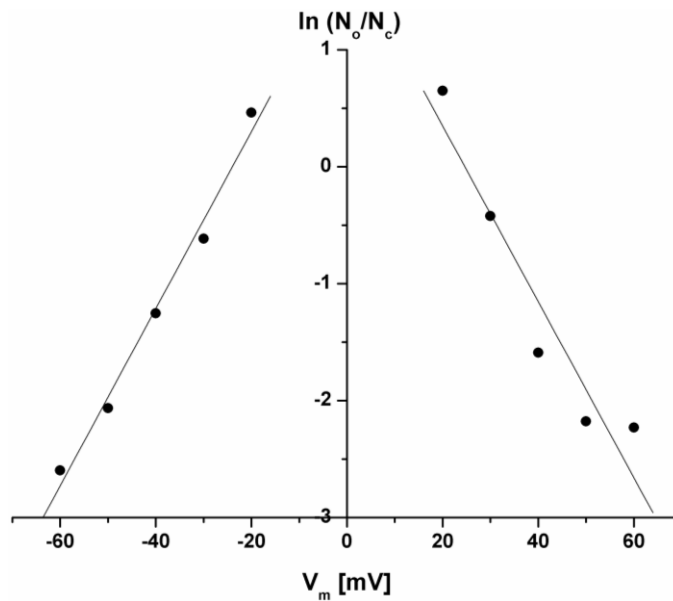
Figure 4.11: Semi-logarithmic plot of the ratio N_O/N_C as a function of the applied transmembrane potential V_m. The data of Fig. 4.10 is fundamental to access the midpoint potential V_0, at which half of the channels are in a closed state configuration ($N_O/N_C = 1$). V_0 is – 24.0 mV and + 24.6 mV for negative and positive potentials, respectively. In both cases 1.9 charges were calculated to cause the voltage-dependent closure of CjPorA channels.

4.4.8 Estimation of the channel diameter of CjPorA

The conductance of the channels formed by CjPorA was a linear function of the bulk aqueous concentration (Fig. 4.8). This means that the *C. jeikeium* channel does not contain point charges near the channel opening excluding a determination of the pore diameter on basis of Nelson`s and McQuarrie`s (1975) formalism as was performed for cell wall channels of other members of the mycolata (Lichtinger *et al.*, 1998; Riess *et al.*, 1998; Trias & Benz, 1993). On the other hand, an estimate of the size of the *C. jeikeium* channel is possible from a fit of the single-channel data for salts of different anions using the Renkin equation (Trias & Benz, 1994). That is because the CjPorA channel was anionic selective under all conditions. Its single-channel conductance was primarily limited by the permeability of the anions passing the channel (Table 4.2). Additionally, the permeability of the anions moving through the channel followed approximately their mobility sequences in the aqueous phase (Br$^-$ > Cl$^-$ > NO$_3^-$ > ClO$_3^-$ > F$^-$ > HCOO$^-$ > CH$_3$COO$^-$) which means that an interaction of the anions with the channel's interior could nearly be ruled out.

The diameter of the *C. jeikeium* channel was determined using a method formerly suggested by Trias & Benz (1994). The permeability of a cylindrical channel towards ions (or other solutes) is proportional to the aqueous diffusion coefficient (*D*) multiplied with the Renkin correction factor, which is given by Equation 4.3:

Equation 4.3
$$\frac{A}{A_0} = \left[1 - (a/r)^2\right]\left[1 - 2.104(a/r) + 2.09(a/r)^3 - 0.95(a/r)^5\right]$$

A in this equation is the effective area of the channel mouth. A_0 is the total cross sectional area of the channel. *r* and *a* are the radii of the channel and the hydrated monovalent ions, respectively, passing through the channel. *a* can be calculated according to the Stokes equation (Equation 4.4) by using λ_i, the limiting molar conductivity of the ions in the aqueous phase (Castellan, 1983).

Equation 4.4
$$a = \frac{Fe}{6\pi\eta\lambda_i}$$

Parameters in this equation are: F (= 96500 As/mol) is the Faraday constant, e (= $1.602*10^{-19}$ As) is the elementary charge and η (= $1.002*10^{-3}$ kg/m*s) is the viscosity of the aqueous phase.

Table 4.4 contains the limiting molar conductivity adopted from Castellan (1983), the hydrated anion radii calculated according to the Stokes equation (Equation 4.4) and the single-channel conductance of the *C. jeikeium* porin that was set to unity relative to the conductance in 0.1 M KBr.

Anion	Radii of the hydrated anions a [nm]	Limited molar conductivity λ_i [Scm^2/mol]	Permeability relative to 0.1 M KBr	
			maximum	
			left-side	right-side
Br$^-$	0.105	78.14	1.0	1.0
Cl$^-$	0.107	76.35	1.0	0.96
NO$_3^-$	0.115	71.46	0.82	0.76
ClO$_3^-$	0.127	64.60	0.68	0.69
F$^-$	0.148	55.40	0.41	0.53
HCOO$^-$	0.150	54.59	0.38	0.46
CH$_3$COO$^-$	0.200	40.90	0.29	0.34

Table 4.4: Radii of the anions, the limited molar conductivity λ_i and the relative permeability of CjPorA in different salt solutions. The radii of the hydrated anions were calculated using the Stokes equation (Equation 4.4) and the limited molar conductivity taken from Castellan (1983). The single-channel conductance of CjPorA for the 0.1 M salt solutions was taken from Table 4.2. The relative permeability of the single anions was calculated by dividing the single-channel conductance of the individual anion by that of 0.1 M KBr. The relative permeability for 0.1 M KBr was set to unity.

The fit of the normalized single-channel conductance (mean of the left- and right-side relative permeability) of CjPorA with the Renkin correction factor (Equation 4.3) times the aqueous diffusion coefficient of the corresponding anion is shown in Fig. 4.12. The best fit of the relative permeability was obtained with r = 0.7 nm (diameter 1.4 nm).
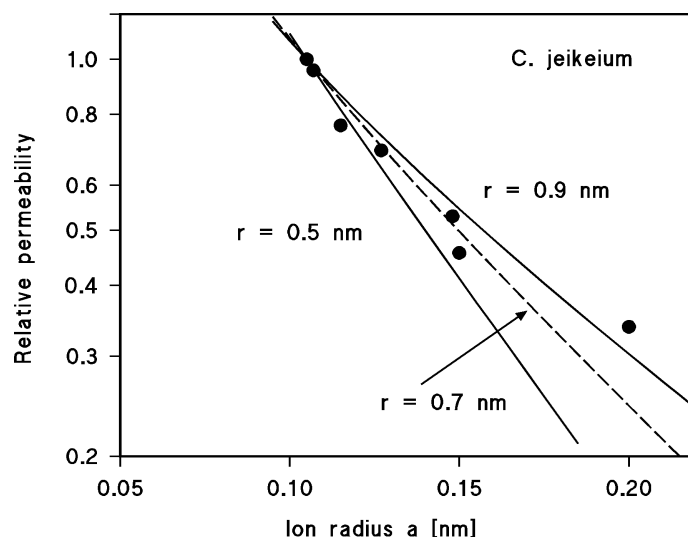
Figure 4.12: Fit of the single-channel conductance data of the CjPorA cell wall channel by using the Renkin correction factor times the aqueous diffusion coefficients of the different anions (Trias & Benz, 1994). The product of both numbers was normalized to 1 for a = 1.05 nm (Br⁻). Single-channel conductance were normalized to the one of 0.1 M KBr and plotted versus the hydrated ion radii taken from Table 4.4. The single-channel conductance correspond to Br⁻, Cl⁻, NO₃⁻, ClO₃⁻, F⁻, HCOO⁻ and CH₃COO⁻ which were all used for the pore diameter estimation. The fit (solid lines) is shown for r = 0.5 nm (lower line) and r = 0.9 nm (upper line). The best fit was achieved with r = 0.7 nm (diameter = 1.4 nm) corresponding to the broken line.

4.5 Discussion

4.5.1 The genome of *C. jeikeium* contains only one gene coding for CjPorA, the main cell wall channel

In this work, we extended our study of channel-forming proteins within the family of *Corynebacteriaceae* to the species *C. jeikeium*. Methodologies used previously for the isolation and characterization of cell wall-associated, channel-forming proteins showed that the supernatant of detergent extracted C. *jeikeium* cells contained channel-forming units. These units increased in black lipid bilayer assays the ion conductance mainly by 1.25 and 2.75 nS steps in 1 M KCl (Fig. 4.1). From preparative tricine-containing SDS-PAGE it became evident that a small-sized protein of *C. jeikeium* was responsible for the pore-forming activity similar to that of PorH and PorA porins of *C. glutamicum*, *C. callunae*, *C. efficiens* and *C. diphtheriae*. Therefore, we searched within the known genome of *C. jeikeium* K411 for homologous proteins to PorH and PorA using the basic local alignment search tool (BLAST). Interestingly, this direct approach to identify the *C. jeikeium* porin was unsuccessful. In an additional approach, the localizations of *porH* and *porA* genes within the chromosomes were compared with the homologous region of *C. jeikeium* (Fig. 4.2). The results suggested that

124

these genes are located in a conserved region flanked by genes coding a chaperonin (GroEL2) and a poly-phosphate kinase (PPK2). Applied to *C. jeikeium*, the region between the genes *jk0267* and *jk0269* was astonishingly smaller than that of the other *Corynebacterium* strains and it contained only one predicted coding DNA sequence, *jk0268*. This gene is coding for a 40 AS polypeptide with a (calculated) MW of 4401 Da. BLAST of the *C. jeikeium* protein to the non-redundant GenBank database (6.494.107 sequences, 02/08, National Center for Biotechnology Information) did not result in a significant match to any other sequence. Six base pairs upstream of the inducer methionine, the *jk0268* gene contains a putative ribosome binding site (5'-AGGAG-3'). On the bases of various predicted rho-independent terminator sequences, we suggest that the gene *jk0268* is transcribed autonomously of the surrounding genes similar to the situation in the genome of *C. glutamicum* (see *Chapter 3*). Our assumption is substantiated downstream of *jk0268* by a high-scored (100) stem-loop structure (5'- CCCCGGCTTCGGCCGGGG -3') and upstream of the gene by structures that are probably able to end GroEL2 mRNA transcription (score values of 39 to 66) (Kingsford *et al.*, 2007).

Only recently it was demonstrated that the major cell wall channels of *C. glutamicum*, *C. efficiens* and *C. diphtheriae* are formed by oligomers of two small peptides, PorH and PorA (see *Chapter 3*). This is also likely to be true for the major cell wall channel of *C. callunae* because CcPorH and CcPorA of this strain possess distinctive homology to the corresponding proteins of *C. glutamicum* and *C. efficiens* (Fig. 4.4). These findings suggested that presumably most corynebacteria possess heteromeric major cell wall channels. However, this study showed that in contrast to this the major cell wall channel of *C. jeikeium* is an oligomer formed solely from one polypeptide, CjPorA. There are two clear findings supporting this. (i) There exists only a single gene (*jk0268*) between *jk0267* (GroEL2) and *jk0269* (PPK2), whereas the same region within the genomes of the other corynebacteria contains two that are transcribed together. (ii) We cloned *jk0268* in an expression plasmid. Its expression in a *C. glutamicum* mutant that lacked the genes coding for CgPorH and CgPorA resulted in the same channels observed from detergent extracts of *C. jeikeium* K411 cells. This result revealed that oligomers of a short 40 amino acids long polypeptide are sufficient to form channels in the cell wall of corynebacteria.

Analogous to the situation of PorH and PorA proteins of *C. glutamicum*, *C. callunae*, *C. efficiens* and *C. diphtheriae,* the *C. jeikeium* CjPorA protein does not contain N- or C-terminal

or twin-arginine sorting signals commonly used by Gram-positive bacteria for Sec- or TAT-transport (Berks *et al.*, 2000; Ton-That *et al.*, 2004; van Wely *et al.*, 2001). This means that the protein presumably uses the same but still unknown transport mechanism for cell wall proteins of corynebacteria to overcome the cytoplasmic membrane to reach the cell wall. However, the single CjPorA monomers themselves are undoubtedly not large enough to form the observed channels. On the other hand, oligomerization was frequently observed in the field of porin research within mycolate actinomycetes suggesting that the *C. jeikeium* channel is also an oligomer (Lichtinger *et al.*, 2000; Niederweis *et al.*, 1999; Riess *et al.*, 1998; Schiffler *et al.*, 2007).

4.5.2 CjPorA forms an anion selective, wide and water-filled pore with no indication for point charges

The conductance of the cell wall channels formed by CjPorA was a linear function of the bulk aqueous concentration (Fig. 4.8). Similarly, the selectivity of the *C. jeikeium* channels was dependent on the mobility of the ions in the aqueous phase (Table 4.3). This means that the CjPorA pore sorts mainly according to the molecular mass of the solutes similar to the function of general diffusion pores in Gram-negative bacteria (Benz, 1994). This result is surprising because up to date many identified cell wall channels within the taxon mycolta contained charges in or near the channel opening. Apart from the CdPorA/CdPorH channel of *C. diphtheriae*, the *C. jeikeium* channel presented in this study is actually the second channel within the *Corynebacterineae* that does not contain point charges. For this reason, the single-channel analysis did not allow estimation of the channel size on the basis of the existence of point net charges, as it was performed for cell wall channels of mycobacteria, nocardia and corynebacteria (Lichtinger *et al.*, 1998; Riess *et al.*, 1998; Trias & Benz, 1993). Otherwise, the CjPorA channel was anion selective under all conditions, which is on the background of a totally charge balanced monomer astonishing (four positive lysines, compared to four negative glutamates and aspartates), since it suggests a slight excess of cationic charges in the channel lumen of the oligomer. However, the anions passing through the channel interior did obviously not interact much with the channel because the permeability of the anions moving through the channel followed approximately their mobility sequence in the aqueous phase (Table 4.4). For this reason, the Renkin equation could be used to estimate the channel diameter which is approximately 1.4 nm. Thus, the *C. jeikeium* porin is ranking into known channel diameters varying from 1.4 over 2.0 to 3.0 nm of different mycolata, such as

Nocardia asteroides (Riess *et al.*, 1999), *Rhodococcus erythropolis* (Lichtinger *et al.*, 2000) and *Mycobacterium smegmatis* (Trias & Benz, 1994). However, the diameter of the *C. jeikeium* channel was considerably smaller than that of the major CgPorA/CgPorH cell wall channel from *C. glutamicum* with 2.2 nm (Lichtinger *et al.*, 1998).

4.5.3   Putative structure of the channel formed by CjPorA

The comparison of the sequences of different PorA and PorH proteins with CjPorA of *C. jeikeium* (Fig. 4.4) showed that the latter one is more comparable in size to the different PorA proteins. In addition, the alignments do not allow a distinctive allocation to PorA or PorH because each class affiliated members show with 13.6% (PorH) and 11.1% (PorA) a remarkable low degree of conserved residues as compared to CjPorA. Nevertheless, there existed something like a structural homology between CjPorA and the other two channel-forming proteins. Secondary structure predictions of all three proteins suggested that they contain a heptameric repeat motive (abcdefg, Fig. 4.13A) indicating the existence of large α-helical structures with hydrophobic and hydrophilic residues localized on different sides of the helices. Figure 9B shows the possible arrangement of the amino acids in CjPorA in an α-helix. This means that this protein could form an amphipathic helix similar to the possible secondary structure in the monomeric PorH and PorA proteins (Hünten *et al.*, 2005a; Hünten *et al.*, 2005b; Lichtinger *et al.*, 2001). In agreement with the experimental data (demanding a water filled pore with 1.4 nm diameter), the *C. jeikeium* channel is postulated to consist of oligomeric α-helical subunits. This is definitely in contradiction to the 3D-structure of Gram-negative bacterial porins (Schulz, 2004) and that of the mycobacterial MspA channel (Faller *et al.*, 2004), which both form β-barrel cylinders. On the other hand, it represents a similar structure as those of antibiotic channels, such as, e.g., alamethicin (Chugh & Wallace, 2001; Woolley, 2007), the cell wall porin CgPorB of *C. glutamicum* (Ziegler *et al.*, 2008) and the ligand-gated ion channel in the inner membrane of *Erwinia chrysanthemi* (ELIC) (Hilf & Dutzler, 2008). For the cell wall channel of *C. jeikeium* this could mean that the CjPorA monomers are orientated with the leucine, isoleucine and phenylalanine residues (Fig. 4.13B; interfaces a, d and g) to the lipid phase, while glycine rich interfaces (c, e) allow close contact to neighbouring units. The four negative aspartates (Asp 3, Asp 28) and glutamates (Glu 7, Glu 31) together with the four lysines (Lys 24, Lys 27, Lys 35 and Lys 40) are oriented to the channel lumen (f, b and e). At least one of the positive residues must take a dominant position

in the otherwise charge-balanced protein causing the determined anion selectivity. The number of CjPorA monomers in the homooligomeric channel is yet not known and need further experimental and structural information about the channel.

A)

B)
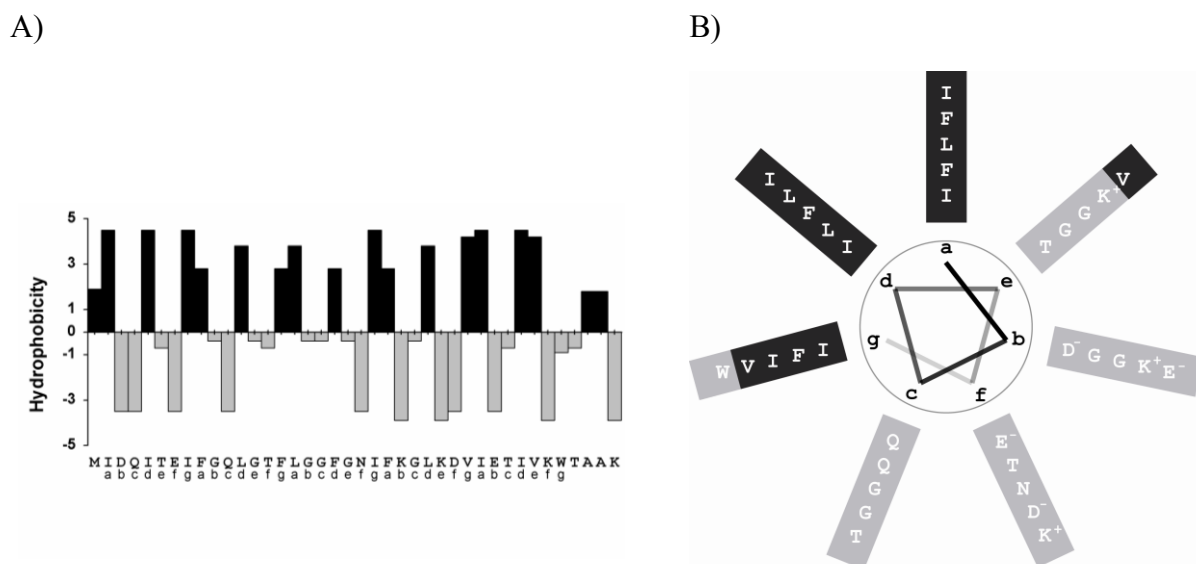
Figure 4.13: Scheme of CjPorA secondary structure. (A) Hydrophobicity indices of the individual amino acids of the *C. jeikeium* protein according to Kyte and Doolittle (1982). Secondary structure prediction using a consensus method (Deleage *et al.*, 1997) at the Pole Bioinformatique Lyonnaise network (http://npsa-pbil.ibcp.fr/cgi-bin/npsa_automat.pl?page=/NPSA/npsa_seccons.html) suggested that the protein forms α-helices (not shown). (B) Amino acid residues arranged on basis of heptameric repeats (a-g) show CjPorA can be separated in a hydrophobic domain supposable surrounded by lipid molecules (dark grey) and a hydrophilic domain (light grey) that is suggested to represent the component orientated to the water filled lumen in the presumed oligomeric *C. jeikeium* cell wall channel.

4.5.4 Is CjPorA of *C. jeikeium* the subunit of the ancestral cell wall channel of corynebacteria?

It is evident that the major cell wall channels of most corynebacteria, i.e. those of *C. glutamicum*, *C. callunae*, *C. efficiens* and *C. diphtheriae*, are oligomers build by two small polypeptides, PorA and PorH. In contrast to this, the major cell wall channel of *C. jeikeium* is an oligomer formed by a single polypeptide, CjPorA. Nevertheless, the many similarities between PorA/PorH and CjPorA suggest that these channel-forming proteins form a family of proteins analogous to the MspABCD cell wall family of *M. smegmatis* and related species (Dörner *et al.*, 2004; Niederweis *et al.*, 1999; Riess *et al.*, 2001; Stephan *et al.*, 2005). Although the CjPorA channel structurally differs in its channel composition from the heterooligomeric PorH/PorA channels within the genus *Corynebacterium* there is a clear evidence for phylogenetic relationships of the channel proteins. The different channel

characteristics (e.g. diameter and selectivity) may reflect minor adaptations to the wide-spread habitats of *Corynebacterium* species ranging from soil to skin and tissue of plants, animals as far as to man. In the first run, mycolata were mainly classified according to properties of the phenotype and the chemical composition of their cell wall (containing meso-diaminopimelic acid, arabinose and glucose as major sugars (Lechevalier *et al.*, 1971)). Analysis of 16S rRNA provided deeper insight into separation of species within the monophyletic *Corynebacteria-Mycobacteria-Nocardia*-group (Khamis *et al.*, 2004; Pascual *et al.*, 1995; Ruimy *et al.*, 1995).
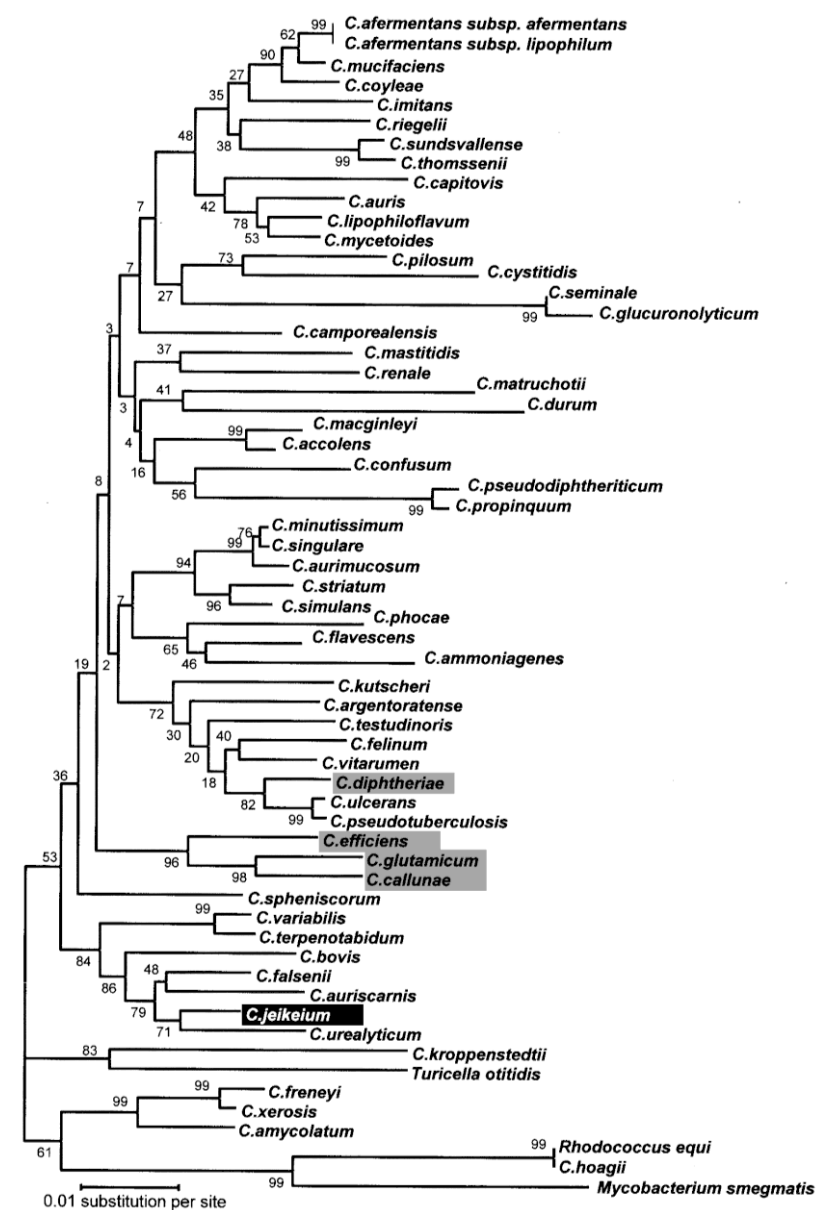
Figure 4.14: Dendrogram of the phylogenetic relationships of *Corynebacterium* species taken from Khamis *et al.* (2004). The tree highlights strains yet known to contain genes that structure bicomponental (grey) and monocomponental (black) major cell wall channels for *Corynebacterium* species. It is based on the neighbour-joining method using aligned 16S rRNA sequences. The support of each branch is shown by the value at each node in percentage, as determined from 1000 bootstraped samples.

Although latter approach cannot claim absolute classification accuracy, strains yet known to be concomitant of *porH* and *porA* genes, namely *C. glutamicum*, *C. efficiens*, *C. diphtheriae* and *C. callunae* likely evolved from an ancestor of *C. jeikeium* (Fig. 4.14). For this reason, *jk0268* of *C. jeikeium* could be related to the ancestor of the genes *porH* and *porA* that may have evolved by gene duplication. Interestingly, corynebacteria devoid of mycolates (*Corynebacterium amycolatum* (Collins *et al.*, 1988), *Corynebacterium kroppenstedtii* (Collins *et al.*, 1998) and *Corynebacterium atypicum* (Hall *et al.*, 2003)) are predicted to originate even earlier than *C. jeikeium*. This implies that the development of the mycolate cell wall and the here described channel could be connected.

Chapter 5

Summary

5.1 Summary

The genus *Corynebacterium* belongs, together with *Mycobacterium*, *Nocardia*, *Rhodococcus* and further closely related genera, to the distinctive suprageneric taxon mycolata. Many species within this diverse group of mycolic acid containing actinomycetes are known either because of their medical or biotechnological relevance. For instance, *Mycobacterium tuberculosis* (TB, at present 1.7 million deaths/a), *Mycobacterium leprae* (leprosy, 225 thousand reported cases in 2007), *Corynebacterium diphtheriae* (diphtheria) and *Nocardia farcinica* (nocardiosis), causer of most dangerous bacterial infectious diseases world-wide, are among this exceptional group of Gram-positive bacteria. Likewise of importance are some harmless mycolata species which, because of special abilities, find use in industrial settings. *Corynebacterium glutamicum* and *Corynebacterium efficiens* are, e.g., potent producers of the flavour enhancer glutamate and the animal feed additive lysine, while several *Rhodococcus* species are applied in the production of acrylic acids.

The cell wall of mycolata species, compared with that of Gram-positive bacteria, exhibits an unusual composition and organization. Besides an arabinogalactan-peptidoglycan complex, the cell walls of most actinomycetes contain large amounts of mycolic acids. Comparable to the outer membrane of Gram-negative bacteria, these long-chained branched fatty acids form a highly impermeable hydrophobic outer layer which provides the basis of the exceptional drug resistance of mycolata species. Like the outer membrane of Gram-negative bacteria, the cell wall of mycolata contains channel-forming proteins that allow the passage of hydrophilic solutes. By permitting and controlling the exchange and communication between the interior of the cell and the environment in which the bacterium lives, the channels play an important role for the function of the bacterial cell envelope. In the last decade, molecular and electrophysiological studies have provided evidence for the existence of channels in, e.g., *Mycobacterium*- and harmless *Corynebacterium* species. However, in contrast to

mycobacterial channels almost nothing is known about the architecture of corynebacterial channels.

The aim of this thesis was to extend our knowledge about cell wall channels in corynebacteria. For this purpose, we examined PorA and PorH proteins that have been associated by previous studies with cell wall pores in *C. glutamicum, C. efficiens* and *Corynebacterium callunae* in order to resolve unanswered questions and to gain structural knowledge. We also investigated cell walls of pathogenic corynebacteria, in particular of *Corynebacterium diphtheriae* and *Corynebacterium jeikeium*, to investigate if these species possessed channels as is the case with their harmless relatives.

Because of two contradictory reports, some unanswered questions developed concerning the prominant cell wall channels of *C. glutamicum*. One report suggests that the cell wall of *C. glutamicum* contains two separate pores with 2.5 and 5.5 nS conductance, namely PorH and PorA. Both pores are assumed to be homooligomers consisting of the 6.2 kDa CgPorH and the 4.7 kDa CgPorA monomer, respectively. However, a second study shows that the cell wall of a PorA deficient mutant of *C. glutamicum* inexplicably does not contain the channel of PorH. Due to the fact that the corresponding genes, i.e. *cgporH* and *cgporA*, are direct neighbours in the *C. glutamicum* chromosome, a possible interaction of both proteins to cooperatively form the major cell wall pores was assumed for this strain. This question was addressed by constructing a Δ*porH* Δ*porA* mutant of *C. glutamicum*. The cell wall of this double porin mutant was essentially free of channel-forming protein, as shown by black lipid membrane experiments. Using the same technique, it was demonstrated that it was possible to restore the removed channels in the mutant by complementing the gene defects. For the successful reconstruction of the pores, the genotype of the mutant had to fully correspond to the genotype of the wild-type strain. Reconstitution experiments in artificial lipid membranes using recombinant expressed and to homogeneity purified CgPorH and CgPorA proteins demonstrated that the *C. glutamicum* major cell wall channel was solely but obligatory dependent on these two proteins. In contrast to previous publications, we concluded that this cell wall channel is a heterooligomer composed of monomeric CgPorH and CgPorA subunits and has a single-channel conductance of 2.5 nS in 1M KCl. Consistent with this assumption, Northern and RT-PCR analysis revealed a bicistronic transcript consisting of *cgporH* and *cgporA* open reading frames. The transcription start point of the genes was determined by RACE approach, allowing a prediction of the -35 and -10 regions of the porin promoter. The

finding that the major cell wall channel of *C. glutamicum* assembled from interacting CgPorH and CgPorA monomers was of great significance in this thesis. Our analysis of PorH and PorA homologs of *C. efficiens* and *C. diphtheriae* showed a similar result. The recent discovery of *ccporH* and *ccporA* genes in *C. callunae* suggests that the major cell wall pore in this strain is also constructed of functional associated CcPorH and CcPorA proteins.

The initial question whether cell wall pores are restricted to benign corynebacterial species has to be negated. In the cell walls of both examined pathogens we detected channel-forming proteins. The pore of *C. diphtheriae* was isolated from whole cells by organic solvent extraction. Preparative SDS-PAGE was applied to the purification of the channel from the cell extract. An enzyme-linked immunosorbent assay established that the channel is located on the surface of the cells. Lipid bilayer analysis indicated that its single-channel conductance is 2.25 nS in 1 M KCl and results from the interaction of two 4.7 and 6.6 kDa proteins. The proteins were identified in the accessible genome of *C. diphtheriae* in which the corresponding genes are arranged in close vicinity to each other. As the channel forming proteins of *C. diphtheriae* shared homology to known PorH and PorA polypeptides, we designated them CdPorH and CdPorA, respectively. The heteromeric *C. diphtheriae* channel is wide and water-filled and forms a slightly cation-selective pore. In comparison with cell wall channels of other mycolata, the *C. diphtheriae* channel does not contain point charges at the channel entry.

The second pathogen to be thoroughly investigated for channel-forming activity was *C. jeikeium*. Detergent extracts of whole *C. jeikeium* cells contained a prominent pore with a single-channel conductance of 1.25 nS in 1 M KCl. The channel-forming protein CjPorA was identified in the published genome of *C. jeikeium* by comparative genomic analysis. The 4.4 kDa protein was produced recombinantly through expression in a Δ*porH* Δ*porA* mutant of *C. glutamicum* and purified to homogeneity by affinity chromatography from detergent extracted cells. Black lipid bilayer analysis indicated that the *C. jeikeium* channel is selective for anions because of a strategically located positive charge in the channel lumen. Like the channel of *C. diphtheriae*, it does not contain point charges in or near the channel mouth. Based on permeation abilities of different sized anions using the Renkin correction factor, the channel diameter is 1.4 nm. Given the fact that the *C. jeikeium* protein consists of only 40 amino acids, which is insufficient to produce a large ion-conducting pore, we presumed that the monomeric CjPorA protein produces a homooligomeric channel. This assumption is in line

with a secondary structure prediction showing that the protein could form an amphipathic α-helix.

In this work we provided evidence for the existence of cell wall channels in two further *Corynebacteria* species, *C. diphtheriae* and *C. jeikeium*. Moreover, we demonstrated that the major cell wall channels of *C. glutamicum*, *C. efficiens* and *C. diphtheriae* consist of two distinctive polypeptides; one of whom belongs to the class of PorH proteins and the other to the class of PorA proteins. This heteromeric structure of channels of corynebacteria represents a novelty for channels of the mycolata. In contrast, the *C. jeikeium* channel is solely constituted by a single protein, CjPorA, arranged as an oligomer. Although the molecular mass of this protein is comparable to those of PorH and PorA proteins, it shares no distinctive homology in its primary sequence with them. However, there is evidence for relationship between CjPorA and PorH/PorA proteins because the gene *jk0268*, coding for CjPorA, is localized in a chromosomal region of *C. jeikeium* that corresponds to the genomic region containing the *porH/porA* genes in the other corynebacteria. This suggests that *jk0268* (coding for the homomeric cell wall channel in *C. jeikeium*) and the *porH/porA* genes of *C. glutamicum*, *C. efficiens* and *C. diphtheriae* (coding for heteromeric cell wall channels) are presumably descendants of a common ancestor gene. This assumption gets support from data on phylogenetic analysis of the genus *Corynebacterium*. Moreover, these data suggest that the here investigated cell wall channels are presumably widespread within this genus. A profound knowledge of cell wall channels, building the main passage of solutes through the outer mycolate membrane in corynebacteria and other members of the mycolata, can be of great economical and medical value. As water-soluble antimicrobial compounds have to cross this permeability barrier to be effective, results of this thesis may provide the basis for the design of more efficient drugs in the future.

5.2 Zusammenfassung

Die Gattung *Corynebacterium* gehört, neben *Mycobacterium*, *Nocardia*, *Rhodococcus* und weiteren nahverwandten Gattungen, dem unverwechselbaren, gattungsübergreifenden Taxon Mycolata an. Viele Spezies aus dieser heterogenen Gruppe Mycolsäure-haltiger Actinomyceten sind entweder aufgrund ihrer medizinischen oder ihrer biotechnologischen Bedeutung bekannt. Beispielsweise zählen *Mycobacterium tuberculosis* (TBC, derzeitig 1,7 Millionen Todesfälle/Jahr), *Mycobacterium leprae* (Lepra, mit 225 Tausend registrierten Fällen im Jahr 2007), *Corynebacterium diphtheriae* (Diphtherie) und *Nocardia farcinica* (Nocardiose), welche weltweit Verursacher besonders gefährlicher bakterieller Infektionskrankheiten sind, zu dieser ungewöhnlichen Gruppe Gram-positiver Bakterien. Ebenso bedeutsam sind einige apathogene Mycolata-Arten, die aufgrund besonderer Fähigkeiten industrielle Anwendung finden. *Corynebacterium glutamicum* und *Corynebacterium efficiens* sind leistungsfähige Bakterien, die zum Beispiel in der Produktion des Geschmacksverstärkers Glutamat und des Tierfuttermittelzusatzes Lysin eingesetzt werden, während verschiedene *Rhodococcus* Spezies Anwendung bei der Herstellung von Acrylsäuren finden.

Die Zellwand der Mycolata zeigt, verglichen mit der klassischer Gram-positiver Bakterien, eine außergewöhnliche Zusammensetzung und Struktur auf. Abgesehen von einem Arabinogalactan-Peptidoglycan-Komplex enthält die Zellwand der meisten Actinomyceten einen hohen Anteil an Mycolsäuren. Diese langkettigen, verzweigten Fettsäuren formen eine, mit der äußeren Membran Gram-negativer Bakterien vergleichbare, stark undurchlässige, hydrophobe äußere Hülle, welche die Grundlage der außergewöhnlichen Medikamentenresistenz bei den Mycolata bildet. Wie die äußere Membran Gram-negativer Bakterien enthält die Zellwand der Mycolata porenformende Proteine, die den Durchlass hydrophiler Substanzen gestatten. Indem sie eine Verbindung zwischen dem Zellinneren und der Umwelt, in der das Bakterium lebt, schaffen und einen kontrollierten Austausch zwischen beiden ermöglichen, tragen die Kanalproteine entscheidend zur Funktion der bakteriellen Zellhülle bei. Im vergangen Jahrzehnt haben molekulare sowie elektrophysiologische Studien erwiesen, dass zum Beispiel *Mycobacterium*- und ungefährliche *Corynebacterium*-Arten Kanalproteine besitzen. Über die Struktur corynebakterieller Kanalproteine ist im Gegensatz zu mycobakteriellen Poren jedoch fast nichts bekannt.

Das Ziel dieser Arbeit war unser Wissen über Zellwandkanäle in Corynebakterien zu erweitern. Deshalb untersuchten wir PorA und PorH Proteine, die basierend auf früheren Studien Zellwandkanälen in *C. glutamicum, C. efficiens* und *Corynebacterium callunae* zugeordnet werden, um ungeklärten Fragen nachzugehen und um Wissen über deren Struktur zu erlangen. Ferner inspizierten wir Zellwände pathogener Corynebakterien, genauer gesagt von *Corynebacterium diphtheriae* und *Corynebacterium jeikeium*, um herauszufinden, ob diese Spezies wie ihre harmlosen Verwandten Kanalproteine besitzen.

Aufgrund zweier, sich widersprechender Berichte entstanden ungeklärte Fragen hinsichtlich der wichtigsten Zellwandkanäle von *C. glutamicum*. Ein Bericht besagt, dass *C. glutamicum* in seiner Zellwand zwei eigenständige Poren mit 2,5 bzw. 5,5 nS Ionenleitfähigkeit besitzt, bekannt als PorH und PorA. Beide Poren werden als Homooligomere, bestehend aus dem 6,2 kDa CgPorH beziehungsweise dem 4,7 kDa CgPorA Monomer angesehen. Indessen besagt ein zweiter Bericht, dass die Zellwand einer PorA defizienten *C. glutamicum* Mutante unerklärlicherweise keinen PorH Kanal enthält. Da die entsprechenden Gene, *cgporH* und *cgporA*, im Chromosom von *C. glutamicum* unmittelbar aneinander grenzen, entstand die Vermutung, dass beide Proteine zusammenwirkend die Hauptporen dieses Bakteriums aufbauen. Durch die Erzeugung einer *C. glutamicum* Δ*porH* Δ*porA* Mutante konnte diese Frage geklärt werden. Versuche mit schwarzen Membranen zeigten, dass die Zellwand dieser Porin Doppelmutante frei von porenformenden Proteinen war. Mittels selbiger Methode konnte gezeigt werden, dass es durch Komplementierung der Gendefekte möglich war, die Zellwandkanäle in der Mutante wieder herzustellen. Für die erfolgreiche Wiederherstellung musste der Genotyp der Mutante völlig dem des Wildtypstammes entsprechen. Rekonstitutionsexperimente in künstlichen Lipidmembranen zeigten unter Verwendung von rekombinant exprimierten und aufgereinigten CgPorH und CgPorA Proteinen, dass der Hauptkanal von *C. glutamicum* alleinig aber zwingend von beiden Proteinen abhing. Entgegen früheren Publikationen folgerten wir, dass dieser Zellwandkanal ein Heterooligomer bestehend aus CgPorH und CgPorA Untereinheiten ist und eine Einzelkanalleitfähigkeit von 2,5 nS in 1 M KCl besitzt. Northern sowie RT-PCR Ergebnisse, die ein *cgporH* und *cgporA* enthaltendes, bicistronisches RNA-Transkript offenbarten, waren stimmig mit der Schlussfolgerung. Mittels RACE-Methode wurde der Transkriptionsstartpunkt beider Gene bestimmt, wodurch eine Vorhersage der -35 und -10 Region des Porin Promotors möglich wurde. Die Feststellung, dass sich der Hauptkanal von *C. glutamicum* aus CgPorH und CgPorA Monomeren zusammensetzte, erwies sich in dieser Arbeit als sehr bedeutsam. Unsere

Untersuchungen der homologen Proteine aus *C. efficiens* und *C. diphtheriae* zeigten ein vergleichbares Ergebnis. Die erst kürzlich entdeckten *ccporH* und *ccporA* Gene in *C. callunae* legen nahe, dass die Hauptpore dieses Stammes auch aus interagierenden CcPorH und CcPorA Proteinen hervorgeht.

Die Anfangsfrage, ob Zellwandporen nur in apathogenen *Corynebacterium*-Arten zu finden sind, muss verneint werden. In den Zellwänden beider untersuchter pathogener Vertreter stellten wir porenformende Proteine fest. Die Pore von *C. diphtheriae* wurde durch Extraktion ganzer Zellen mit organischen Lösungsmitteln isoliert. Für die Aufreinigung des Kanals aus dem Zellextrakt wurde die Methode der präparativen Polyacrylamid-Gelelektrophorese angewandt. Ein enzymgekoppelter Immunadsorptionstest bestätigte, dass sich der Kanal an der Zelloberfläche befindet. Untersuchungen mit schwarzen Lipidmembranen zeigten, dass die Einzelkanalleitfähigkeit der Pore 2,25 nS in 1 M KCl Lösung beträgt und aus der Interaktion zweier 4,7 und 6,6 kDa Proteine resultiert. Die Proteine wurden im veröffentlichten Genom von *C. diphtheriae* identifiziert, in welchem sich die entsprechenden Gene in unmittelbarer Nachbarschaft zueinander befinden. Aufgrund der Homologie zu bekannten PorH und PorA Proteinen, wurden die Poren-formenden Proteine von *C. diphtheriae* als CdPorH bzw. CdPorA bezeichnet. Der heteromere Zellwandkanal aus *C. diphtheriae* ist eine offene, mit Wasser gefüllte und leicht kationenselektive Pore. Im Vergleich zu Zellwandkanälen anderer Mycolata besitzt der Zellwandkanal von *C. diphtheriae* keine Punktladungen am Kanaleingang.

Das zweite auf Zellwandkanäle näher untersuchte pathogene Bakterium war *C. jeikeium*. Detergenz-Extrakte ganzer *C. jeikeium* Zellen enthielten eine markante Pore mit einer Einzelkanalleitfähigkeit von 1,25 nS in 1 M KCl Lösung. Mithilfe der vergleichenden Genomanalyse wurde das porenformende Protein CjPorA in dem veröffentlichten Genom von *C. jeikeium* identifiziert. Dieses 4,4 kDa Protein wurde rekombinant durch Expression in einer Δ*porH* Δ*porA* *C. glutamicum* Mutante hergestellt und durch Affinitätschromatografie aus Detergenz-extrahierten Zellen aufgereinigt. Die *C. jeikeium* Pore ist, wie Bilayer Ergebnisse andeuteten, aufgrund eines sich im Kanal befindlichen Filters selektiv für Anionen. Ebenso wie bei der Pore von *C. diphtheriae* sind bei dem *C. jeikeium* Kanal keine Punktladungen an der Kanalöffnung oder in deren Nähe vorhanden. Der anhand der Permeationsfähigkeit verschieden großer Anionen ermittelte Kanaldurchmesser beträgt unter Verwendung des Renkin Korrekturfaktors 1,4 nm. Angesichts der Tatsache, dass das CjPorA Protein mit nur

40 Aminosäuren zu klein ist um eine wassergefüllte Pore zu bilden, vermuteten wir, dass das monomere CjPorA Protein einen homooligomeren Kanal bildet. Diese Annahme ist stimmig mit einer Sekundärstrukturvorhersage, die andeutet, dass das Protein eine lange amphipathische α-Helix bilden kann.

In dieser Arbeit wiesen wir mit *C. diphtheriae* und *C. jeikeium* in zwei weiteren *Corynebacterium*-Arten Zellwandkanäle nach. Des Weiteren zeigten wir, dass sich die Zellwandkanäle von *C. glutamicum*, *C. efficiens* und *C. diphtheriae* aus zwei Proteinen zusammensetzen, einem zugehörig zu der Gruppe der PorH Proteine und einem weiteren aus der Gruppe der PorA Proteine. Diese heteromere Struktur von Zellwandkanälen bei Corynebakterien stellt ein Novum für Zellwandkanäle bei den Mycolata dar. Indessen besteht der Zellwandkanal von *C. jeikeium* aus nur einem Protein, CjPorA, angeordnet zu einem Oligomer. Obgleich das Molekulargewicht dieses Proteins mit dem von PorH und PorA Proteinen vergleichbar ist, weißt seine Primärsequenz keine eindeutige Homologie zu diesen auf. Dennoch deutet vieles auf eine Verwandtschaft zwischen CjPorA und PorH/PorA Proteinen hin, da das Gen *jk0268*, welches für CjPorA kodiert, sich in einer Region des *C. jeikeium* Chromosoms befindet, die der Genomregion entspricht in welcher die *porH/porA* Gene der anderen Corynebakterien lokalisiert sind. Dies lässt vermuten, dass *jk0268* (welches für den homomeren Zellwandkanal in *C. jeikeium* kodiert) und die *porH/porA* Gene von *C. glutamicum*, *C. efficiens* und *C. diphtheriae* (die einen heteromeren Zellwandkanal kodieren) wahrscheinlich Nachkommen eines gemeinsamen Vorläufergens sind. Phylogenetische Analysen der Gattung *Corynebacterium* unterstützen diese Annahme. Desweitern legen sie nahe, dass die hier untersuchten Zellwandkanäle innerhalb dieser Gattung wahrscheinlich weit verbreitet sind. Ein umfassendes Wissen über Zellwandkanäle, denen beim Transport gelöster Stoffe über die äußere Membran in Corynebakterien und anderen Mitgliedern der Mycolata eine entscheidende Rolle zukommt, könnte von großem wirtschaftlichem und medizinischem Nutzen sein. Da wasserlösliche antimikrobielle Präparate diese Permeabilitätsbarriere überqueren müssen um wirken zu können, könnten Ergebnisse aus dieser Arbeit künftig die Grundlage für die Entwicklung effektiverer Arzneimittel bilden.

Chapter 6

Appendix

6.1 References

Altschul, S. F., Gish, W., Miller, W., Myers, E. W. & Lipman, D. J. (1990). Basic local alignment search tool. *J Mol Biol* **215**, 403-410.

Altschul, S. F., Madden, T. L., Schaffer, A. A., Zhang, J., Zhang, Z., Miller, W. & Lipman, D. J. (1997). Gapped BLAST and PSI-BLAST: a new generation of protein database search programs. *Nucleic Acids Res* **25**, 3389-3402.

Anderson, G. S. & Penfold, J. B. (1973). An outbreak of diphtheria in a hospital for the mentally subnormal. *J Clin Pathol* **26**, 606-615.

Asselineau, C. P., Montrozier, H. L., Prome, J. C., Savagnac, A. M. & Welby, M. (1972). Polyunsaturated glycolipids synthesized by *Mycobacterium phlei*. *Eur J Biochem* **28**, 102-109.

Barksdale, L. (1959). Lysogenic conversions in bacteria. *Bacteriol Rev* **23**, 202-212.

Barksdale, L. (1970). *Corynebacterium diphtheriae* and its relatives. *Bacteriol Rev* **34**, 378-422.

Barksdale, L. (1981). The genus *Corynebacterium*. In *The prokaryotes*, pp. 1827-1837. Edited by M. P. Starr, H. Stoll, H. Trüper, H. G. Balows & H. G. Schlegel. Berlin: Springer-Verlag.

Barreiro, C., Gonzalez-Lavado, E., Patek, M. & Martin, J. F. (2004). Transcriptional analysis of the *groES-groEL1*, *groEL2*, and *dnaK* genes in *Corynebacterium glutamicum*: characterization of heat shock-induced promoters. *J Bacteriol* **186**, 4813-4817.

Barry, C. E., 3rd, Lee, R. E., Mdluli, K., Sampson, A. E., Schroeder, B. G., Slayden, R. A. & Yuan, Y. (1998). Mycolic acids: structure, biosynthesis and physiological functions. *Prog Lipid Res* **37**, 143-179.

Belisle, J. T., Vissa, V. D., Sievert, T., Takayama, K., Brennan, P. J. & Besra, G. S. (1997). Role of the major antigen of *Mycobacterium tuberculosis* in cell wall biogenesis. *Science* **276**, 1420-1422.

Benz, R., Janko, K., Boos, W. & Lauger, P. (1978). Formation of large, ion-permeable membrane channels by the matrix protein (porin) of *Escherichia coli*. *Biochim Biophys Acta* **511**, 305-319.

Benz, R., Janko, K. & Lauger, P. (1979). Ionic selectivity of pores formed by the matrix protein (porin) of *Escherichia coli*. *Biochim Biophys Acta* **551**, 238-247.

Benz, R. (1988). Structure and function of porins from Gram-negative bacteria. *Annu Rev Microbiol* **42**, 359-393.

Benz, R., Schmid, A., Maier, C. & Bremer, E. (1988). Characterization of the nucleoside-binding site inside the Tsx channel of *Escherichia coli* outer membrane. Reconstitution experiments with lipid bilayer membranes. *Eur J Biochem* **176**, 699-705.

Benz, R. (1994). Solute uptake through the bacterial outer membrane. In *Bacterial cell wall*, pp. 397-423. Edited by J. M. Ghuysen & R. Hakenbeck. Amsterdam: Elsevier Sciene B.V.

Benz, R. (2003). Porins - structure and function. In *Microbial transport systems*, pp. 227-246. Edited by G. Winkelmann. Weinheim: Wiley-VCH.

Berks, B. C., Sargent, F. & Palmer, T. (2000). The Tat protein export pathway. *Mol Microbiol* **35**, 260-274.

Besra, G. S., McNeil, M. R. & Brennan, P. J. (1992). Characterization of the specific antigenicity of *Mycobacterium fortuitum*. *Biochemistry* **31**, 6504-6509.

Blum, H., Beier, H. & Gross, H. J. (1987). Improved silver staining of plant proteins, RNA and DNA in polyacrylamide gels. *Electrophoresis* **8**, 93-99.

Bonnet, J. M. & Begg, N. T. (1999). Control of diphtheria: guidance for consultants in communicable disease control. World Health Organization. *Commun Dis Public Health* **2**, 242-249.

Braun, V. & Rehn, K. (1969). Chemical characterization, spatial distribution and function of a lipoprotein (murein-lipoprotein) of the *E. coli* cell wall. The specific effect of trypsin on the membrane structure. *Eur J Biochem* **10**, 426-438.

Brennan, P. J. & Nikaido, H. (1995). The envelope of mycobacteria. *Annu Rev Biochem* **64**, 29-63.

Bricaire, F. (1996). Diphtheria: apropos of an epidemic. *Presse Med* **25**, 327-329.

Brock, T. D., Madigan, M. T., Martinko, J. M. & Parker, J. (2001). *Brock Mikrobiologie*, 9 edn. Berlin: Spekrtum Verlag.

Brune, I., Becker, A., Paarmann, D., Albersmeier, A., Kalinowski, J., Pühler, A. & Tauch, A. (2006). Under the influence of the active deodorant ingredient 4-hydroxy-3-methoxybenzyl alcohol, the skin bacterium *Corynebacterium jeikeium* moderately responds with differential gene expression. *J Biotechnol* **127**, 21-33.

Burkovski, A. (1997). Rapid detection of bacterial surface proteins using an enzyme-linked immunosorbent assay system. *J Biochem Biophys Methods* **34**, 69-71.

Caroff, M. & Karibian, D. (2003). Structure of bacterial lipopolysaccharides. *Carbohydr Res* **338**, 2431-2447.

Castellan, G. W. (1983). The ionic current in aqueous solutions. In *Physical chemistry*, pp. 769-780. Reading, MA: Addison-Wesley.

Cerdeno-Tarraga, A. M., Efstratiou, A., Dover, L. G. & other authors (2003). The complete genome sequence and analysis of *Corynebacterium diphtheriae* NCTC13129. *Nucleic Acids Res* **31**, 6516-6523.

Chatterjee, D. (1997). The mycobacterial cell wall: structure, biosynthesis and sites of drug action. *Curr Opin Chem Biol* **1**, 579-588.

Chugh, J. K. & Wallace, B. A. (2001). Peptaibols: models for ion channels. *Biochem Soc Trans* **29**, 565-570.

Collins, M. D., Burton, R. A. & Jones, D. (1988). *Corynebacterium amycolatum* sp. nov., a new mycolic acid-less *Corynebacterium* species from human skin. *FEMS Microbiol Lett* **49**, 349-352.

Collins, M. D., Falsen, E., Akervall, E., Sjoden, B. & Alvarez, A. (1998). *Corynebacterium kroppenstedtii* sp. nov., a novel corynebacterium that does not contain mycolic acids. *Int J Syst Bacteriol* **48 Pt 4**, 1449-1454.

Costa-Riu, N., Burkovski, A., Kramer, R. & Benz, R. (2003a). PorA represents the major cell wall channel of the Gram-positive bacterium *Corynebacterium glutamicum*. *J Bacteriol* **185**, 4779-4786.

Costa-Riu, N., Maier, E., Burkovski, A., Kramer, R., Lottspeich, F. & Benz, R. (2003b). Identification of an anion-specific channel in the cell wall of the Gram-positive bacterium *Corynebacterium glutamicum*. *Mol Microbiol* **50**, 1295-1308.

Crick, D. C., Mahapatra, S. & Brennan, P. J. (2001). Biosynthesis of the arabinogalactan-peptidoglycan complex of *Mycobacterium tuberculosis*. *Glycobiology* **11**, 107R-118R.

Cullis, P. & Hope, M. J. (1985). Physical properties and functional roles of lipids in membranes. In *Biochemistry of Lipids and Membranes*, pp. 25-72. Edited by D. E. Vance & J. E. Vance. New York (USA): Benjamin/Cummings

Daffe, M., Brennan, P. J. & McNeil, M. (1990). Predominant structural features of the cell wall arabinogalactan of *Mycobacterium tuberculosis* as revealed through characterization of oligoglycosyl alditol fragments by gas chromatography/mass spectrometry and by 1H and 13C NMR analyses. *J Biol Chem* **265**, 6734-6743.

Daffe, M. & Draper, P. (1998). The envelope layers of mycobacteria with reference to their pathogenicity. *Adv Microb Physiol* **39**, 131-203.

Deleage, G., Blanchet, C. & Geourjon, C. (1997). Protein structure prediction. Implications for the biologist. *Biochimie* **79**, 681-686.

Demchick, P. & Koch, A. L. (1996). The permeability of the wall fabric of *Escherichia coli* and *Bacillus subtilis*. *J Bacteriol* **178**, 768-773.

Dijkstra, A. J. & Keck, W. (1996). Peptidoglycan as a barrier to transenvelope transport. *J Bacteriol* **178**, 5555-5562.

Dixon, J. M. S., Noble, W. C. & Smith, G. R. (1990). Dipththeria; other corynebacterial and coryneform infections. In *Principles of bacteriology, virology and immunity*, pp. 55-79. Edited by M. T. Parker & L. H. Collier. London: Toppley and Wilson`s.

Dmitriev, B. A., Ehlers, S. & Rietschel, E. T. (1999). Layered murein revisited: a fundamentally new concept of bacterial cell wall structure, biogenesis and function. *Med Microbiol Immunol* **187**, 173-181.

Dmitriev, B. A., Ehlers, S., Rietschel, E. T. & Brennan, P. J. (2000). Molecular mechanics of the mycobacterial cell wall: from horizontal layers to vertical scaffolds. *Int J Med Microbiol* **290**, 251-258.

Dörner, U., Maier, E. & Benz, R. (2004). Identification of a cation-specific channel (TipA) in the cell wall of the Gram-positive mycolata *Tsukamurella inchonensis*: the gene of the channel-forming protein is identical to *mspA* of *Mycobacterium smegmatis* and *mppA* of *Mycobacterium phlei*. *Biochim Biophys Acta* **1667**, 47-55.

Eggeling, L. & Sahm, H. (1999). L-glutamate and L-lysine: traditional products with impetuous developments. *Appl Microbiol Biotechnol* **52**, 146-153.

Eggeling, L. & Sahm, H. (2001). The cell wall barrier of *Corynebacterium glutamicum* and amino acid efflux. *Journal of Bioscience and Bioengineering* **92**, 201-213.

Faller, M., Niederweis, M. & Schulz, G. E. (2004). The structure of a mycobacterial outer-membrane channel. *Science* **303**, 1189-1192.

Freudl, R. (1992). Protein secretion in Gram-positive bacteria. *J Biotechnol* **23**, 231-240.

Fudou, R., Jojima, Y., Seto, A., Yamada, K., Kimura, E., Nakamatsu, T., Hiraishi, A. & Yamanaka, S. (2002). *Corynebacterium efficiens* sp. nov., a glutamic-acid-producing species from soil and vegetables. *Int J Syst Evol Microbiol* **52**, 1127-1131.

Funke, G., von Graevenitz, A., Clarridge, J. E., 3rd & Bernard, K. A. (1997). Clinical microbiology of coryneform bacteria. *Clin Microbiol Rev* **10**, 125-159.

Galazka, A. M. & Robertson, S. E. (1995). Diphtheria: changing patterns in the developing world and the industrialized world. *Eur J Epidemiol* **11**, 107-117.

Gebhardt, H., Meniche, X., Tropis, M., Kramer, R., Daffe, M. & Morbach, S. (2007). The key role of the mycolic acid content in the functionality of the cell wall permeability barrier in *Corynebacterineae*. *Microbiology* **153**, 1424-1434.

Georgi, T., Rittmann, D. & Wendisch, V. F. (2005). Lysine and glutamate production by *Corynebacterium glutamicum* on glucose, fructose and sucrose: roles of malic enzyme and fructose-1,6-bisphosphatase. *Metab Eng* **7**, 291-301.

Ghuysen, J. M. (1968). Use of bacteriolytic enzymes in determination of wall structure and their role in cell metabolism. *Bacteriol Rev* **32**, 425-464.

Gilson, E., Alloing, G., Schmidt, T., Claverys, J. P., Dudler, R. & Hofnung, M. (1988). Evidence for high affinity binding-protein dependent transport systems in Gram-positive bacteria and in *Mycoplasma. EMBO J* **7**, 3971-3974.

Goodfellow, M., Collins, M. D. & Minnikin, D. E. (1976). Thin-layer chromatographic analysis of mycolic acid and other long-chain components in whole-organism methanolysates of coryneform and related taxa. *J Gen Microbiol* **96**, 351-358.

Hall, V., Collins, M. D., Hutson, R. A., Lawson, P. A., Falsen, E. & Duerden, B. I. (2003). *Corynebacterium atypicum* sp. nov., from a human clinical source, does not contain corynomycolic acids. *Int J Syst Evol Microbiol* **53**, 1065-1068.

Hallin, P. F. & Ussery, D. W. (2004). CBS Genome Atlas Database: a dynamic storage for bioinformatic results and sequence data. *Bioinformatics* **20**, 3682-3686.

Hansmeier, N., Chao, T. C., Daschkey, S., Musken, M., Kalinowski, J., Pühler, A. & Tauch, A. (2007). A comprehensive proteome map of the lipid-requiring nosocomial pathogen *Corynebacterium jeikeium* K411. *Proteomics* **7**, 1076-1096.

Harley, C. B. & Reynolds, R. P. (1987). Analysis of *E. coli* promoter sequences. *Nucleic Acids Res* **15**, 2343-2361.

Harnisch, J. P., Tronca, E., Nolan, C. M., Turck, M. & Holmes, K. K. (1989). Diphtheria among alcoholic urban adults. A decade of experience in Seattle. *Ann Intern Med* **111**, 71-82.

Hashimoto, K., Kawasaki, H., Akazawa, K., Nakamura, J., Asakura, Y., Kudo, T., Sakuradani, E., Shimizu, S. & Nakamatsu, T. (2006). Changes in composition and content of mycolic acids in glutamate-overproducing *Corynebacterium glutamicum. Biosci Biotechnol Biochem* **70**, 22-30.

Helmann, J. D. (1995). Compilation and analysis of *Bacillus subtilis* sigma A-dependent promoter sequences: evidence for extended contact between RNA polymerase and upstream promoter DNA. *Nucleic Acids Res* **23**, 2351-2360.

Hermann, T. (2003). Industrial production of amino acids by coryneform bacteria. *J Biotechnol* **104**, 155-172.

Hilf, R. J. & Dutzler, R. (2008). X-ray structure of a prokaryotic pentameric ligand-gated ion channel. *Nature* **452**, 375-379.

Holmes, R. K. (2000). Biology and molecular epidemiology of diphtheria toxin and the *tox* gene. *J Infect Dis* **181 Suppl 1**, S156-167.

Holt, J. G., Krieg, N. R., Sneath, P. H. A., Staley, J. T. & Williams, S. T. (1994). Nocardioform actinomycetes. In *Bergey`s manual of determinative biology, 9th edn*, pp. 625-650. Baltimore: The Williams and Wilkins Co.

Holtje, J. V. (1998). Growth of the stress-bearing and shape-maintaining murein sacculus of *Escherichia coli. Microbiol Mol Biol Rev* **62**, 181-203.

Hünten, P., Costa-Riu, N., Palm, D., Lottspeich, F. & Benz, R. (2005a). Identification and characterization of PorH, a new cell wall channel of *Corynebacterium glutamicum. Biochim Biophys Acta* **1715**, 25-36.

Hünten, P., Schiffler, B., Lottspeich, F. & Benz, R. (2005b). PorH, a new channel-forming protein present in the cell wall of *Corynebacterium efficiens* and *Corynebacterium callunae. Microbiology* **151**, 2429-2438.

Hunter, S. W., Gaylord, H. & Brennan, P. J. (1986). Structure and antigenicity of the phosphorylated lipopolysaccharide antigens from the leprosy and tubercle bacilli. *J Biol Chem* **261**, 12345-12351.

Hunter, S. W. & Brennan, P. J. (1990). Evidence for the presence of a phosphatidylinositol anchor on the lipoarabinomannan and lipomannan of *Mycobacterium tuberculosis*. *J Biol Chem* **265**, 9272-9279.

Ikeda, M. & Nakagawa, S. (2003). The *Corynebacterium glutamicum* genome: features and impacts on biotechnological processes. *Appl Microbiol Biotechnol* **62**, 99-109.

Jackman, P. J., Pitcher, D. G., Pelczynska, S. & Borman, P. (1987). Classification of corynebacteria associated with endocarditis (group JK) as *Corynebacterium jeikeium* sp. nov. . *Syst Appl Microbiol* **9**, 83-90.

Jarlier, V. & Nikaido, H. (1990). Permeability barrier to hydrophilic solutes in *Mycobacterium chelonei*. *J Bacteriol* **172**, 1418-1423.

Johnson, W. D. & Kaye, D. (1970). Serious infections caused by diphtheroids. *Ann N Y Acad Sci* **174**, 568-576.

Kalinowski, J., Bathe, B., Bartels, D. & other authors (2003). The complete *Corynebacterium glutamicum* ATCC 13032 genome sequence and its impact on the production of L-aspartate-derived amino acids and vitamins. *J Biotechnol* **104**, 5-25.

Kaplan, G., Gandhi, R. R., Weinstein, D. E., Levis, W. R., Patarroyo, M. E., Brennan, P. J. & Cohn, Z. A. (1987). *Mycobacterium leprae* antigen-induced suppression of T cell proliferation in vitro. *J Immunol* **138**, 3028-3034.

Kartmann, B., Stenger, S. & Niederweis, M. (1999). Porins in the cell wall of *Mycobacterium tuberculosis*. *J Bacteriol* **181**, 6543-6546.

Keilhauer, C., Eggeling, L. & Sahm, H. (1993). Isoleucine synthesis in *Corynebacterium glutamicum*: molecular analysis of the *ilvB-ilvN-ilvC* operon. *J Bacteriol* **175**, 5595-5603.

Khamis, A., Raoult, D. & La Scola, B. (2004). *rpoB* gene sequencing for identification of *Corynebacterium* species. *J Clin Microbiol* **42**, 3925-3931.

Kingsford, C. L., Ayanbule, K. & Salzberg, S. L. (2007). Rapid, accurate, computational discovery of Rho-independent transcription terminators illuminates their relationship to DNA uptake. *Genome Biol* **8**, R22.

Kinoshita, S., Udaka, S. & Shimono, M. (2004). Studies on the amino acid fermentation. Part 1. Production of L-glutamic acid by various microorganisms. *J Gen Appl Microbiol* **50**, 331-343.

Kumagai, Y., Hirasawa, T., Hayakawa, K., Nagai, K. & Wachi, M. (2005). Fluorescent phospholipid analogs as microscopic probes for detection of the mycolic acid-containing layer in *Corynebacterium glutamicum*: detecting alterations in the mycolic acid-containing layer following ethambutol treatment. *Biosci Biotechnol Biochem* **69**, 2051-2056.

Kyhse-Andersen, J. (1984). Electroblotting of multiple gels: a simple apparatus without buffer tank for rapid transfer of proteins from polyacrylamide to nitrocellulose. *J Biochem Biophys Methods* **10**, 203-209.

Kyte, J. & Doolittle, R. F. (1982). A simple method for displaying the hydropathic character of a protein. *J Mol Biol* **157**, 105-132.

Laemmli, U. K. (1970). Cleavage of structural proteins during the assembly of the head of bacteriophage T4. *Nature* **227**, 680-685.

Lakshman, M. & Raghavendra Rao, M. R. (1980). Excretion of lysine by *Micrococcus glutamicus*. *J Biosci* **3**, 51-55.

Lambert, P. A. (2002). Cellular impermeability and uptake of biocides and antibiotics in Gram-positive bacteria and mycobacteria. *Symp Ser Soc Appl Microbiol*, 46S-54S.

Lechevalier, H. A., Lechevalier, M. P. & Gerber, N. N. (1971). Chemical composition as a criterion in the classification of actinomycetes. *Adv Appl Microbiol* **14**, 47-72.

Lee, R. E., Brennan, P. J. & Besra, G. S. (1996). *Mycobacterium tuberculosis* cell envelope. *Curr Top Microbiol Immunol* **215**, 1-27.

Leigh, C. D. & Bertozzi, C. R. (2008). Synthetic studies toward *Mycobacterium tuberculosis* sulfolipid-I. *J Org Chem* **73**, 1008-1017.

Leuchtenberger, W. (1996). Amino acids - technical production and use. Products of primary metabolism. In *Biotechnology*, pp. 465-502. Edited by H. J. Rehm, A. Pühler, G. Reed & P. J. W. Stadler. Weinheim: Wiley-VCH.

Lichtinger, T., Burkovski, A., Niederweis, M., Kramer, R. & Benz, R. (1998). Biochemical and biophysical characterization of the cell wall porin of *Corynebacterium glutamicum*: the channel is formed by a low-molecular-mass polypeptide. *Biochemistry* **37**, 15024-15032.

Lichtinger, T., Heym, B., Maier, E., Eichner, H., Cole, S. T. & Benz, R. (1999). Evidence for a small anion-selective channel in the cell wall of *Mycobacterium bovis* BCG besides a wide cation-selective pore. *FEBS Lett* **454**, 349-355.

Lichtinger, T., Reiss, G. & Benz, R. (2000). Biochemical identification and biophysical characterization of a channel-forming protein from *Rhodococcus erythropolis*. *J Bacteriol* **182**, 764-770.

Lichtinger, T., Riess, F. G., Burkovski, A., Engelbrecht, F., Hesse, D., Kratzin, H. D., Kramer, R. & Benz, R. (2001). The low-molecular-mass subunit of the cell wall channel of the Gram-positive *Corynebacterium glutamicum*. Immunological localization, cloning and sequencing of its gene *porA*. *Eur J Biochem* **268**, 462-469.

Lindner, S. N., Vidaurre, D., Willbold, S., Schoberth, S. M. & Wendisch, V. F. (2007). NCgl2620 encodes a class II polyphosphate kinase in *Corynebacterium glutamicum*. *Appl Environ Microbiol* **73**, 5026-5033.

Liu, J., Rosenberg, E. Y. & Nikaido, H. (1995). Fluidity of the lipid domain of cell wall from *Mycobacterium chelonae*. *Proc Natl Acad Sci U S A* **92**, 11254-11258.

Ludwig, O., De Pinto, V., Palmieri, F. & Benz, R. (1986). Pore formation by the mitochondrial porin of rat brain in lipid bilayer membranes. *Biochim Biophys Acta* **860**, 268-276.

MacGregor, R. R. (1995). *Corynebacterium diphtheriae*. In *Principles and practices of infectious diseases, 4th edn*, pp. 1865-1872. Edited by G. L. Mandell, J. E. Bennett & R. Dolin. New York: Churchill Livingston.

Mailaender, C., Reiling, N., Engelhardt, H., Bossmann, S., Ehlers, S. & Niederweis, M. (2004). The MspA porin promotes growth and increases antibiotic susceptibility of both *Mycobacterium bovis* BCG and *Mycobacterium tuberculosis*. *Microbiology* **150**, 853-864.

Marienfeld, S., Uhlemann, E. M., Schmid, R., Kramer, R. & Burkovski, A. (1997). Ultrastructure of the *Corynebacterium glutamicum* cell wall. *Antonie Van Leeuwenhoek* **72**, 291-297.

Matias, V. R., Al-Amoudi, A., Dubochet, J. & Beveridge, T. J. (2003). Cryo-transmission electron microscopy of frozen-hydrated sections of *Escherichia coli* and *Pseudomonas aeruginosa*. *J Bacteriol* **185**, 6112-6118.

Matias, V. R. & Beveridge, T. J. (2006). Native cell wall organization shown by cryo-electron microscopy confirms the existence of a periplasmic space in *Staphylococcus aureus*. *J Bacteriol* **188**, 1011-1021.

McGinley, K. J., Labows, J. N., Zechman, J. M., Nordstrom, K. M., Webster, G. F. & Leyden, J. J. (1985). Analysis of cellular components, biochemical reactions, and habitat of human cutaneous lipophilic diphtheroids. *J Invest Dermatol* **85**, 374-377.

McNeil, M. R. & Brennan, P. J. (1991). Structure, function and biogenesis of the cell envelope of mycobacteria in relation to bacterial physiology, pathogenesis and drug resistance; some thoughts and possibilities arising from recent structural information. *Res Microbiol* **142**, 451-463.

Merchante, R., Pooley, H. M. & Karamata, D. (1995). A periplasm in *Bacillus subtilis*. *J Bacteriol* **177**, 6176-6183.

Minnikin, D. E., Patel, P. & Goodfellow, M. (1974). Mycolic acids of representative strains of Nocardia and the 'rhodochrous' complex. *FEBS Lett* **39**, 322-324.

Minnikin, D. E. (1982). Lipids: complex lipids, their chemistry, biosynthesis and roles. In *The Biology of the Mycobacteria*, pp. 95-184. Edited by C. Ratledge & J. C. Stanford. New York (USA): Academic Press.

Minnikin, D. E. (1987). Chemical targets in cell envelops. In *Chemotherapy of tropical diseases*, pp. 19-43. Edited by M. Hopper. Chichester: John Wiley & Sons Ltd.

Minnikin, D. E., Dobson, G., Parlett, J. H., Goodfellow, M. & Magnusson, M. (1987). Analysis of dimycocerosates of glycosylphenolphthiocerols in the identification of some clinically significant mycobacteria. *Eur J Clin Microbiol* **6**, 703-707.

Molle, V., Saint, N., Campagna, S., Kremer, L., Lea, E., Draper, P. & Molle, G. (2006). pH-dependent pore-forming activity of OmpATb from *Mycobacterium tuberculosis* and characterization of the channel by peptidic dissection. *Mol Microbiol* **61**, 826-837.

Mookadam, F., Cikes, M., Baddour, L. M., Tleyjeh, I. M. & Mookadam, M. (2006). *Corynebacterium jeikeium* endocarditis: a systematic overview spanning four decades. *Eur J Clin Microbiol Infect Dis* **25**, 349-353.

Navarre, W. W. & Schneewind, O. (1999). Surface proteins of Gram-positive bacteria and mechanisms of their targeting to the cell wall envelope. *Microbiol Mol Biol Rev* **63**, 174-229.

Neuhoff, V., Arold, N., Taube, D. & Ehrhardt, W. (1988). Improved staining of proteins in polyacrylamide gels including isoelectric focusing gels with clear background at nanogram sensitivity using Coomassie Brilliant Blue G-250 and R-250. *Electrophoresis* **9**, 255-262.

Niederweis, M., Maier, E., Lichtinger, T., Benz, R. & Kramer, R. (1995). Identification of channel-forming activity in the cell wall of *Corynebacterium glutamicum*. *J Bacteriol* **177**, 5716-5718.

Niederweis, M., Ehrt, S., Heinz, C., Klocker, U., Karosi, S., Swiderek, K. M., Riley, L. W. & Benz, R. (1999). Cloning of the *mspA* gene encoding a porin from *Mycobacterium smegmatis*. *Mol Microbiol* **33**, 933-945.

Niederweis, M. (2003). Mycobacterial porins-new channel proteins in unique outer membranes. *Mol Microbiol* **49**, 1167-1177.

Nigou, J., Gilleron, M. & Puzo, G. (2003). Lipoarabinomannans: from structure to biosynthesis. *Biochimie* **85**, 153-166.

Nikaido, H. & Rosenberg, E. Y. (1983). Porin channels in *Escherichia coli*: studies with liposomes reconstituted from purified proteins. *J Bacteriol* **153**, 241-252.

Nikaido, H. & Jarlier, V. (1991). Permeability of the mycobacterial cell wall. *Res Microbiol* **142**, 437-443.

Nikaido, H. (1992). Porins and specific channels of bacterial outer membranes. *Mol Microbiol* **6**, 435-442.

Nikaido, H., Kim, S. H. & Rosenberg, E. Y. (1993). Physical organization of lipids in the cell wall of *Mycobacterium chelonae*. *Mol Microbiol* **8**, 1025-1030.

Nikaido, H. (2003). Molecular basis of bacterial outer membrane permeability revisited. *Microbiol Mol Biol Rev* **67**, 593-656.

Noll, H., Bloch, H., Asselineau, J. & Lederer, E. (1956). The chemical structure of the cord factor of *Mycobacterium tuberculosis*. *Biochim Biophys Acta* **20**, 299-309.

Ochi, K. (1995). Phylogenetic analysis of mycolic acid-containing wall-chemotype IV actinomycetes and allied taxa by partial sequencing of ribosomal protein AT-L30. *Int J Syst Bacteriol* **45**, 653-660.

Ohnishi, J., Hayashi, M., Mitsuhashi, S. & Ikeda, M. (2003). Efficient 40 degrees C fermentation of L-lysine by a new *Corynebacterium glutamicum* mutant developed by genome breeding. *Appl Microbiol Biotechnol* **62**, 69-75.

Osborn, M. J., Gander, J. E., Parisi, E. & Carson, J. (1972). Mechinism of assembly of the outer membrane of *Salmonella typhimurium*. Isolation and characterization of cytoplasmic and outer membrane. *J Biol Chem* **247**, 3962-3972.

Oteo, J., Aracil, B., Ignacio Alos, J. & Luis Gomez-Garces, J. (2001). Significant bacteremias by *Corynebacterium amycolatum*: an emergent pathogen. *Enferm Infecc Microbiol Clin* **19**, 103-106.

Pappenheimer, A. M., Jr. & Murphy, J. R. (1983). Studies on the molecular epidemiology of diphtheria. *Lancet* **2**, 923-926.

Pascual, C., Lawson, P. A., Farrow, J. A., Gimenez, M. N. & Collins, M. D. (1995). Phylogenetic analysis of the genus *Corynebacterium* based on 16S rRNA gene sequences. *Int J Syst Bacteriol* **45**, 724-728.

Patek, M., Nesvera, J., Guyonvarch, A., Reyes, O. & Leblon, G. (2003). Promoters of *Corynebacterium glutamicum*. *J Biotechnol* **104**, 311-323.

Pathak, A. K., Pathak, V., Seitz, L., Gurcha, S. S., Besra, G. S., Riordan, J. M. & Reynolds, R. C. (2007). Disaccharide analogs as probes for glycosyltransferases in *Mycobacterium tuberculosis*. *Bioorg Med Chem* **15**, 5629-5650.

Peyret, J. L., Bayan, N., Joliff, G., Gulik-Krzywicki, T., Mathieu, L., Schechter, E. & Leblon, G. (1993). Characterization of the *cspB* gene encoding PS2, an ordered surface-layer protein in *Corynebacterium glutamicum*. *Mol Microbiol* **9**, 97-109.

Plesiat, P. & Nikaido, H. (1992). Outer membranes of Gram-negative bacteria are permeable to steroid probes. *Mol Microbiol* **6**, 1323-1333.

Prospero, E., Raffo, M., Bagnoli, M., Appignanesi, R. & D'Errico, M. M. (1997). Diphtheria: epidemiological update and review of prevention and control strategies. *Eur J Epidemiol* **13**, 527-534.

Puech, V., Chami, M., Lemassu, A., Laneelle, M. A., Schiffler, B., Gounon, P., Bayan, N., Benz, R. & Daffe, M. (2001). Structure of the cell envelope of corynebacteria: importance of the non-covalently bound lipids in the formation of the cell wall permeability barrier and fracture plane. *Microbiology* **147**, 1365-1382.

Radmacher, E., Stansen, K. C., Besra, G. S., Alderwick, L. J., Maughan, W. N., Hollweg, G., Sahm, H., Wendisch, V. F. & Eggeling, L. (2005). Ethambutol, a cell wall inhibitor of *Mycobacterium tuberculosis*, elicits L-glutamate efflux of *Corynebacterium glutamicum*. *Microbiology* **151**, 1359-1368.

Rastogi, N. (1991). Recent observations concerning structure and function relationships in the mycobacterial cell envelope: elaboration of a model in terms of mycobacterial pathogenicity, virulence and drug-resistance. *Res Microbiol* **142**, 464-476.

Raynaud, C., Etienne, G., Peyron, P., Laneelle, M. A. & Daffe, M. (1998). Extracellular enzyme activities potentially involved in the pathogenicity of *Mycobacterium tuberculosis*. *Microbiology* **144 (Pt 2)**, 577-587.

Reeves, P. (1994). Biosynthesis and assembly if lipopolysaccharide. In *Bacterial cell wall New comprehensive biochemistry*, pp. 281-317. Edited by J. M. Ghuysen & R. Hakenbeck. Amsterdam: Elsevier.

Riess, F. G., Lichtinger, T., Cseh, R., Yassin, A. F., Schaal, K. P. & Benz, R. (1998). The cell wall porin of *Nocardia farcinica*: biochemical identification of the channel-forming protein and biophysical characterization of the channel properties. *Mol Microbiol* **29**, 139-150.

Riess, F. G., Lichtinger, T., Yassin, A. F., Schaal, K. P. & Benz, R. (1999). The cell wall porin of the Gram-positive bacterium *Nocardia asteroides* forms cation-selective channels that exhibit asymmetric voltage dependence. *Arch Microbiol* **171**, 173-182.

Riess, F. G. & Benz, R. (2000). Discovery of a novel channel-forming protein in the cell wall of the non-pathogenic *Nocardia corynebacteroides*. *Biochim Biophys Acta* **1509**, 485-495.

Riess, F. G., Dörner, U., Schiffler, B. & Benz, R. (2001). Study of the properties of a channel-forming protein of the cell wall of the Gram-positive bacterium *Mycobacterium phlei*. *J Membr Biol* **182**, 147-157.

Riess, F. G., Elflein, M., Benk, M., Schiffler, B., Benz, R., Garton, N. & Sutcliffe, I. (2003). The cell wall of the pathogenic bacterium *Rhodococcus equi* contains two channel-forming proteins with different properties. *J Bacteriol* **185**, 2952-2960.

Ruimy, R., Boiron, P., Boivin, V. & Christen, R. (1994). A phylogeny of the genus Nocardia deduced from the analysis of small-subunit ribosomal DNA sequences, including transfer of *Nocardia amarae* to the genus *Gordona* as *Gordona amarae* comb. nov. *FEMS Microbiol Lett* **123**, 261-267.

Ruimy, R., Riegel, P., Boiron, P., Monteil, H. & Christen, R. (1995). Phylogeny of the genus *Corynebacterium* deduced from analyses of small-subunit ribosomal DNA sequences. *Int J Syst Bacteriol* **45**, 740-746.

Sahm, H., Eggeling, L., Eikmanns, B. & Kramer, R. (1996). Construction of L-lysine-, L-threonine-, and L-isoleucine-overproducing strains of *Corynebacterium glutamicum*. *Ann N Y Acad Sci* **782**, 25-39.

Sambrook, J. & Russell, D. (2001). *Molecular Cloning: A Laboratory Manual* 3rd edn. New York: Cold Spring Habor.

Schäfer, A., Tauch, A., Jager, W., Kalinowski, J., Thierbach, G. & Pühler, A. (1994). Small mobilizable multi-purpose cloning vectors derived from the *Escherichia coli* plasmids pK18 and pK19: selection of defined deletions in the chromosome of *Corynebacterium glutamicum*. *Gene* **145**, 69-73.

Schägger, H. & von Jagow, G. (1987). Tricine-sodium dodecyl sulfate-polyacrylamide gel electrophoresis for the separation of proteins in the range from 1 to 100 kDa. *Anal Biochem* **166**, 368-379.

Schägger, H. & von Jagow, G. (1991). Blue native electrophoresis for isolation of membrane protein complexes in enzymatically active form. *Anal Biochem* **199**, 223-231.

Schiffler, B., Barth, E., Daffe, M. & Benz, R. (2007). *Corynebacterium diphtheriae*: identification and characterization of a channel-forming protein in the cell wall. *J Bacteriol* **189**, 7709-7719.

Schleifer, K. H. & Kandler, O. (1972). Peptidoglycan types of bacterial cell walls and their taxonomic implications. *Bacteriol Rev* **36**, 407-477.

Schmid, K., Ebner, R., Jahreis, K., Lengeler, J. W. & Titgemeyer, F. (1991). A sugar-specific porin, ScrY, is involved in sucrose uptake in enteric bacteria. *Mol Microbiol* **5**, 941-950.

Schneewind, O., Mihaylova-Petkov, D. & Model, P. (1993). Cell wall sorting signals in surface proteins of Gram-positive bacteria. *EMBO J* **12**, 4803-4811.

Schulz, G. E. (2004). The structures of general porins. In *Bacterial and Eukaryotic Porins*, pp. 25-40. Edited by R. Benz. Weinheim: Wiley-VCH.

Seltmann, G. & Holst, O. (2002). *The bacterial cell wall*. Heidelberg: Springer-Verlag.

Senaratne, R. H., Mobasheri, H., Papavinasasundaram, K. G., Jenner, P., Lea, E. J. & Draper, P. (1998). Expression of a gene for a porin-like protein of the OmpA family from *Mycobacterium tuberculosis* H37Rv. *J Bacteriol* **180**, 3541-3547.

Shah, N. S., Wright, A., Bai, G. H. & other authors (2007). Worldwide emergence of extensively drug-resistant tuberculosis. *Emerg Infect Dis* **13**, 380-387.

Simic, P., Sahm, H. & Eggeling, L. (2001). L-threonine export: use of peptides to identify a new translocator from *Corynebacterium glutamicum*. *J Bacteriol* **183**, 5317-5324.

Spargo, B. J., Crowe, L. M., Ioneda, T., Beaman, B. L. & Crowe, J. H. (1991). Cord factor (alpha,alpha-trehalose 6,6'-dimycolate) inhibits fusion between phospholipid vesicles. *Proc Natl Acad Sci U S A* **88**, 737-740.

Stackebrandt, E., Rainey, F. A. & Ward-Rainey, N. L. (1997). Proposal for a New Hierarchic Classification System, Actinobacteria classis nov. *Int J Syst Bacteriol* **47**, 479-491.

Stahl, C., Kubetzko, S., Kaps, I., Seeber, S., Engelhardt, H. & Niederweis, M. (2001). MspA provides the main hydrophilic pathway through the cell wall of *Mycobacterium smegmatis*. *Mol Microbiol* **40**, 451-464.

Stephan, J., Bender, J., Wolschendorf, F., Hoffmann, C., Roth, E., Mailander, C., Engelhardt, H. & Niederweis, M. (2005). The growth rate of *Mycobacterium smegmatis* depends on sufficient porin-mediated influx of nutrients. *Mol Microbiol* **58**, 714-730.

Sutcliffe, I. C. & Russell, R. R. (1995). Lipoproteins of Gram-positive bacteria. *J Bacteriol* **177**, 1123-1128.

Sutcliffe, I. C. (1997). Macroamphiphilic cell envelope components of *Rhodococcus equi* and closely related bacteria. *Vet Microbiol* **56**, 287-299.

Sutcliffe, I. C. (1998). Cell envelope composition and organisation in the genus *Rhodococcus*. *Antonie Van Leeuwenhoek* **74**, 49-58.

Szmelcman, S. & Hofnung, M. (1975). Maltose transport in *Escherichia coli* K-12: involvement of the bacteriophage lambda receptor. *J Bacteriol* **124**, 112-118.

Tatituri, R. V., Alderwick, L. J., Mishra, A. K. & other authors (2007). Structural characterization of a partially arabinosylated lipoarabinomannan variant isolated from a *Corynebacterium glutamicum ubiA* mutant. *Microbiology* **153**, 2621-2629.

Tauch, A., Bischoff, N., Pühler, A. & Kalinowski, J. (2004). Comparative genomics identified two conserved DNA modules in a corynebacterial plasmid family present in clinical isolates of the opportunistic human pathogen *Corynebacterium jeikeium*. *Plasmid* **52**, 102-118.

Tauch, A., Kaiser, O., Hain, T. & other authors (2005). Complete genome sequence and analysis of the multiresistant nosocomial pathogen *Corynebacterium jeikeium* K411, a lipid-requiring bacterium of the human skin flora. *J Bacteriol* **187**, 4671-4682.

Tauch, A., Trost, E., Tilker, A. & other authors (2008). The lifestyle of *Corynebacterium urealyticum* derived from its complete genome sequence established by pyrosequencing. *J Biotechnol*.

Ton-That, H., Marraffini, L. A. & Schneewind, O. (2004). Protein sorting to the cell wall envelope of Gram-positive bacteria. *Biochim Biophys Acta* **1694**, 269-278.

Towbin, H., Staehelin, T. & Gordon, J. (1979). Electrophoretic transfer of proteins from polyacrylamide gels to nitrocellulose sheets: procedure and some applications. *Proc Natl Acad Sci U S A* **76**, 4350-4354.

Trias, J., Jarlier, V. & Benz, R. (1992). Porins in the cell wall of mycobacteria. *Science* **258**, 1479-1481.

Trias, J. & Benz, R. (1993). Characterization of the channel formed by the mycobacterial porin in lipid bilayer membranes. Demonstration of voltage gating and of negative point charges at the channel mouth. *J Biol Chem* **268**, 6234-6240.

Trias, J. & Benz, R. (1994). Permeability of the cell wall of *Mycobacterium smegmatis*. *Mol Microbiol* **14**, 283-290.

Tropis, M., Meniche, X., Wolf, A. & other authors (2005). The crucial role of trehalose and structurally related oligosaccharides in the biosynthesis and transfer of mycolic acids in *Corynebacterineae*. *J Biol Chem* **280**, 26573-26585.

Trotschel, C., Deutenberg, D., Bathe, B., Burkovski, A. & Kramer, R. (2005). Characterization of methionine export in *Corynebacterium glutamicum*. *J Bacteriol* **187**, 3786-3794.

Uchida, K. & Aida, K. (1979). Taxonomic significance of cell-wall acyl type in *Corynebacterium-Mycobacterium-Nocardia* group by a glycolate test. *J Gen Appl Microbiol* **25**, 169-183.

Vaara, M., Plachy, W. Z. & Nikaido, H. (1990). Partitioning of hydrophobic probes into lipopolysaccharide bilayers. *Biochim Biophys Acta* **1024**, 152-158.

van der Rest, M. E., Lange, C. & Molenaar, D. (1999). A heat shock following electroporation induces highly efficient transformation of *Corynebacterium glutamicum* with xenogeneic plasmid DNA. *Appl Microbiol Biotechnol* **52**, 541-545.

van Wely, K. H., Swaving, J., Freudl, R. & Driessen, A. J. (2001). Translocation of proteins across the cell envelope of Gram-positive bacteria. *FEMS Microbiol Rev* **25**, 437-454.

Vasicova, P., Patek, M., Nesvera, J., Sahm, H. & Eikmanns, B. (1999). Analysis of the *Corynebacterium glutamicum dapA* promoter. *J Bacteriol* **181**, 6188-6191.

Vollmer, W. (2008). Structural variation in the glycan strands of bacterial peptidoglycan. *FEMS Microbiol Rev* **32**, 287-306.

Vrljic, M., Sahm, H. & Eggeling, L. (1996). A new type of transporter with a new type of cellular function: L-lysine export from *Corynebacterium glutamicum*. *Mol Microbiol* **22**, 815-826.

Ward, J. B. (1981). Teichoic and teichuronic acids: biosynthesis, assembly, and location. *Microbiol Rev* **45**, 211-243.

Weiss, M. S., Kreusch, A., Schiltz, E., Nestel, U., Welte, W., Weckesser, J. & Schulz, G. E. (1991). The structure of porin from *Rhodobacter capsulatus* at 1.8 A resolution. *FEBS Lett* **280**, 379-382.

Wolschendorf, F., Mahfoud, M. & Niederweis, M. (2007). Porins are required for uptake of phosphates by *Mycobacterium smegmatis*. *J Bacteriol* **189**, 2435-2442.

Woolley, G. A. (2007). Channel-forming activity of alamethicin: effects of covalent tethering. *Chem Biodivers* **4**, 1323-1337.

Yano, I. & Saito, K. (1972). Gas chromatographic and mass spectrometric analysis of molecular species of corynomycolic acids from *Corynebacterium ulcerans*. *FEBS Lett* **23**, 352-356.

Yukawa, H., Omumasaba, C. A., Nonaka, H. & other authors (2007). Comparative analysis of the *Corynebacterium glutamicum* group and complete genome sequence of strain R. *Microbiology* **153**, 1042-1058.

Ziegler, K., Benz, R. & Schulz, G. E. (2008). A Putative alpha-Helical Porin from *Corynebacterium glutamicum*. *J Mol Biol*.

Zuber, B., Chami, M., Houssin, C., Dubochet, J., Griffiths, G. & Daffe, M. (2008). Direct visualization of the outer membrane of mycobacteria and corynebacteria in their native state. *J Bacteriol* **190**, 5672-5680.

6.2 Curriculum vitae

Name: Enrico Barth

Address: Prager Ring 23,

                                     97084 Würzburg

Date and place of birth: 24/07/1977   Chemnitz/ Germany

Marital status: unmarried

Education:

    09/1984 – 06/1988   Elementary school, Würzburg

    09/1988 – 06/1997   Deutschhaus-Gymnasium, Würzburg

    06/1997   Abitur

Military service:

    09/1997 – 06/1998   Ellwangen and Veitshöchheim

Course of study:

    11/1998 – 12/2004   Study of biology at the University of Würzburg
        Major subject: Biotechnology
        Minor subjects: Microbiology and Biochemistry
        Diploma thesis: „*Purification and characterization of membrane proteins from mycolata*“

    12/2004   Diploma

    01/2005   Start of Ph.D. - thesis - in the laboratory of Prof. Dr. Dr. h.c. Roland Benz at the University of Würzburg

6.3   Publications

Schiffler, B., Barth, E., Daffe M. & Benz, R. (2007). *Corynebacterium diphtheriae*: identification and characterization of a channel-forming protein in the cell wall. *J Bacteriol* **189,** 7709-19.

Barth, E., Agullo Barcello, M., Kläckta, C. & Benz, R. (2008). Study of the major cell wall channel of *Corynebacterium glutamicum*, *Corynebacterium efficiens* and *Corynebacterium diphtheriae* in dependence of PorH and PorA proteins. (in preparation)

Barth, E., Tauch, A. & Benz, R. (2008). *Corynebacterium jeikeium jk0268* constitutes for CjPorA, which forms a homooligomeric and anion-selective cell wall channel. (manuscript prepared for publication)

6.4 Acknowledgments

meiner Freundin Patricia für…

… deine Hilfe und Unterstützung sowie deine aufbauenden Worte!